2015

GUMBOS as Matrices for Matrix-Assisted Laser Desorption Ionization Time of Flight Mass Spectrometry

Hashim Abdullah Al Ghafly
Louisiana State University and Agricultural and Mechanical College, halgha3@lsu.edu

GUMBOS AS MATRICES FOR MATRIX-ASSISTED LASER DESORPTION IONIZATION TIME OF FLIGHT MASS SPECTROMETRY

A Dissertation

Submitted to the Graduate Faculty of the
Louisiana State University and
Agricultural and Mechanical College
in partial fulfillment of the
requirements for the degree of
Doctor of Philosophy

in

The Department of Chemistry

by
Hashim Al Ghafly
B.S., King Saudi University Riyadh, 1997
M.S., University of Nebraska Omaha, 2009
May 2015

To my Parents Abdullah Al Ghafly and Norah Bouhlaqa
To my children, my wife and my friends for their continuous love, encouragement and support throughout the years.

ACKNOWLEDGEMENTS

I deeply appreciate the excellent guidance, dedicated teaching, constant encouragement, kind assistance, and the precious time devoted by my supervisor, Professor Isiah M. Warner. I am confident that the experience I gained in the Warner lab will tremendously help me to succeed in my future endeavors. I also express thanks to the members of my doctoral committee i.e. Professors Graca Vicente and Hsiao-Chun Wu for their time and helpful suggestions.

Next, I am grateful to Professor Kermit K. Murray for helping me learn about mass spectrometry and for his guidance and encouragement. I also want to recognize Dr. Jeonghoon Lee and Ms. Connie David at the Louisiana State University Mass Spectrometry Facility for their training on the mass spectrometers.

In addition, I acknowledge the guidance of former and current members of Professor Warner's research group, especially the postdoctoral researchers: Dr. Noureen Siraj, Dr. Susmita Das, and Dr. Farhana Hasan for teaching me the relevant instrumental techniques utilized for the synthesis and characterization of ionic liquids. I also appreciate them for their helpful suggestions and assistance with proofreading my dissertation and published manuscripts.

Finally, I thank the Culture Mission of the Royal Embassy of Saudi Arabia, and the National Science Foundation (NSF) grants CHE-1307611 and CHE-1152106 for financial support.

Overall, I dedicate this work to my lovely wife, Dr. Zahra Al Ghafli, and our children, Kawthar, Fatimah, Ali, and Haydar for their love, support, and prayers, which enabled me to successfully complete this research.

TABLE OF CONTENTS

LIST OF TABLES

LIST OF FIGURES

LIST OF ABBREVIATIONS

A	Absorbance
ACN	Acetonitrile
CHCA	α-cyano-hydroxycinnamic acid
DHB	2,5-Dihydroxy benzoic acid
ESI	Electrospray ionization
IL	Ionic liquid
ITO	Indium tin oxide
GUMBOS	Group of uniform materials based on organic salts
LDI	Laser desorption ionization
m/z	Mass-to-charge ratio
MALDI	Matrix-assisted laser desorption/ionization
MS	Mass spectrometry
NMR	Nuclear magnetic resonance
RSD	Relative standard deviation
S/N	Signal-to-nose
TFA	Trifluoroacetic acid

ABSTRACT

This work involves the investigation of a *g*roup of *u*niform *m*aterials *b*ased on *o*rganic *s*alts (GUMBOS) as matrices for matrix assisted laser desorption ionization time of flight mass spectrometry (MALDI-TOF) for analysis of hydrophobic biomolecules. GUMBOS are new class of materials that show great promise as MALDI matrices because they are able to form a thin-layer on the MS target, thereby enhancing the sample homogeneity, signal intensity, and shot-to-shot reproducibility. The detection of hydrophobic peptides using MALDI-TOF MS remains a challenge because the majority of matrices utilized are hydrophilic thereby exhibiting low affinity for hydrophobic molecules. To address this, I have developed novel matrices of varying hydrophobicity based on aminopyrine (AP) to enhance the detection of such molecules. In the first part of this work, I outline the synthesis of a series of AP-based GUMBOS in which various counter-ions such as chloride, ascorbate, and bis(trifluoromethane) sulfonamide were used to tune the hydrophobicity of a matrix. The hydrophobicities of these compounds relative to α-cyano-4-hydroxycinnamic acid (CHCA), a common MALDI matrix, indicated that the AP-based GUMBOS can be tuned to greater hydrophobicity than CHCA. In addition, a clear trend was observed between the signal intensity of the hydrophobic peptides and the hydrophobicity of the matrix. In the second part of this work, I present a unique approach for predicting matrix-analyte interactions in MALDI using fluorescence spectroscopy. Interactions of analytes with matrices that are composed of AP and AP-based GUMBOS were investigated using a hydrophobic (gramicidin) and a hydrophilic peptide (angiotensin II). Fluorescence anisotropy and Scatchard analysis

were used to investigate the interaction between matrices and peptides. Hydrophobic AP and AP-based GUMBOS revealed stronger interactions with hydrophobic peptides and enhanced detection of these peptides, which correlate well with the MALDI MS results. Finally, I have synthesized a hydrophobic GUMBOS-based matrix using CHCA and oleylamine (OA). The [OA][CHCA] GUMBOS was used as a matrix for MALDI MS for the detection of lipids in tissues and compared with 2,5-dihydroxybenzoic acid (DHB) had better signal reproducibility and improved homogeneity. These enhancements were used to examine the distribution and localization of different classes of lipids in tissue.

CHAPTER 1: THE EVALUATION OF MASS SPECTROMETRY AND THE POTENTIAL OF IONIC LIQUIDS FOR MALDI MATRECES

1.1 Mass Spectrometry

Mass spectrometry (MS) is an important tool for the analysis of complex samples such as biomolecules, tissues, cell cultures, and polymers.[1] Recently in the MS field, imaging mass spectrometry (IMS) has emerged as technique for screening analytes such as lipids, peptides, proteins, and drugs.[2-8] Over the years, MS has become a powerful, and highly selective analytical tool used to evaluate the mass composition of a sample by separating the ions based on their mass-to-charge ratio (*m/z*).[9, 10] The two most recently, developed ionization methods in MS are electrospray ionization (ESI)[11] and matrix-assisted laser desorption/ionization time of flight mass spectrometry (MALDI-TOF MS).[12] MALDI is a soft ionization technique, in which the gas phase ions are formed without fragmentation.[13] This technique has been extensively utilized to analyze of the wide range of biomolecules. This technique is particularly useful for characterizing the large thermally labile biomolecules and has recently found applications in imaging and clinical research.[1] The advantages of this approach include robustness, high throughput, high sensitivity and applicability to a wide range of compounds.

A mass spectrometer (MS) is composed of three components: ionization source, mass analyzer, and detector. A schematic of a mass spectrometer is shown in Figure 1.1. An inlet is used to transfer samples from atmospheric pressure into the ion source chamber where the analytes are converted into gaseous ions. Once the ions reach the mass analyzer, the analytes in the sample are then separated based on their mass-to-

charge ratio and transported under a magnetic field. The separated chemical ions are then detected and the produced signals are transferred to data analysis.[14]

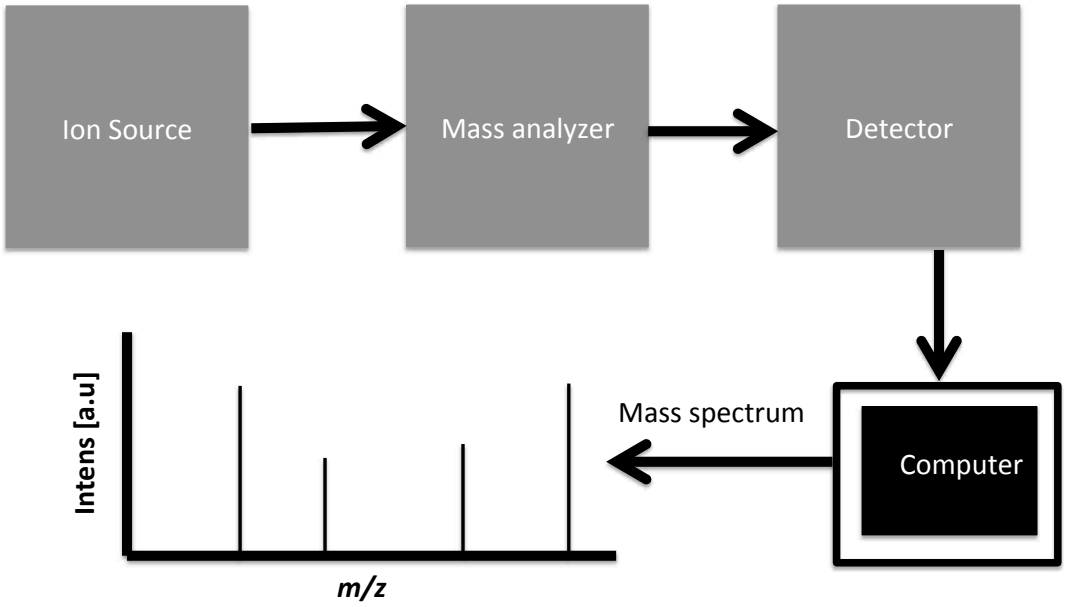

Figure 1.1. Schematic of a mass spectrometry of basic components.

1.2 Matrix Assisted Laser Desorption Ionization Time of Flight Mass Spectrometry (MALDI-TOF MS)

MALDI-TOF MS has evolved as an excellent tool for rapid, sensitive (femtomole or attomole), and accurate mass identification [1, 15, 16] and characterization of analytes.[17] This technique has the ability to detect low molecular weight compounds of peptides or amino acids.[18, 19] In 1988, Karas and Hillenkamp[12] demonstrated that MALDI-TOF-MS provide the advantage of rapid and accurate identification and characterization of such analytes with minimal sample introduction. Since its development, MALDI-TOF MS has been increasingly used in the biological sciences particularly for the characterization of proteins, peptides, and nucleic acids.[20]

The development of MALDI was influenced by laser desorption ionization (LDI), which is used to ionize compounds less than 1000 Da.[14] Though, LDI has been previously used for the ionization of highly volatile molecules.[14] Though, LDI has been previously used for the ionization of highly volatile molecules, it is difficult to control excessive thermal degradation and some compounds are unable to absorb laser irradiation in LDI.[21]

1.2.1 Operational Mode of MALD IMS

The operation of MALDI-MS involves three steps. The first step involves the use of a matrix that in the MALDI mechanism will donate a proton to the analyte. During this first step, the matrix and analyte are mixed and then spotted on target and left at room temperature until the solvent evaporated. Once the solvent is vaporized, a uniform co-crystal of the matrix and analyte that depends on the type of matrix, surface, evaporation, etc., is generated. Typically, the analyte and matrix are prepared at a molar ratio of 1:1000 and 1:10,000 for the analysis of peptides and proteins, respectively.[22] Next, the crystalline mixture is irradiated with a laser pulse from sources such as 337 nm nitrogen laser or 355 nm Nd:YAG laser. The matrix absorbs energy and transfers protons to the analyte.[23] This energy is used for desorption and ionization of the analyte which is subsequently focused towards the mass analyzer. Upon ionization, analytes are accelerated using high voltage and then separated under high vacuum.[24] Such separation is achieved based on the mass-to-charge ratio of the ions. A schematic of the MALDI-MS process is shown in Figure 1.2.

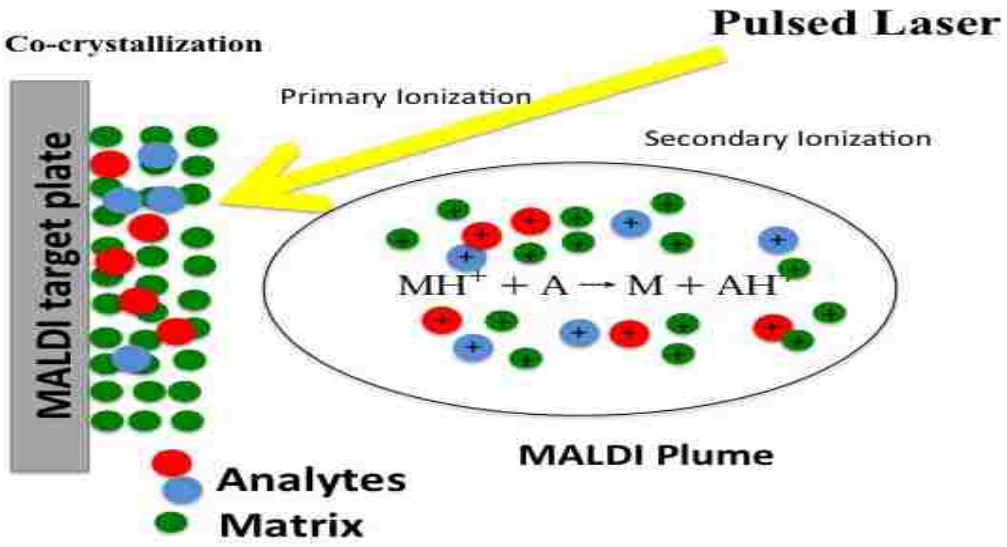

Figure 1.2. Schematic diagram of the matrix and analytes co-crystallized on the MALDI target followed by irradiation with a laser pulse. The matrix absorbs the energy from the laser then transfers the proton to the analyte. Protonation occurs by transferring protons to the analyte via gas-phase collisions or cluster ionization. M represents matrix and A represents analyte.

1.2.2 Time of Flight Mass Spectrometry (TOFMS)

While this MALDI ionization technique can be coupled with various mass analyzers such as Time of Flight (TOF), Fourier Transform Mass Spectrometry (FTMS), Quadruple Time of Flight (QTOF), etc., this research will focus on applications with TOF. Time of Flight (TOF) measurement is an analytical technique that is used to analyze the mass of a sample. The TOF based technique was developed by Cameron has been further improved for higher mass resolution and sensitivity through the use of time-lag focusing techniques. [25, 26] Today TOF is frequently used with MALDI MS and it is employed in either reflectron or linear mode, which will be described later.

TOF mass spectrometry has many advantages over other instruments such as high ion transmission, low cost, and theoretically unlimited mass (more than 100 kDa). The entire mass spectrum can be obtained in each cycle of measurement without scanning voltage or

current, which makes TOF a fast technique, taking only a few microseconds.[27-30] A major advantage of TOF MS[30] is the entire mass spectrum can be recorded. Moreover, this approach has good transmission of ions and fast repetition rate. [2, 26]

The TOF technique allows determination of the *m/z* ratio of the ions by measuring the flight time of ions in a field free region. The construction and operation of TOF is simple, which consists of an acceleration region, field free drift region, and a detector all housed inside a chamber.[31] The ions move from the ion source into the flight tube where they are accelerated by an electric field. When the ions reach the field free drift region, the acceleration gives all ions the same kinetic energy (KE) if they have the same charge. Kinetic energy is defined by the following equation:

$$KE = \frac{mv^2}{2} \qquad (1)$$

where KE represents the kinetic energy of the ions, which is determined by acceleration voltage, m is the mass of ions, and v is the velocity. Heavier ions reach the detector later than lighter ions. The mass-to-charge ratio (*m/z*) can be calculated based on the time it takes for ions in the field-free flight to reach the detector at the end of the tube.[31, 32] Ions with different mass to charge ratios that are accelerated into the field free drift region will have different velocities. Based on this concept, the KE of the ions can be calculated from voltage, (V), as they travel through the field-free tube, L, by Equation 1:

$$zV = \frac{mv^2}{2} \qquad (2)$$

where m is mass, z is the charge, and v is velocity. Equations 1 and 2 can be rearranged to solve for the flight time (t):

$$t = \frac{L}{v} = L\sqrt{\frac{m}{2zV}} \qquad (3)$$

where L is the length of the flight path and t is the time it takes the ion to travel a particular distance.[33]

Linear and reflectron are two types of TOF MS. Figure 1.3 shows a schematic of the linear mode TOF MS. In this method, the ions enter the field-free flight tube by acceleration and continue to move inside the flight tube until they hit the detector. Ions with different *m/z*, will have different velocities, thus travel inside the field-free region at different speeds.[34] Notably, ions that have similar (*m/z*), but have different velocities and initial positions, can reach the detector at different times. These factors directly affect the resolution of the linear TOF because even if the ions have the same *m/z* ratio, they do not necessarily reach the detector at the same time. For these reasons, the linear mode has a lower resolution. [35].

Mass resolution (R) of mass spectrometry is defined as follows:

$$R = \frac{m}{\Delta m} = \frac{t}{2\Delta t} \quad (4)$$

where m is the observed mass and Δm is the difference in the mass error of ions, t is the flight time and Δt is difference in times at the full width at half maximum (FWHM) of a peak. Mass accuracy is defined as the difference between the exact mass and the observed mass. Mass accuracy can be calculated in part per million (ppm).

$$\text{Mass Accuracy} = 10^6 \times \frac{(M_m - M_t)}{M_t} \quad (5)$$

where M_m represents observed mass and M_t represent exact mass

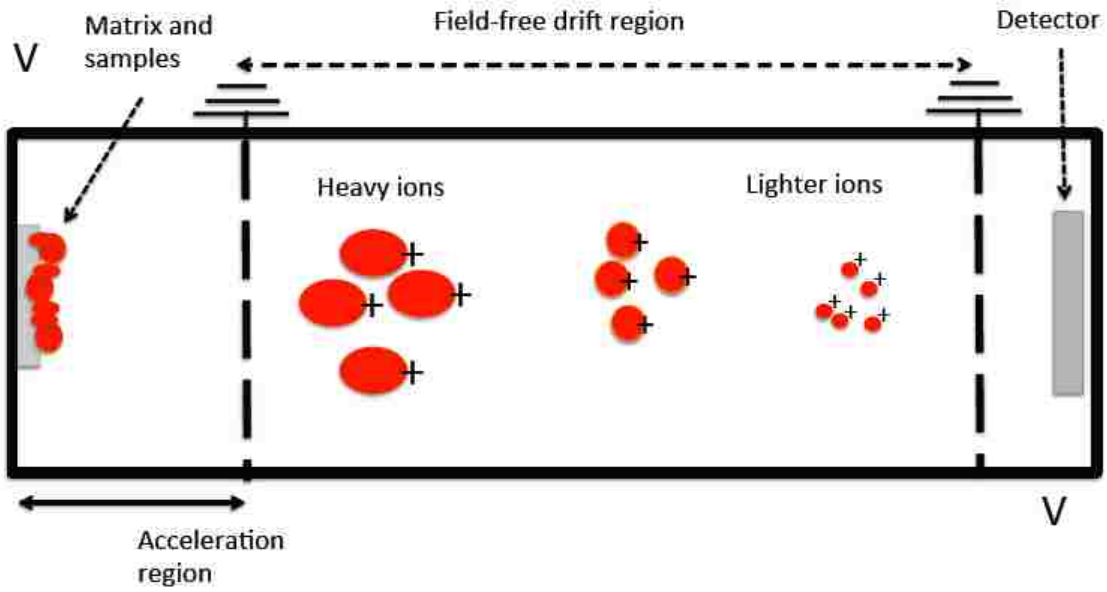

Figure 1.3. Schematic of mass separation by linear-TOF mass analyzer. The lighter ions reach the detector sooner than heavy ions with the same charge.

Linear mode TOF exhibits low mass resolution (~1000),[36] which affects mass accuracy. When using linear mode, the isotopic distribution of ions cannot be distinguished. Mass accuracy with high resolution is important for complex samples such as tissues. In order to solve this problem, TOF in ion reflectron mode can be used. Reflectron mode TOF can easily obtain a mass with resolution greater than 10,000.[30]This mode has good resolution due to the addition of an ion mirror at the end of the flight tube region.[32] Figure 1.4 shows a reflectron TOF mass analyzer that is used to maximize the resolution for ions with the same mass to charge ratio. Some ions can have higher velocity and the others have lower velocity due to same mass. The ions with a higher energy not only travel faster but also penetrate deeper and spend more time in the ion mirror [33] On the other hand, ions with lower velocity do not penetrate as deeply as a result they spend less time in the ion mirror. When the detector position is adjusted properly, the ions of the same mass-to-charge ratio will arrive at the detector at the same

time. Additionally, resolution can be improved by increasing the path length of the reflectron (L_1+L_2). All ions that have the same (*m/z*) ratio will reach the detector, located at the end of flight path L_2.[35]

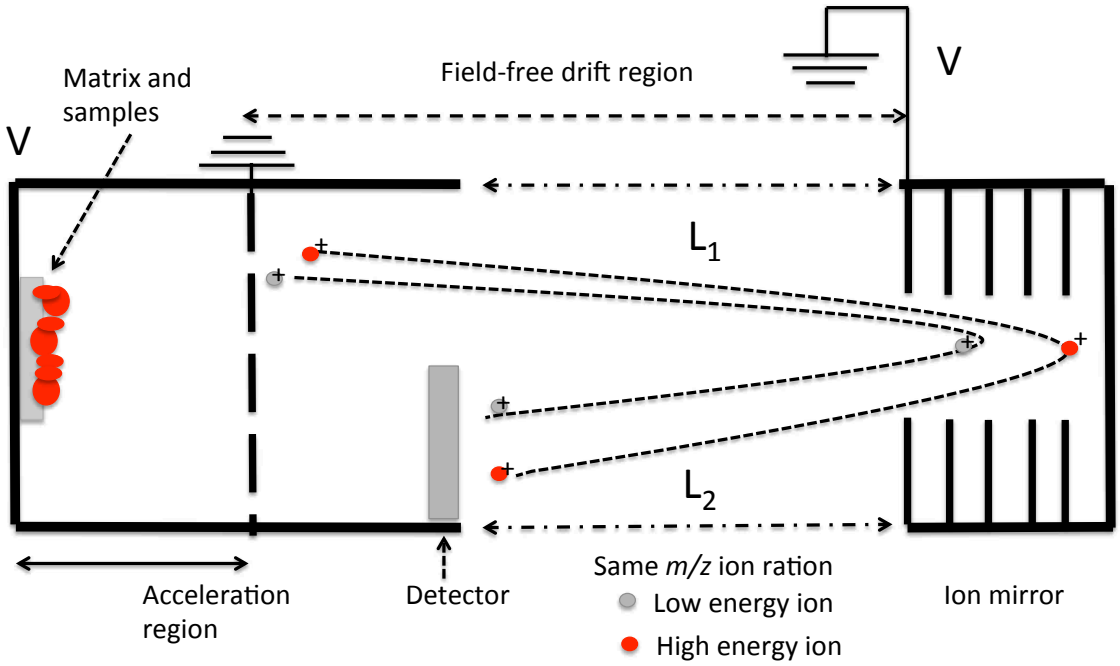

Figure 1.4. Schematic of the reflectron-TOF mass analyzer. All the *m/z* ions have different kinetic energy. They arrive at the same time at the detector that is located at the end of path flight L_2.

Another method used to improve resolution is delayed ion extraction.[37, 38] In this method, ions are extracted from an ion source after laser irradiation of the sample. This occurs after a short time delay, on the order of one hundred nanoseconds. If an ion has a lower velocity, it is accelerated more when the extraction potential is applied. Conversely, the ions with a high velocity are accelerated less when the extraction potential is applied because the position of these ions is farther from the extraction grid.

1.2.3 Matrix Ionization

Although MALDI has been used for decades, the exact mechanism of ionization is still being debated.[39] Matrix ionization occurs in two steps; the first is called primary ionization, in which a laser is used to irradiate the matrix; the second is called secondary ionization, which happens in the gas phase to form a plume on the top of the target as shown in Figure 1.2. In primary ionization, the matrix (M) absorbs a photon from laser irradiation leading to an excited (M^*).[40] The matrix transfers the proton to the analyte species in the laser-induced plume during the secondary ionization when the matrix and analyte collide.[40-42]

An alternative mechanism forms ions in clusters. In this method, clusters are assumed to be formed in the desorption plume by trapping the numerous charged ions and counter ions that are derived from the analyte. The charges separated in the clusters have a deficit. The ions of analyte are formed by evaporation from the matrix, which has rich clusters.[43]

1.2.4 Sample Preparation

There are several important factors that affect the signal intensity in a MALDI mass spectrum.[44] One of these factors is sample preparation, more specifically, the co-crystallization of analyte and matrix.[45] The homogeneity of a sample plays a role in the reproducibility and signal intensity of ion yields. Several techniques have been used to improve sample preparation. One of which is the dried-droplet technique,[46] in this method, 1 μL of the matrix and sample is respectively spotted onto the target, mixed and dried slowly under ambient air.[46] Another method used to improve homogeneity is the rapid evaporation method.[33] In this case, the matrix is prepared in a highly volatile

solvent such as acetone with the analyte prepared in water. A few microliters of the matrix is spotted on the target then left until the solvent is evaporated and a film generated. Next, a few microliters of analyte is dropped on the target and the solvent is dried slowly under room temperature. The sandwich method is yet another technique used to improve homogeneity.[47] A few microliters of a matrix is deposited until a thin layer of the matrix is formed. Then the analyte is deposited upon the matrix. Finally, an additional layer of matrix is applied; thereafter, the mixture is then dried in ambient air.

Electrospray method[48, 49] is also occasionally used to generate more homogenous samples. Briefly, the analyte and matrix solutions pass through a capillary at high potential and are deposited on the target plate to yield much smaller crystals and dried under a stream of nitrogen gas. Parameters such as flow rate and applied voltage can be controlled to optimize the method.

Prior to the use of MALDI, calibration with a suitable reference (standard) compound(s) should be performed. For example, specifically for the Bruker instrument used for these studies a peptide standard, which contains seven standard peptides, can be used. Angiotensin II, angiotensin I, substance P, ACTH clip 1-17, ACTH 18-39 and Somalostain 28 are few examples of the peptides that can be used for calibration. To ensure high resolution and reproducibility, standards of highest purity must be used for calibrating MALDI. A mass spectrum for calibration is shown in Figure1.5.

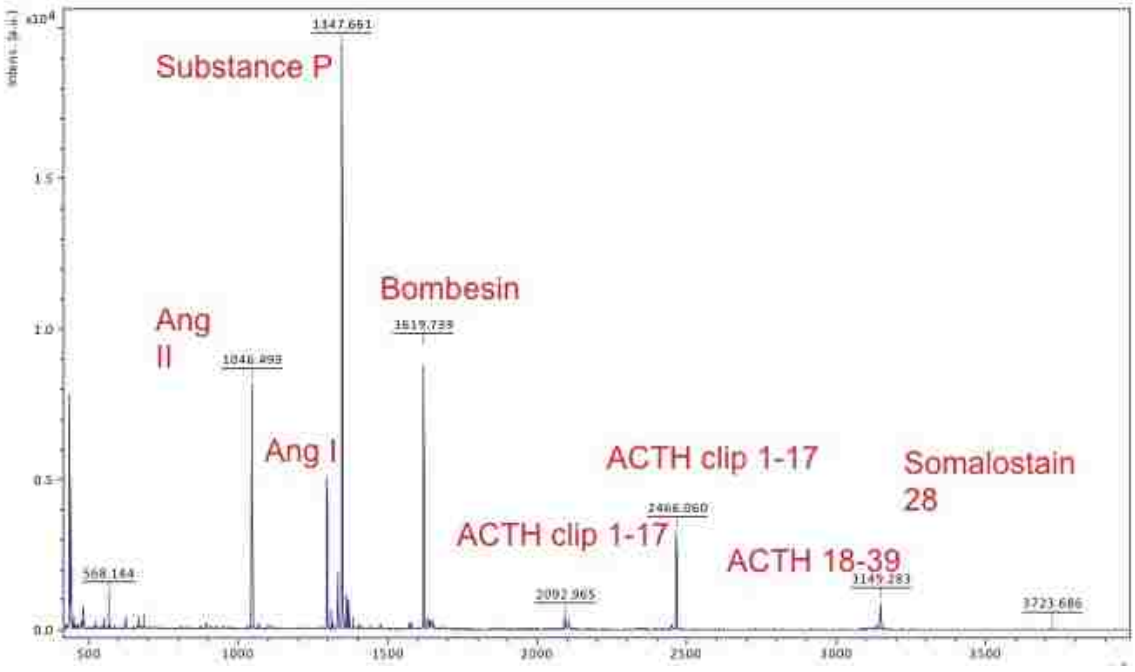

Figure 1.5. 1 µL each from Peptide calibration standard and CHCA dried droplet mixed on plate target.

1.3 MALDI Matrices

In general, typical MALDI matrices must possess some specific properties that include: strong absorption at the wavelength laser,[50] and the ability to effectively disperse analytes.[51] Synthesized matrices must have the ability to be dissolved in the same solvent that is used for analytes. Moreover, matrices should also serve as good protonating or deprotonating agents. [23, 52, 53]

1.3.1 Organic Matrices

A variety of organic compounds can be used to prepare solid matrices. There are several characteristics that are required to make a good matrix. First, the material must strongly absorb at the same wavelength of the laser, 337 or 355 nm. They must dissolve in the same solvent that is used for analytes and be stable in vacuum, donate protons to

the analyte, and be inert to reaction with analytes. Finally, they must have the capacity to crystallize and have a low heat of sublimation. [44]

Solid matrices such as α-cyano-4-hydroxycinnamic acid (CHCA) have been used for the analysis of proteins and peptides with molecular weights below 10 kDa, while 2,5-dihydroxbenzoic acid (DHB) and sinapinic acid (SA) have been used for the analysis of proteins with higher molecular weights.[54-56] Table 1.1 shows the structures and biological applications of commonly used matrices.

A notable challenge in the quantification of analytes using MALDI is the poor sample-to-sample and shot-to-shot reproducibility due to the formation of several sweet spots as a result of non-homogenous distribution of the matrix and analyte on the target.[51, 57-60] The extent of inhomogeneity depends on the type of matrix employed and deposition.[61] The non-homogeneous distribution of analytes increases the measurement time because analytes can be detected only in such spots. Therefore, in order to improve reproducibility, the selection of a suitable matrix that can produce homogeneous MALDI spots is important. [54]

One method of increasing the homogeneity of these MALDI spots involves the use of nitrocellulose substrates. The increased homogeneity that this method provides improved spot-to-spot reproducibility and the higher precision of peptides quantitation of MALDI. Nitrocellulose substrates help to increase the uniformity of analyte distribution on the sample surface and increase interaction and binding between the analyte and matrix. Another advantage of using nitrocellulose is the reduction of contaminants in the sample, which leads to an increase in the yield of the $[M+H]^+$ ion signal. This is due to

the ability of the nitro groups in nitrocellulose to electrostatically bind to analytes, allowing impurities to be rinsed away without reduction in analyte concentration.[62]

Table 1.1. Structure of common matrices used for MALDI.

Matrix	Structure	Application
α-cyano-4-hydroxycinnamic acid (α-CHCA)[60]	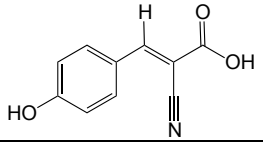	Peptides
2,5-dihydroxy benzoic acid (DHB)	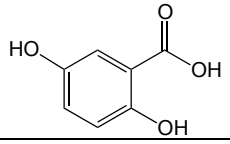	Lipids/ proteins
(Sinapinic acid, SA)	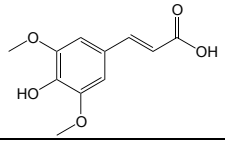	Proteins
1,5-Diaminonaphthalene (DAN)[63]	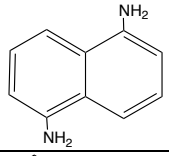	Lipids
Picolinic acid (PA)[64]	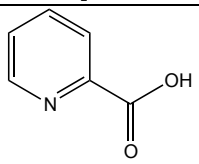	Oligonucleotides
Dithranol	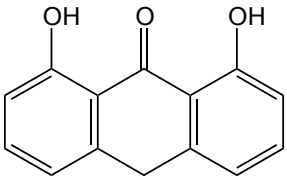	Polymers
6-Aza-2-thiothymine (ATT)	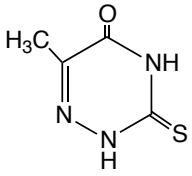	Oligonucleotides

1.3.2 Inorganic Matrices

Improved homogeneity and signal intensity have been reported when using inorganic salts for example copper, cobalt, silver, and gold as MALDI matrices.[65] These materials are dissolved with the appropriate nonvolatile solvents such as glycerol and are suitable for analysis of low molecular weight compounds such as methyl stearate, as well as, other non-polar and polar analytes since they generate low background noise. In addition, these matrices have been known to form small sized crystals and provide rapid heating, which is necessary to desorb and ionize analytes without causing decomposition of the analytes. These inorganic matrices generate the lowest background noise and highest intensity when used in MALDI-TOF.[66] The use of graphite based inorganic matrices works similarly and is termed Surface Assisted Laser Desorption Ionization (SALDI). In addition to this SALDI technique, two other techniques that use inorganic matrices such as porous silicon and silicon nanowires are Desorption Ionization on Silicon (DIOS) and Nanowire Assisted Desorption Ionization (NALDI) respectively.[67-69]

1.3.3 Liquid Matrices

Although most matrices are composed of solid organic compounds, the use of liquid matrices has some advantages such as shot-to-shot reproducibility and the ease of miscibility with both hydrophobic and hydrophilic analyte.[70-72] For example, glycerol is a suitable liquid matrix for infrared IR-MALDI mass spectrometry; though, glycerol cannot be used in ultraviolet UV-MALDI mass spectrometry since it is incompatible with 337 nm nitrogen laser.[73] However, nitro benzyl alcohol can use for UV MALDI. The physical characteristics of liquid matrices are similar to aqueous solutions. Also, the use

of liquid matrices can likewise avoid non-covalent complex dissociation, which is usually apparent in solid matrices during the co-crystallization process.[70] Contamination at the source and high backing pressures under vacuum are major drawbacks that have prevented liquids matrices from being utilized in routine analysis.[72]

1.4 Ionic Liquids

Ionic liquids (ILs) are compounds composed of bulky organic ions with melting points equal to or less than 100°C. Typically, inorganic salts such as sodium chloride possess melting points higher than 800°C. Replacing the cation or anion with a bulky organic ion results in a lower melting point through the poor coordination between the bulky organic and inorganic ions.[74] ILs have been categorized into room temperature ionic liquids (RTILs) (melting point < 25°C) and frozen ionic liquids (FILs) (melting point range of 25 - 100°C).

In general, the cations used in ILs are organic moieties of low symmetry.[75] In the main, cations are derived from ammonium, phosphonium, pyridinium, or imidazolium ions. Inorganic or organic anions such as tetrafluoroborate or nitrate have been used as counterions.[75] Figure 1.6 shows both common cations and anions used in the synthesis of ionic liquids.

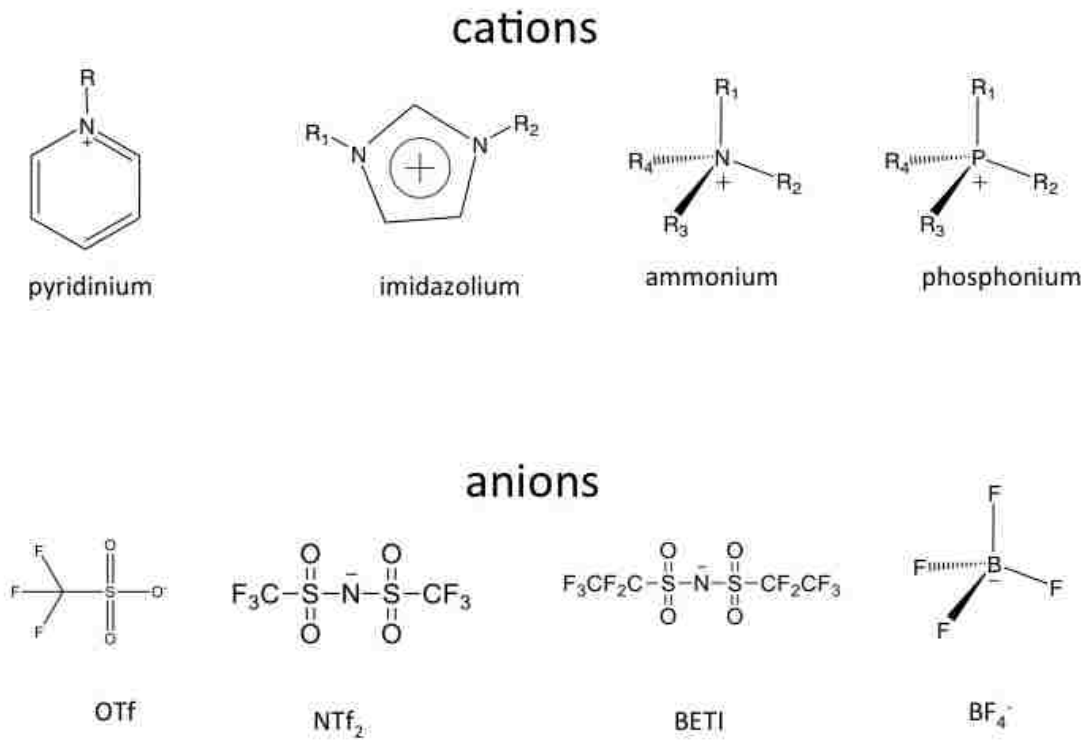

Figure 1.6. Common cations and anions used in ionic liquids (ILs). OTF (trifluoromethanesulfonatev), NTf_2 (bis(trifluoromethanesulfonyl)imide), BETI (bis(trifluoromethylsulfonyl)imide), BF_4 (tetrafluoroborate).

Ionic liquids possess many advantages over common solvents including non-flammability, negligible vapor pressure, non-explosiveness and excellent stability at elevated temperatures. They are called designer solvents because of the tunability of various physical properties such as density, melting point, polarity and viscosity.[76] Further, their cations or anions can be replaced to increase or decrease their hydrophobicity depending on the desired application. As a result of the many features of ILs, they have become attractive for application in a number of techniques such as gas chromatography,[77], electrochemical studies[78], and even organic synthesis.[79]

Armstrong and coworkers [54, 80, 81] introduced the concept of using room temperature ionic liquids (RTILs) as MALDI matrices; they produce a more homogeneous sample, which allows for better shot-to-shot reproducibility.[76] A comparison of ionic liquid matrices (ILMs) with solid matrices in MALDI revealed that ILMs exhibit improved reproducibility, higher sensitivity, and lower detection limits.[54] Although, using ILs alone does not promote analyte ion formation, the performance of ILs in MALDI can be improved by synthesizing them from organic matrices such as 2,5-dihydroxy benzoic acid, or α-cyno-4-hydroxy benzoic acid.[54]

1.4.1 Synthesis of Ionic Liquids

The simplicity in the synthesis of ILs makes them potential candidates for the development of MALDI matrices in routine analysis. The synthesis of water immiscible ILs utilizes a metathesis or ion-exchange reaction. For example, 1-butyl-3-methylimidazolium hexafluorophosphate is prepared by a biphasic reaction of 1-butyl-3-methylimidazolium chloride and sodium hexafluorophosphate in the presence of water plus an organic solvent such as dichloromethane (DCM).[82] In this method, a biphasic reaction is used with an organic solvent such as dichloromethane (DCM) and water. Since both solvents are immiscible, the hydrophobic IL can be extracted into the organic phase while the salt by-product (NaCl in this case) remains in the water layer. The general reaction equation is represented in Figure 1.7.

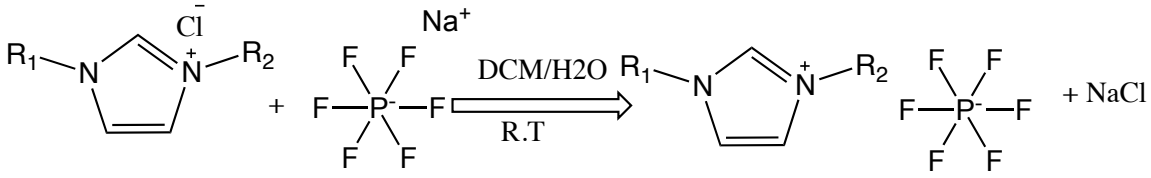

Figure 1.7. Synthesis of 1-alkyl-3-methylimidazolium hexaflurophosphate. R_1: alkyl and R_2: methyl.

Alternatively, ILs can been prepared via the acid-base reaction.[83] For example, ethyl ammonium nitrate was prepared by reacting ethylamine with nitric acid. Both reactants were dissolved in water at a temperature of 4°C. Upon reaction completion, water was removed by lyophilization(see Figure 1.8).

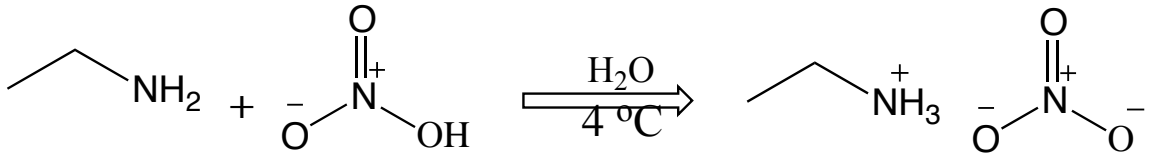

Figure 1.8. Reaction of ethyl ammonium nitrate.

Another example of an acid-base reaction is the synthesis of [Py][CHCA] using equimolar amounts of α-cyno-4-hydroxy benzoic acid (CHCA) and pyridine (Py). Both compounds were dissolved in methanol and mixed. When completed, methanol was removed at reduced pressure (see Figure 1.9).[80]

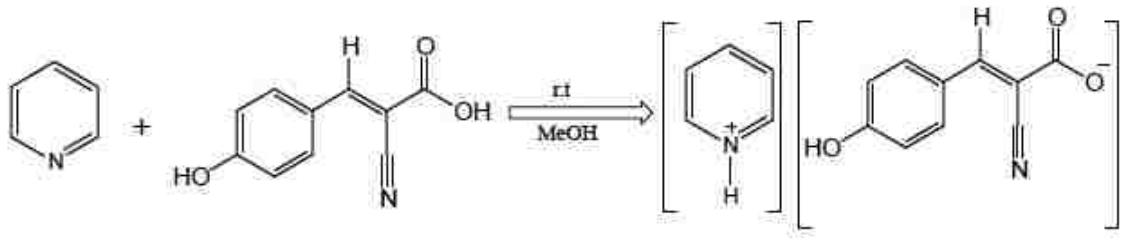

Figure 1.9. Reaction between pyridine and α-cyno-4-hydroxy benzoic acid in solvent MeOH.

1.4.2 Physical and Chemical Properties of Ionic Liquids

Based on their vast range of unique properties, ionic liquids (ILs) have been widely used in many fields.[84, 85] They exhibit low vapor pressure as a result of the strong interaction between the ions.[86] ILs have emerged as green solvents because of their ability to be recycled.[74] Moreover, they are conductive since they are composed of ions, which have high mobility in liquids or in aqueous solutions. The melting point of ILs can be tuned by changing the structure of the ions. As the length of alkyl chain increases, the magnitude of van der Waals forces also increases; thus, reducing the lattice energy and the melting point.[87] Another factor that affects the melting point of ionic liquids, compared with inorganic salts, is the size and symmetry of the bulky organic ions, which causes poor crystal packing.[88]

1.5 Group of Uniform Materials Based on Organic Salts (GUMBOS)

The development and applications of the group of uniform materials based on organic salts (GUMBOS) have been extensively reported.[89] These compounds are similar to ILs with the exception of higher melting points, from 25 to 250°C (see Figure 1.10). Since FILs also have a range of melting points from 25 to 100°C, there is an overlap between GUMBOS and FILs. The physical and chemical properties of GUMBOS are similar to FILs and they are synthesized in a similar manner. These similar properties include high conductivity, high thermal stability, low vapor pressure, and non-flammability and these properties can be tuned by varying the counter ions. For example, using cations that possess anticancer or fluorescent properties with an anion that possesses magnetic properties, multifunctional GUMBOS can be synthesized. Recently, GUMBOS have been used in various applications such as anticancer drug delivery, and

for light harvesting.[85, 90]

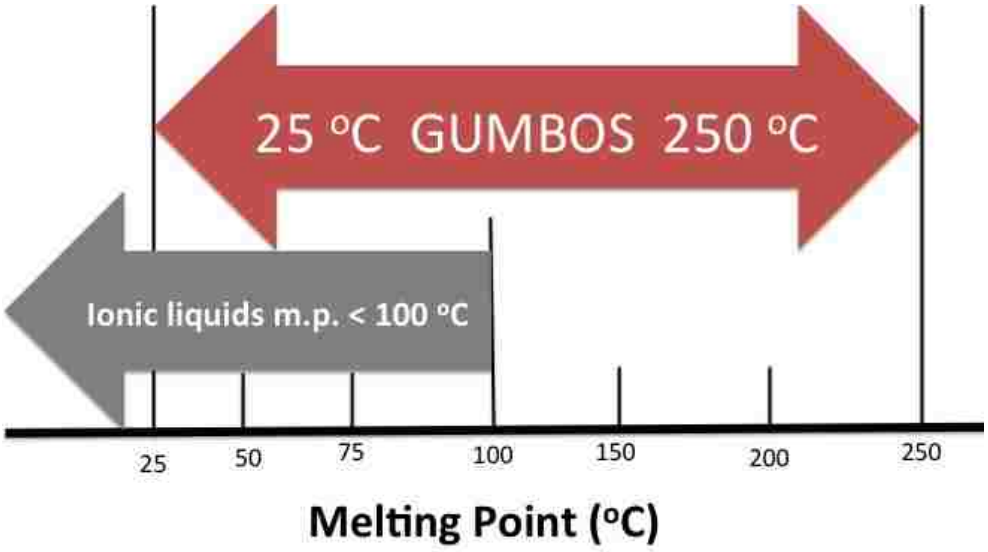

Figure 1.10. Temperature difference between GUMBOS and ionic liquids.

1.6 Tissue Imaging Using MALDI

As previously discussed, MALDI is a powerful technique that can be utilized for the analysis of complex biological samples such as cells and direct tissue analysis. This method eliminates the need for sample preparation except sectioning of the tissue and addition of the matrix making the approach is less time consuming as compared to other imaging techniques such as staining.[91] Caprioli and coworkers [92] introduced MALDI imaging. This method has been used to detect intact proteins, drugs, and metabolites directly from tissue and have revealed reported successes in the study and identification of protein and lipids biomarkers in cancer cells and tissues.[93]

1.6.1 Tissue Preparation

Tissue samples can be isolated from any part of an animal, such as the brain or the liver. First, the proteins and peptides must be protected from degradation. To accomplish this, the sample is wrapped in aluminum foil then frozen in liquid nitrogen, which helps to preserve the shape and greatly slow down biological degradation.[94] In a recent study, a sample of brain tissue was frozen at -80°C within 30 min of surgical resection and stored in a sample container.[95]

For sample analysis by MALDI imaging mass spectrometry, frozen tissue sections are cut by a cryostat to a thickness of 5 to 15 μm.[96] Optimization of the thickness of the tissue is important and this can be easily controlled and manipulated. Thin tissue is prone to tearing. Depending on the analyte of interest, specific size of tissue can be used. If the analyte is a protein and the size of the protein is between 3 to 20 kDa, a tissue 5 – 15 μm thick can be cut.[97] Frozen tissues are mounted on the cryostat head with the use of an embedding medium such as agar or a polymer (OCT). The cut sample is typically maintained around -25°C with the temperature dependent on the kind of tissue. The blade used to cut the tissue is rinsed with methanol and acetone to prevent contamination.[2, 98] Tissue samples are mounted on microscope slide that is coated with a thin (approximately 130 Å) conductive film of indium tin oxide (ITO). A schematic of tissue analysis is shown in Figure 1.11. After this, the tissue is kept in a dessicator for 15 min and the matrix is applied on the tissue sample. The raster moves across the entire surface of the tissue that has been covered with matrix. The use of software allows the visualization of the spatial distribution using different colors for each *m/z* distributions and the intensity of an ion across the tissue surface.[2, 99, 100]

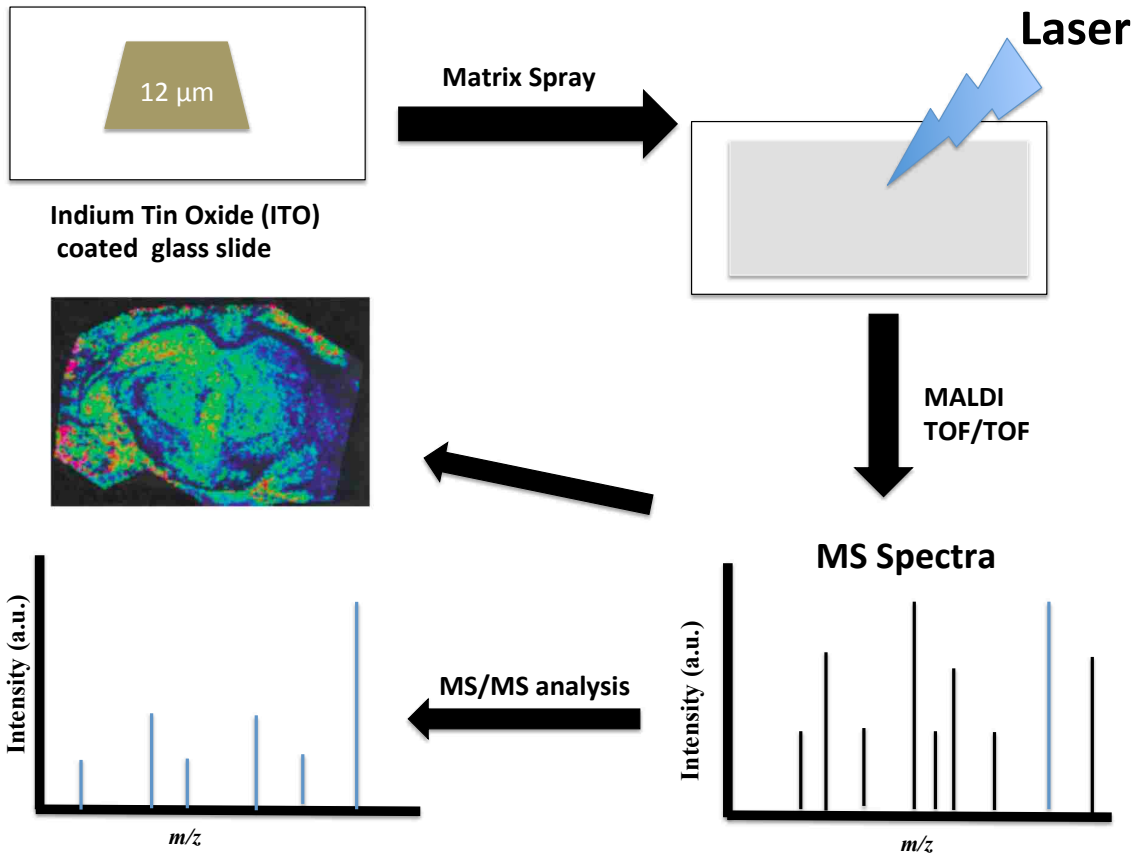

Figure 1.11. Schematic diagrams showing the stages involved in the direct tissue imaging by MALDI IMS.

1.6.2 Matrix Selection and Application

After mounting the tissue sample on the ITO coated glass plate, the matrix is applied. Imaging mass spectrometry (IMS) requires a homogenous matrix for optimal interaction with the tissue surface. Typically, it is important that the matrix is able to absorb laser energy and cause the analyte to desorb from the sample surface and ionize. There are many suitable matrices for tissue analysis depending on the analyte. For example, 3,5-dimethoxy-4-hydroxy-cinnamic acid (SA) is used to detect proteins, while 2,5-dihydodroxybenzoic acid (DHB) is used to detect lipids and proteins. Additionally, α-

cyano-4-hydroxycinnamic acid (CHCA) is used to detect peptides or proteins.[96] Common solvents used to dissolve matrices are 50:50 acetonitrile or ethanol and water mixture.[91] Ethanol is recommended for tissues applications because it prevents the matrix from spreading.[91, 96]

Several methods are utilized to deposit the matrix on tissues for MALDI imaging in order to obtain better homogeneity and resolution. Typically, the matrix is deposited across the tissue section to avoid analyte migration. This is important for imaging tissue sample to study the distribution of the analyte (such as lipids, peptides and proteins) in tissue. A popular method for depositing the matrix is robotic spotting, which involves spotting along the XY direction of the matrix to apply uniform crystals on tissue. Though it has been shown to produce high signal-to-noise ratios and reproducible results, the imaging resolution is limited by the size and spacing of the matrix spots.[101] Similarly, spray coating, which is another method utilized for depositing the matrix on tissue, has the disadvantage of causing analyte delocalization if the tissue becomes too wet. Spray coating does however, allow for the highest spatial resolution, as densely spotted arrays show higher reproducibility and generally better spectra quality.[95] In the dry coating method, the matrix (such as CHCA or DHB) is ground to small particles. Then the matrix is filtered through a 20 μm pore size sieve. In the main, this method allows for good reproducibility and high resolution, however, it forms large crystals.[101, 102] Another method that has been used is spray or electrospray.[103] Noteworthy is the sublimation method which converts the solid matrix directly to gas without forming a liquid phase. This method has been reported to minimize the lateral movement of tissue lipids by MALDI imaging and does not require the use of solvents to dissolve the lipids as does

electrospray or airbrush.[103]

1.7 Additional Analytical Techniques

1.7.1 Ultraviolet-Visible Spectroscopy

Ultraviolet-visible spectroscopy (UV-vis) is a technique that is used to analyze molecules that absorb light in the ultraviolet and visible region of the electromagnetic spectrum. UV-vis measures the amount of energy absorbed by the molecules when exposed to light (see Figure 1.12).

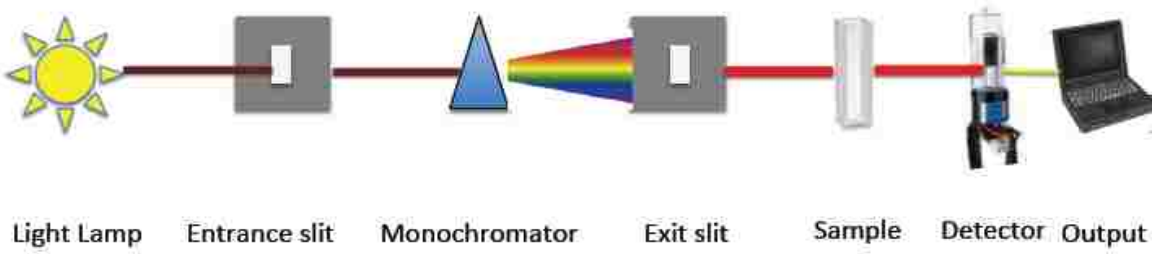

Figure 1.12. Schematic diagram of UV-vis spectrometry.

After light passes through a monochromator, which selects the desired wavelength, the sample absorbs some of the light. Using the Beer Lambert law, the concentration of a sample can be related to the amount of light absorbed using the equation:

$$A = \text{Log}\left(\frac{I_o}{I}\right) = \varepsilon C b \,, \qquad (6)$$

where A is absorbance, I_o is the intensity of the incident light, I is the transmitted intensity, ε is the molar absorptivity, C is the concentration of sample and b is the absorption path length. The sample can be exposed to light of a range of wavelength and a spectrum of the absorbance versus wavelength can be generated. Unknown

concentrations of samples can be obtained from a calibration curve generated using a range of concentrations of standard.

In this work, octanol/water partition coefficients were determined by UV-vis to evaluate the hydrophobicity of matrices.[104] A solution of 1-octanol with water was shaken for 24 hours before use in order to pre-saturate the octanol with the minimal volume of water that is soluble within it. The 1-octanol and water were then separated; and, known equal volumes of pre-saturated 1-octanol and water were mixed with equal concentrations of each matrix and stirred for 24 hours.[104] UV-vis detection was used to analyze the upper (1-octanol) phase and water phase. Calibration curves for the matrices were made using increasing concentrations of each matrix and measuring the respective absorption. Using the calibration curve, the concentration of the matrix in each phase was determined.[85] Hence, the partition coefficient can be calculated by using the following equation:

$$K_{o/w} = \frac{[X]_{o,e}}{[X]_{w,e}} \qquad (7)$$

where $K_{o/w}$ represents the octanol/water partition coefficient, $[X]_{o,e}$ represent the concentration of matrix in octanol at equilibrium and $[X]_{w,e}$ represent the concentration of matrix in water at equilibrium.

1.7.2 Fluorescence Spectroscopy

Fluorescence spectroscopy is a sensitive analytical technique that determines the amount of analyte present in a sample by monitoring the amount of photons emitted when an atom or molecule relaxes to the electronic ground state (S_0), from an excited electronic state (S_1). Briefly, fluorophores are irradiated with light and are promoted to excited

electronic states (S_n). After molecules reach the excited state, they return to the ground state causing emission. However, if excited molecules transfer to the triplet state by intersystem crossing, the emission from the triplet state is called phosphorescence. A typical Jablonski energy level diagram is shown in Figure 1.13. Since most biological molecules being analyzed are non-fluorescent, they are labelled with fluorescent dyes to aid in their detection.

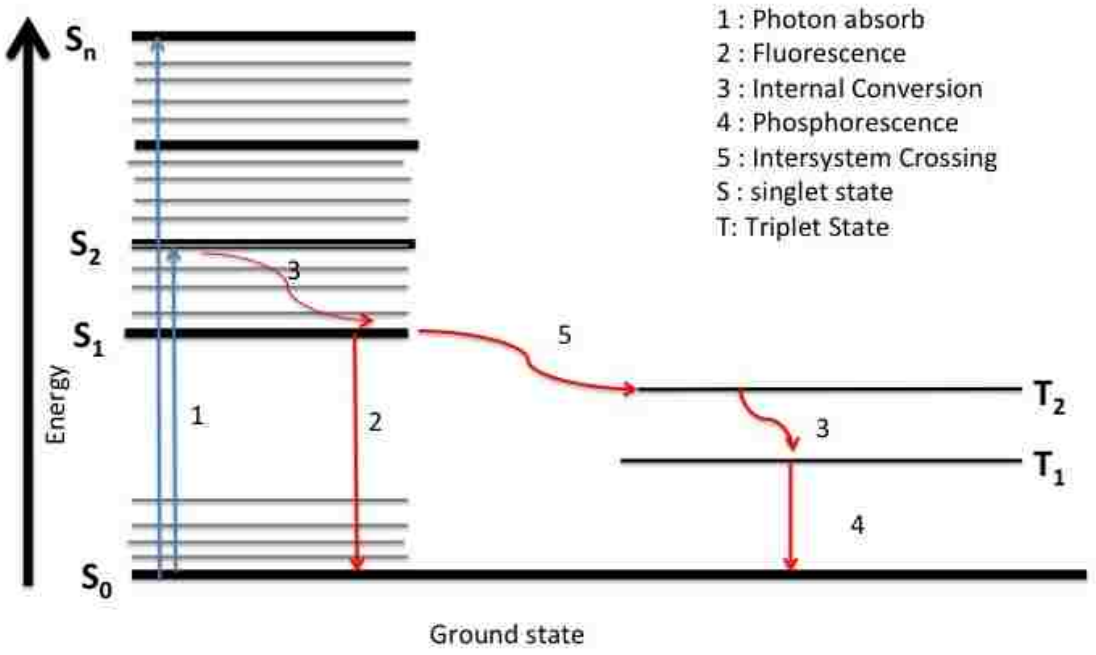

Figure 1.13. The Jablonski diagram.

1.7.2.1 Intrinsic Protein Fluorescence

There are three aromatic amino acids; phenylalanine (phe), tyrosine (tyr), and tryptophan (try) (see Figure 1.14). These compounds display intrinsic fluorescence with the highest fluorescence seen from tryptophan with light absorbance light at wavelengths

between 295-305 nm.[105] A protein's intrinsic fluorescence is used to help in understanding the changes in the protein such as protein interaction or ligand binding.

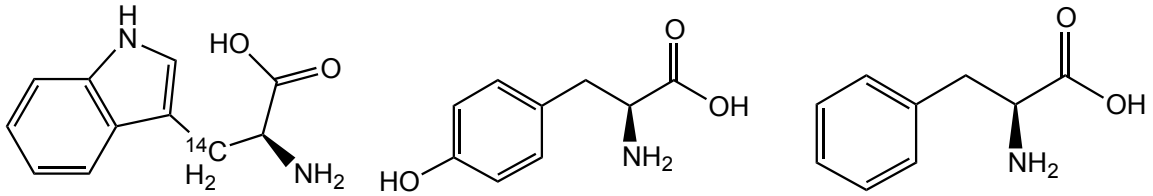

A B C

Figure 1.14. Intrinsic protein fluorescence A) tryptophan B) tyrosine C) phenylalanine.

1.7.2.2 Binding Isotherm Models

There are four characteristic regions of a binding isotherm that are displayed as the concentration of ionic liquids or surfactant and analyte increases (see Figure 1.15). The initial region, (A), is called specific binding and it occurs at low concentrations at high-energy sites on the analyte. The next region, (B), starts rising on a plateau of isotherm. In region (C), there is a massive increase in binding due to cooperative interactions. The last region, (D), may result from saturation suggesting that there is no further binding between ionic liquids/surfactant and analyte.[106]

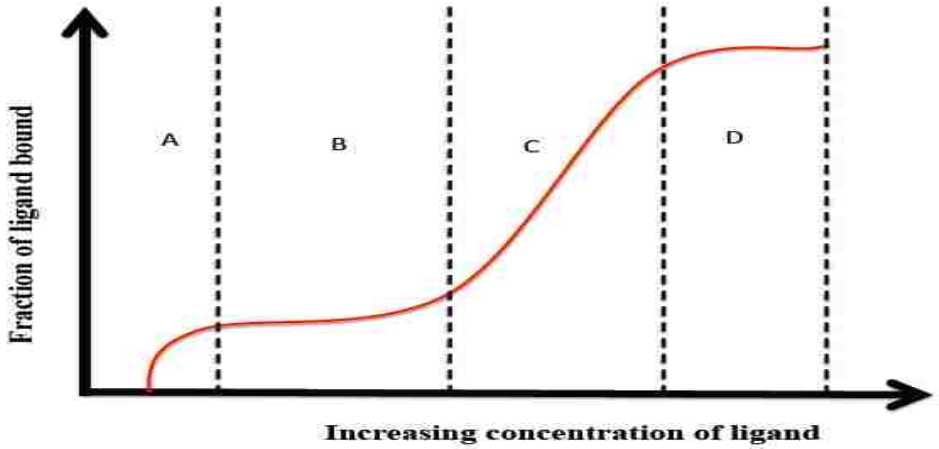

Figure 1.15. Schematic plot of a binding isotherm.

1.7.3 Fluorescence Anisotropy

Fluorescence anisotropy (r) is studied in a steady state by measuring and monitoring the binding of small molecules with peptides or proteins. This tool/phenomenon is also used to study conformational changes of proteins and provides information about the size and shape of protein. In this method, the molecule absorbs photons whose electric vectors are parallel to the transition moment of the fluorophores. After the molecules are excited in vertical polarized light, the electrical vector of excitation light will be oriented parallel to the vertical with the intensity of the emitted light, which is then measured through a polarizer.[107] The anisotropy is calculated based on the equation:

$$r = \frac{I_{vv} - GI_{vh}}{I_{vv} + 2GI_{vh}} \quad , \qquad (8)$$

where r is the anisotropy, I_{vv}, represent the vertically polarized excitation and the vertically polarized emission, I_{vh} is the vertically polarized excitation and the horizontally polarized emission and G is the grating factor for instrument responses

1.8 Scope of the Dissertation

The overall objective of this work is to develop new matrices for MALDI with a good signal-to-noise intensity and spatial resolution in the detection of hydrophobic molecules. This dissertation is composed of three parts. In the first part, the organic matrix, aminopyrene (AP), and a series of AP-based GUMBOS, were used to vary the hydrophobicity of the MALDI matrix to detect various hydrophobic and hydrophilic peptides in comparison to a traditional matrix such as (CHCA). In the second part, studies the interaction between matrices and both hydrophobic and hydrophilic peptides are described. Scatchard plots and fluorescence anisotropy were used to analyze the binding between hydrophobic and hydrophilic matrices with hydrophobic and hydrophilic peptides. In the concluding part, a hydrophobic CHCA matrix is tuned by changing cation to add the counter ion oleylamine (OA) is described. [OA][CHCA] hydrophobic matrix, possesses a long hydrocarbon chain, and is used for the detection of hydrophobic proteins and lipids directly from tissue. The hydrophobic GUMBOS matrix was used for MALDI imaging mass spectrometry of rat tissue to study the distribution of lipids in tissue.

1.9 References

[1] K. Dreisewerd. Recent methodological advances in MALDI mass spectrometry. *Anal. Bioanal. Chem.* **2014**, *406*, 2261.

[2] S. Nimesh, S. Mohottalage, R. Vincent, P. Kumarathasan. Current status and future perspectives of mass spectrometry imaging. *Int. J. Mol. Sci.* **2013**, *14*, 11277.

[3] J. Bunch, M. R. Clench, D. S. Richards. Determination of pharmaceutical compounds in skin by imaging matrix-assisted laser desorption/ionisation mass spectrometry. *Rapid Commun. Mass Spectrom.* **2004**, *18*, 3051.

[4] A. Rompp, S. Guenther, Z. Takats, B. Spengler. Mass spectrometry imaging with high resolution in mass and space (HR2 MSI) for reliable investigation of drug compound distributions on the cellular level. *Anal. Bioanal. Chem.* **2011**, *401*, 65.

[5] R. B. Chen, X. Y. Jiang, M. C. P. Conaway, I. Mohtashemi, L. M. Hui, R. Viner, L. J. Li. Mass spectral analysis of neuropeptide expression and distribution in the nervous system of the lobster homarus americanus. *J. Proteome. Res.* **2010**, *9*, 818.

[6] M. Stoeckli, D. Staab, M. Staufenbiel, K. H. Wiederhold, L. Signor. Molecular imaging of amyloid beta peptides in mouse brain sections using mass spectrometry. *Anal. Biochem.* **2002**, *311*, 33.

[7] K. Schwamborn, R. M. Caprioli. MALDI imaging mass spectrometry - painting molecular pictures. *Mol. Oncol.* **2010**, *4*, 529.

[8] S. Steurer, C. Borkowski, S. Odinga, M. Buchholz, C. Koop, H. Huland, M. Becker, M. Witt, D. Trede, M. Omidi, O. Kraus, A. S. Bahar, A. S. Seddiqi, J. M. Singer, M. Kwiatkowski, M. Trusch, R. Simon, M. Wurlitzer, S. Minner, T. Schlomm, G. Sauter, H. Schluter. MALDI mass spectrometric imaging based identification of clinically relevant signals in prostate cancer using large-scale tissue microarrays. *Int. J. Cancer.* **2013**, *133*, 920.

[9] K. Chughtai, R. M. A. Heeren. Mass spectrometric imaging for biomedical tissue analysis. *Chem. Rev.* **2010**, *110*, 3237.

[10] L. A. McDonnell, R. M. A. Heeren. Imaging mass spectrometry. *Mass Spectrom. Rev.* **2007**, *26*, 606.

[11] J. B. Fenn, M. Mann, C. K. Meng, S. F. Wong, C. M. Whitehouse. Electrospray ionization for mass spectrometry of large biomolecules. *Science.* **1989**, *246*, 64.

[12] M. Karas, F. Hillenkamp. Laser desorption ionization of proteins with molecular masses exceeding 10,000 daltons. *Anal. Chem.* **1988**, *60*, 2299.

[13] K. K. Murray, R. K. Boyd, M. N. Eberlin, G. J. Langley, L. Li, Y. Naito. Definitions of terms relating to mass spectrometry (IUPAC recommendations 2013). *Pure Appl. Chem.* **2013**, *85*, 1515.

[14] Das, C. *Fundamentals of Contemporary Mass Spectrometry*. Wiley & Sons Inc., New Jersey, **2007**.

[15] D. A. Lake, M. V. Johnson, C. N. McEwen, B. S. Larsen. Sample preparation for high throughput accurate mass analysis by matrix-assisted laser

desorption/ionization time-of-flight mass spectrometry. *Rapid Commun. Mass Spectrom.* **2000**, *14*, 1008.

[16] P. Kovarik, C. Grivet, E. Bourgogne, G. Hopfgartner. Method development aspects for the quantitation of pharmaceutical compounds in human plasma with a matrix-assisted laser desorption/ionization source in the multiple reaction monitoring mode. *Rapid Commun. Mass Spectrom.* **2007**, *21*, 911.

[17] B. Fuchs. Analysis of phospolipids and glycolipids by thin-layer chromatography-matrix-assisted laser desorption and ionization mass spectrometry. *J. Chromatogr. A.* **2012**, *1259*, 62.

[18] L. H. Cohen, A. I. Gusev. Small molecule analysis by MALDI mass spectrometry. *Anal. Bioanal. Chem.* **2002**, *373*, 571.

[19] A. Svatos. Mass spectrometric imaging of small molecules. *Trends Biotechnol.* **2010**, *28*, 425.

[20] I. Garaguso, R. Halter, J. Krzeminski, S. Amin, J. Borlak. Method for the rapid detection and molecular characterization of DNA alkylating agents by MALDI-TOF mass spectrometry. *Anal. Chem.* **2010**, *82*, 8573.

[21] H. L. Wang, Y. J. Hu, D. Xing. Recent progress of two-step laser desorption/laser ionization mass spectrometry and Its application. *Chinese J. Anal. Chem.* **2011**, *39*, 276.

[22] H. Franz., P.-K. Jasa, *MALDI MS A Practical Guide to Instrumentation, Methods, and Applications*, Second Edition ed., Wiley-VCH Verlag GmbH & Co. KGaA, Germany, **2014**.

[23] T. W. Jaskolla, M. Karas. Compelling evidence for lucky survivor and gas phase protonation: The unified MALDI analyte protonation mechanism. *J. Am. Soc. Mass Spectrom.* **2011**, *22*, 976.

[24] S. Trimpin, M. L. Deinzer. Solvent-free MALDI-MS for the analysis of a membrane protein via the mini ball mill approach: Case study of bacteriorhodopsin. *Anal. Chem.* **2007**, *79*, 71.

[25] Cameron, A.E. and Eggers, D.F. An ion elecitron. *Rev. Cci. Instrum.* **1945**, *19*, 1150.

[26] W. C. Wiley, I. H. McLaren. Time-of-flight mass spectrometer with improved resolution. *Rev. Sci. Instrum.* **1955**, *26*, 1150.

[27] R. B. Opsal, K. G. Owens, J. P. Reilly. Resolution in the linear time-of-flight mass spectrometer. *Anal. Chem.* **1985**, *57*, 1884.

[28] Hoffman, E.D., Stroobant,V. *Mass Spectrometry*. Third ed, Wiley & Sons Ltd., West Sussex, England, **2007**.

[29] M. Guilhaus. Principles and instrumentation in time-of-flight mass spectrometry-physical and instrumental concepts. *J. Mass Spectrom.* **1995**, *30*, 1519.

[30] Cotter, R. J. *Time-of-Flight Mass Spectrometry*: *Instrumentation and Applications in Biological Research*. American Chemical Society, Washington D.C., **1997**.

[31] R. J. Cotter. The new time-of-flight mass spectrometry. *Anal. Chem.* **1999**, *71*, 445A.

[32] B. A. Mamyrin. Laser assisted reflectron time-of-flight mass spectrometry. *Int. J. Mass Spectrom. Ion Processes.* **1994**, *131*, 1.

[33] O. Vorm, P. Roepstorff, M. Mann. Improved resolution and very high-sensitivity in MALDI TOF of matrix surfaces made by fast evaporation. *Anal. Chem.* **1994**, *66*, 3281.

[34] U. Bahr, M. Karas, F. Hillenkamp. Analysis of biopolymers by matrix-assisted laser-desorption ionization maldi mass-spectrometry. *Fresenius J. Anal. Chem.* **1994**, *348*, 783.

[35] F. Hillenkamp, M. Karas, R. C. Beavis, B. T. Chait. Matrix-assisted laser desorption ionization mass-spectrometry of biopolymers. *Anal. Chem.* **1991**, *63*, A1193.

[36] C. Weickhardt, F. Moritz, J. Grotemeyer. Time-of-flight mass spectrometry: State-of-the-art in chemical analysis and molecular science. *Mass Spectrom. Rev.* **1996**, *15*, 139.

[37] R. M. Whittal, L. M. Russon, S. R. Weinberger, L. Li. Functional wave time-lag focusing matrix-assisted laser desorption ionization in a linear time-of flight mass spectrometer: Improved mass accuracy. *Anal. Chem.* **1997**, *69*, 2147.

[38] M. L. Vestal. Modern MALDI time-of-flight mass spectrometry. *J. Mass Spectrom.* **2009**, *44*, 303.

[39] R. Knochenmuss. MALDI ionization mechanisms: the coupled photophysical and chemical dynamics model correctly predicts 'temperature'-selected spectra. *J. Mass Spectrom.* **2013**, *48*, 998.

[40] R. Knochenmuss, R. Zenobi. MALDI ionization: the role of in-plume processes. *Chem. Rev.* **2003**, *103*, 441.

[41] R. Zenobi, R. Knochenmuss. Ion formation in MALDI mass spectrometry. *Mass Spectrom. Rev.* **1998**, *17*, 337.

[42] R. Knochenmuss, F. Dubois, M. J. Dale, R. Zenobi. The matrix suppression effect and ionization mechanisms in matrix-assisted laser desorption/ionization. *Rapid Commun. Mass Spectrom.* **1996**, *10*, 871.

[43] M. Karas, M. Gluckmann, J. Schafer. Ionization in matrix-assisted laser desorption/ionization: singly charged molecular ions are the lucky survivors. *J. Mass Spectrom.* **2000**, *35*, 1.

[44] E. J. Zaluzec, D. A. Gage, J. T. Watson. Matrix-assisted laser desorption ionization mass spectrometry: applications in peptide and protein characterization. *Protein Express Purif.* **1995**, *6*, 109.

[45] D. J. Harvey. Matrix-assisted laser desorption ionisation mass spectrometry of oligosaccharides and glycoconjugates. *J. Chromatogr. A.* **1996**, *720*, 429.

[46] J. M. Hettick, D. L. McCurdy, D. C. Barbacci, D. H. Russell. Optimization of sample preparation for peptide sequencing by MALDI-TOF photofragment mass spectrometry. *Anal. Chem.* **2001**, *73*, 5378.

[47] M. Kussmann, E. Nordhoff, H. RahbekNielsen, S. Haebel, M. RosselLarsen, L. Jakobsen, J. Gobom, E. Mirgorodskaya, A. KrollKristensen, L. Palm, P. Roepstorff. Matrix-assisted laser desorption/ionization mass spectrometry sample preparation techniques designed for various peptide and protein analytes. *J. Mass Spectrom.* **1997**, *32*, 593.

[48] J. Axelsson, A. M. Hoberg, C. Waterson, P. Myatt, G. L. Shield, J. Varney, D. M. Haddleton, P. J. Derrick. Improved reproducibility and increased signal intensity in matrix-assisted laser desorption/ionization as a result of electrospray sample preparation. *Rapid Commun. Mass Spectrom.* **1997**, *11*, 209.

[49] H. Wei, K. Nolkrantz, D. H. Powell, J. H. Woods, M. C. Ko, R. T. Kennedy. Electrospray sample deposition for matrix-assisted laser desorption/ionization (MALDI) and atmospheric pressure MALDI mass spectrometry with attomole detection limits. *Rapid Commun. Mass Spectrom.* **2004**, *18*, 1193.

[50] X. J. Chen, J. A. Carroll, R. C. Beavis. Near-ultraviolet-induced matrix-assisted laser desorption/ionization as a function of wavelength. *J. Am. Soc. Mass Spectrom.* **1998**, *9*, 885.

[51] A. Tholey, E. Heinzle. Ionic (liquid) matrices for matrix-assisted laser desorption/ionization mass spectrometry-applications and perspectives. *Anal. Bioanal. Chem.* **2006**, *386*, 24.

[52] K. Dreisewerd. Recent methodological advances in MALDI mass spectrometry. *Anal. Bioanal. Chem.* **2014**, *406*, 2261.

[53] V. Horneffer, K. Dreisewerd, H. C. Ludemann, F. Hillenkamp, M. Lage, K. Strupat. Is the incorporation of analytes into matrix crystals a prerequisite for

matrix-assisted laser desorption/ionization mass spectrometry? A study of five positional isomers of dihydroxybenzoic acid. *Int. J. Mass Spectrom.* **1999**, *185*, 859.

[54] D. W. Armstrong, L. K. Zhang, L. F. He, M. L. Gross. Ionic liquids as matrixes for matrix-assisted laser desorption/ionization mass spectrometry. *Anal. Chem.* **2001**, *73*, 3679.

[55] R. Tummala, K. B. Green-Church, P. A. Limbach. Interactions between sodium dodecyl sulfate micelles and peptides during matrix-assisted laser desorption/ionization mass spectrometry (MALDI-MS) of proteolytic digests. *J. Am. Soc. Mass Spectrom.* **2005**, *16*, 1438.

[56] A. Berthod, J. A. Crank, K. L. Rundlett, D. W. Armstrong. A second-generation ionic liquid matrix-assisted laser desorption/ionization matrix for effective mass spectrometric analysis of biodegradable polymers. *Rapid Commun. Mass Spectrom.* **2009**, *23*, 3409.

[57] E. Szajli, T. Feher, K. F. Medzihradszky. Investigating the quantitative nature of MALDI-TOF MS. *Mol. Cell Proteomics.* **2008**, *7*, 2410.

[58] W. R. Wilkinson, A. I. Gusev, A. Proctor, M. Houalla, D. M. Hercules. Selection of internal standards for quantitative analysis by matrix assisted laser desorption ionization (MALDI) time-of-flight mass spectrometry. *Fresenius J. Anal. Chem.* **1997**, *357*, 241.

[59] K. Minakata, H. Nozawa, I. Yamagishi, K. Hasegawa, A. Wurita, K. Gonmori, M. Suzuki, K. Watanabe, O. Suzuki. MALDI-TOF mass spectrometric determination of four amphetamines in blood. *Forensic Toxicology.* **2014**, *32*, 299.

[60] R. C. Beavis, T. Chaudhary, B. T. Chait. Alpha-cyano-4hydroxycinnamic acid as a matrix for matrix- assisted laser desorption mass-spectrometry. *Org. Mass Spectrom.* **1992**, *27*, 156.

[61] E. Szajli, T. Feher, K. F. Medzihradszky. Investigating the quantitative nature of MALDI-TOF MS. *Mol. Cell Proteomics.* **2008**, *7*, 2410.

[62] L. M. Preston, K. K. Murray, D. H. Russell. Reproducibility and quantitation of matrix-assisted laser desorption ionization mass spectrometry: effects of nitrocellulose on peptide ion yields. *Biol. Mass Spectrom.* **1993**, *22*, 544.

[63] J. H. Yang, R. M. Caprioli. Matrix precoated targets for direct lipid analysis and imaging of tissue. *Anal. Chem.* **2013**, *85*, 2907.

[64] K. Tang, N. I. Taranenko, S. L. Allman, C. H. Chen, L. Y. Chang, K. B. Jacobson. Picolinic acid as a matrix for laser mass spectrometry of nucleic acids and proteins. *Rapid Commun. Mass Spectrom.* **1994**, *8*, 673.

[65] D. S. Peterson. Matrix-free methods for laser desorption/ionization mass spectrometry. *Mass Spectrom. Rev.* **2007**, *26*, 19.

[66] T. Kinumi, T. Saisu, M. Takayama, H. Niwa. Matrix-assisted laser desorption/ionization time-of-flight mass spectrometry using an inorganic particle matrix for small molecule analysis. *J. Mass Spectrom.* **2000**, *35*, 417.

[67] C. S. Pan, S. Y. Xu, H. J. Zhou, Y. Fu, M. L. Ye, H. F. Zou. Recent developments in methods and technology for analysis of biological samples by MALDI-TOF-MS. *Anal. Bioanal. Chem.* **2007**, *387*, 193.

[68] M. F. Wyatt, S. J. Ding, B. K. Stein, A. G. Brenton, R. H. Daniels. Analysis of various organic and organometallic compounds using nanostructure-assisted laser desorption/ionization time-of-flight mass spectrometry (NALDI-TOFMS). *J. Am. Soc. Mass Spectrom.* **2010**, *21*, 1256.

[69] N. Shenar, J. Martinez, C. Enjalbal. Laser desorption/ionization mass spectrometry on porous silica and alumina for peptide mass fingerprinting. *J. Am. Soc. Mass Spectrom.* **2008**, *19*, 632.

[70] P. Zollner, E. R. Schmid, G. Allmaier. K-4 Fe(CN)(6) /glycerol - A new liquid matrix system for matrix-assisted laser desorption/ionization mass spectrometry of hydrophobic compounds. *Rapid Commun. Mass Spectrom.* **1996**, *10*, 1278.

[71] R. Cramer, S. Corless. Liquid ultraviolet matrix-assisted laser desorption/ionization mass spectrometry for automated proteomic analysis. *Proteomics.* **2005**, *5*, 360.

[72] K. Turney, W. W. Harrison. Liquid supports for ultraviolet atmospheric pressure matrix-assisted laser desorption/ionization. *Rapid Commun. Mass Spectrom.* **2004**, *18*, 629.

[73] R. Cramer, A. L. Burlingame. Employing target modifications for the investigation of liquid infrared matrix-assisted laser desorption/ionization mass spectrometry. *Rapid Commun. Mass Spectrom.* **2000**, *14*, 53.

[74] J. S. Wilkes. A short history of ionic liquids - from molten salts to neoteric solvents. *Green Chem.* **2002**, *4*, 73.

[75] B. Clare, A. Sirwardana, D. R. Macfarlane. Synthesis, purification and characterization of ionic liquids. *Top. Curr. Chem.* **2010**, *290*.

[76] J. L. Anderson, D. W. Armstrong, G. T. Wei. Ionic liquids in analytical chemistry. *Anal. Chem.* **2006**, *78*, 2892.

[77] D. W. Armstrong, L. F. He, Y. S. Liu. Examination of ionic liquids and their interaction with molecules, when used as stationary phases in gas chromatography. *Anal. Chem.* **1999**, *71*, 3873.

[78] E. Dickinson, M. E. Williams, S. M. Hendrickson, H. Masui, R. W. Murray. Hybrid redox polyether melts based on polyether-tailed counterions. *J. Am. Chem. Soc.* **1999**, *121*, 613.

[79] J. S. Wilkes, M. J. Zaworotko. Air and water stable I-ehyl-3-methylimidazolium based ionic liquids. *J. Chem. Soc. Chem. Comm.* **1992**, 965.

[80] S. Carda-Broch, A. Berthod, D. W. Armstrong. Ionic matrices for matrix-assisted laser desorption/ionization time-of-flight detection of DNA oligomers. *Rapid Commun. Mass Spectrom.* **2003**, *17*, 553.

[81] J. A. Crank, D. W. Armstrong. Towards a second generation of ionic liquid matrices (ILMs) for MALDI-MS of peptides, proteins, and carbohydrates. *J. Am. Soc. Mass Spectrom.* **2009**, *20*, 1790.

[82] H. Kasai, H. S. Nalwa, H. Oikawa, S. Okada, H. Matsuda, N. Minami, A. Kakuta, K. Ono, A. Mukoh, H. Nakanishi. A novel preparation method of organic microcrystals. *Jpn. J. Appl. Phys.* **1992**, *31*, L1132.

[83] Walden, P. *Bull.* Molecular weights and electrical conductivity of several fused salts. *Acad. Imper. Sci. (St. Petersburg).* **1914,** *(1800)*, 405-422.

[84] H. Al Ghafly, N. Siraj, S. Das, B. P. Regmi, P. K. S. Magut, W. I. S. Galpothdeniya, K. K. Murray, I. M. Warner. GUMBOS matrices of variable hydrophobicity for matrix-assisted laser desorption/ionization mass spectrometry. *Rapid Commun. Mass Spectrom.* **2014**, *28*, 2307.

[85] P. K. S. Magut, S. Das, V. E. Fernand, J. Losso, K. McDonough, B. M. Naylor, S. Aggarwal, I. M. Warner. Tunable cytotoxicity of rhodamine 6G via anion variations. *J. Am. Chem. Soc.* **2013**, *135*, 15873.

[86] M. Vranes, S. Papovic, A. Tot, N. Zec, S. Gadzuric. Density, excess properties, electrical conductivity and viscosity of 1-butyl-3-methylimidazolium bis(trifluoromethylsulfonyl)imide plus gamma-butyrolactone binary mixtures. *J. Chem. Thermodyn.* **2014**, *76*, 161.

[87] C. P. Fredlake, J. M. Crosthwaite, D. G. Hert, S. Aki, J. F. Brennecke. Thermophysical properties of imidazolium-based ionic liquids. *J. Chem. Eng. Data.* **2004**, *49*, 954.

[88] M. G. Del Popolo, G. A. Voth. On the structure and dynamics of ionic liquids. *J. Phys. Chem. B.* **2004**, *108*, 1744.

[89] I. M. Warner, B. El-Zahab, N. Siraj. Perspectives on moving ionic liquid chemistry into the solid phase. *Anal. Chem.* **2014**, *86*, 7184.

[90] A. N. Jordan, S. Das, N. Siraj, S. L. de Rooy, M. Li, B. El-Zahab, L. Chandler, G. A. Baker, I. M. Warner. Anion-controlled morphologies and spectral features of

cyanine-based nanoGUMBOS - an improved photosensitizer. *Nanoscale.* **2012**, *4*, 5031.

[91] L. S. Eberlin, X. H. Liu, C. R. Ferreira, S. Santagata, N. Y. R. Agar, R. G. Cooks. Desorption electrospray ionization then MALDI mass spectrometry imaging of lipid and protein distributions in single tissue sections. *Anal. Chem.* **2011**, *83*, 8366.

[92] R. M. Caprioli, T. B. Farmer, J. Gile. Molecular imaging of biological samples: Localization of peptides and proteins using MALDI-TOF MS. *Anal. Chem.* **1997**, *69*, 4751.

[93] L. H. Cazares, D. A. Troyer, B. H. Wang, R. R. Drake, O. J. Semmes. MALDI tissue imaging: from biomarker discovery to clinical applications. *Anal. Bioanal. Chem.* **2011**, *401*, 17.

[94] R. J. A. Goodwin, A. M. Lang, H. Allingham, M. Boren, A. R. Pitt. Stopping the clock on proteomic degradation by heat treatment at the point of tissue excision. *Proteomics.* **2010**, *10*, 1751.

[95] W. P. Mounfield, T. J. Garrett. Automated MALDI matrix coating system for multiple tissue samples for imaging mass spectrometry. *J. Am. Soc. Mass Spectrom.* **2012**, *23*, 563.

[96] S. A. Schwartz, M. L. Reyzer, R. M. Caprioli. Direct tissue analysis using matrix-assisted laser desorption/ionization mass spectrometry: practical aspects of sample preparation. *J. Mass Spectrom.* **2003**, *38*, 699.

[97] R. J. A. Goodwin, S. R. Pennington, A. R. Pitt. Protein and peptides in pictures: Imaging with MALDI mass spectrometry. *Proteomics.* **2008**, *8*, 3785.

[98] R. L. Caldwell, R. M. Caprioli. Tissue profiling by mass spectrometry - A review of methodology and applications. *Mol. Cell Proteomics.* **2005**, *4*, 394.

[99] L. Li, J. J. Han, Z. P. Wang, J. A. Liu, J. C. Wei, S. X. Xiong, Z. W. Zhao. Mass spectrometry methodology in lipid analysis. *Int. J. Mol. Sci.* **2014**, *15*, 10492.

[100] A. Zavalin, J. Yang, K. Hayden, M. Vestal, R. M. Caprioli. Tissue protein imaging at 1 μm laser spot diameter for high spatial resolution and high imaging speed using transmission geometry MALDI TOF MS. *Anal. Bioanal. Chem.* **2015**, *10.1007/s00216-015-8532-6*.

[101] S. M. Puolitaival, K. E. Burnum, D. S. Cornett, R. M. Caprioli. Solvent-free matrix dry-coating for MALDI imaging of phospholipids. *J. Am. Soc. Mass Spectrom.* **2008**, *19*, 882.

[102] T. J. Garrett, M. C. Prieto-Conaway, V. Kovtoun, H. Bui, N. Izgarian, G. Stafford, R. A. Yost. Imaging of small molecules in tissue sections with a new

intermediate-pressure MALDI linear ion trap mass spectrometer. *Int. J. Mass Spectrom.* **2007**, *260*, 166.

[103] J. A. Hankin, R. M. Barkley, R. C. Murphy. Sublimation as a method of matrix application for mass spectrometric imaging. *J. Am. Soci. Mass Spectrom.* **2007**, *18*, 1646.

[104] S. H. Lee, S. B. Lee. Octanol/water partition coefficients of ionic liquids. *J. Chem. Technol. Biotechnol.* **2009**, *84*, 202.

[105] S. I. Snovida, V. C. Chen, H. Perreault. Use of a 2,5-dihydroxybenzoic acid/aniline MALDI matrix for improved detection and on-target derivatization of glycans: A preliminary report. *Anal. Chem.* **2006**, *78*, 8561.

[106] N. J. Turro, X. G. Lei, K. P. Ananthapadmanabhan, M. Aronson. Spectroscopic probe analysis of protein-surfactant interactions: The BSA/SDS System. *Langmuir.* **1995**, *11*, 2525.

[107] Lakowicz, J. R. *Principle of Fluorescence Spectroscopy*. Third ed, Springer., Baltimore, Maryland, **2006**.

CHAPTER 2: GUMBOS MATRICES OF VARIABLE HYDROHOBICITY FOR MALDI MASS SPECTROMETRY *

2.1 Introduction

Matrix assisted laser desorption-ionization (MALDI) mass spectrometry (MS) is an important tool for rapid and sensitive analyses of biomolecules.[1] In MALDI analysis, the matrix is an essential component, and selection of a suitable matrix is critically important because the optimal performance of many matrices has been found to depend on the chemical characteristics of the analyte.[2-4] Therefore, there have been intense efforts towards development as well as evaluation of novel and effective matrices for MALDI-MS analyses of different analytes.[5-17] In general, MALDI matrices must possess specific properties that include, but are not limited to, strong absorption of laser radiation, ability to effectively disperse analytes, good miscibility with the solvent and analytes, efficient energy transfer to analyte for ionization and desorption, ability to serve as a good protonating and deprotonating agent, and also vacuum stability.[9]

The majority of MALDI matrices studied so far possess hydrophilic characteristics, which are particularly well suited for detection of hydrophilic biomolecules.[17, 18] However, detection of hydrophobic biomolecules remains an elusive limitation for MALDI analyses. This stems from the fact that hydrophilic matrices exhibit low affinities for hydrophobic biomolecules. It must be emphasized that a protein

*This chapter previously appeared as H. Al Ghafly, N. Siraj, S. Das, B. P. Regmi, P. K. S. Magut, W. I. S. Galpothdeniya, K. K. Murray, I. M. Warner. GUMBOS matrices of variable hydrophobicity for matrix-assisted laser desorption/ionization mass spectrometry. *Rapid Commun. Mass Spectrom.* **2014**, *28*, 2307.

contains both hydrophilic and hydrophobic residues, and hence it is critical to also analyze hydrophobic peptides.[17, 19]

An additional problem in the analyses of hydrophobic peptides is their limited solubility in commonly used solvents for MALDI-MS. To overcome this limitation, detergents have been employed to solubilize hydrophobic peptides in aqueous media.[17] These detergents, being amphiphilic, improve the solubility of hydrophobic proteins. However, use of surfactants at critical micelle concentrations can cause deterioration of the spectral quality of peptides, yielding poor signal-to-noise ratios, as well as poor mass resolution.[17, 20]

Despite several attempts to develop new matrices for hydrophobic peptides and proteins,[16, 19, 21-26] limited success has been achieved in MALDI detection of hydrophobic biomolecules. For this reason, synthesis and evaluation of new matrices are still a priority for selective detection of hydrophobic biomolecules within complex biological samples. It has been observed that it is simple to detect hydrophobic biomolecules with hydrophobic matrices since hydrophobic matrices have good affinities for hydrophobic analytes.[17] Therefore, there have been several efforts to synthesize new hydrophobic matrices for analyses of hydrophobic biomolecules.[27-30] However, synthesis of such matrices often involves complex synthetic procedures, which are time consuming and at the same time often produce low product yields.

Ionic liquids (ILs) have been introduced as matrices for MALDI-MS due to several advantages when compared to conventional matrices.[8-11, 16, 31-34] ILs are organic salts with melting points below 100 ^{o}C and these molecules possess several favorable characteristics such as high thermal stability, negligible vapor pressure, and most

importantly, a simple approach to "tuning" properties. Due to ease of synthesis, new matrices with varying hydrophobicity can be designed simply by modifying the cation or anion.[1] Based on results in the literature, a comparison of ionic liquid matrices (ILMs) with solid matrices in MALDI reveals that ILMs exhibit improved reproducibility, sensitivity, sample homogeneity, and detection limits.[8] However, no current studies can be cited which focus on tuning the hydrophobicity of ILMs through changes in the counter ions.

In our laboratory, we are investigating a variety of applications for RTILs and related solid phase organic salts with melting points up to 250 °C which we term a ***g***roup of ***u***niform ***m***aterials ***b***ased on ***o***rganic ***s***alts (GUMBOS). In other words, organic salts with melting points up to 25 ºC are referred to as RTILs, while solids with melting point from 25 to 250 ºC are referred to as GUMBOS. GUMBOS and RTILs have been used for a variety of applications, primarily due to the ease with which these materials can be engineered for specific needs.[35-38] The hydrophobicity of such compounds can be easily tuned simply by changing the counter ion, which results in savings of time and energy. Thus, this approach is an economical method to obtain a desired product with excellent yield.

Herein, we report on an investigation of 1-aminopyrene (AP) and AP-based GUMBOS as MALDI matrices for detection of peptides. AP was selected for these studies because it exhibits strong absorption at the wavelength of laser radiation (337 or 335 nm), displays hydrophobic characteristics, and shows ability to protonate analytes. In this study, we synthesized a series of AP-based GUMBOS, i.e. [AP][Cl], [AP][Asc], and [AP][NTf_2], to achieve variable hydrophobicity simply by changing the anion. The

relative hydrophobicities of these compounds and CHCA were obtained by measuring their 1-octanol/water partition coefficients ($K_{o/w}$), which indicated that these compounds are much more hydrophobic than CHCA. These compounds were then examined as MALDI matrices for analyses of hydrophobic (valinomycin and gramicidin) as well as hydrophilic (bradykinin, and angiotensin II) peptides. These new MALDI matrices showed better performance, and at the same time controllable affinity for different peptides, which is indicated by changes in the signal intensity for peptides of different hydrophobicities. As expected, we observed that hydrophobic matrices showed better signal intensity for hydrophobic peptides, and that hydrophilic matrices produced improved signal intensity for hydrophilic peptides. To the best of our knowledge, there are no literature reports on the use of AP and AP-based salts as matrices for MALDI-MS.

2.2 Experimental Section

2.2.1 Materials

The reagents α-cyano-4-hydroxycinnamic acid (CHCA), acetonitrile, acetone, methanol, ethanol, butanol, trifluoroacetic acid (TFA 99%), bis(trifluoromethane)sulfonimide ($HNTf_2$, 99.95%), 1-aminopyrine (AP, 98%), bradykinin fragment 1-7, angiotensin II human , valinomycin , gramicidin from Bacillus aneurinolyticus, and ascorbic acid (99%) were purchased from Sigma-Aldrich (St Louis, MO, USA). Dichloromethane (99%) DCM and Hydrochloric acid (HCl) were purchased from Fisher Scientific. All chemicals were used as received without further purification.

2.2.2 Synthesis and Characterization of GUMBOS

Equimolar amounts of AP and hydrochloric acid were reacted to yield [AP][Cl]. Briefly, 1 g of AP (4.6 mmol) dissolved in 10 mL DCM was reacted with 5 mL of 0.460 M aqueous HCl and stirred for 3 h. The solid [AP][Cl] product was washed several times with water to remove excess acid. The DCM was removed using rotary evaporation and water was removed by lyophilization. [AP][Asc], was prepared by mixing equimolar amounts of AP and ascorbic acid in methanol and stirring for 24 h. Likewise, [AP][NTf_2] was prepared by reacting equimolar amounts of AP and $HNTf_2$ in methanol and stirring for 24 h. In both cases, methanol was removed by use of rotary evaporation. The melting points of these compounds were determined using a melting point apparatus (DigitMelt MPA 160, Stanford Research Systems).

2.2.3 Determination of Relative Hydrophobicity

The 1-octanol/water partition coefficient was used to gauge the relative hydrophobicities of CHCA, AP, and AP-based GUMBOS. The partition coefficients were determined using a procedure previously developed in our group with very slight modifications.[35] Briefly, 1-octanol and water were shaken for 24 hours before use in order to correct for mutual solubility of the two solvents. A known amount of these compounds was then stirred in a mixture of saturated 1-octanol and water (volume ratio 1:1) for 24 h to allow partitioning. The concentration of the compound in the 1-octanol phase was then determined using UV-Visible spectroscopy and the concentration in water by use of mass balance. Finally, the partition coefficient was calculated by use of the following equation

$$\mathrm{K_{o/w}} = \frac{[\mathrm{X}]_{\mathrm{o,e}}}{[\mathrm{X}]_{\mathrm{w,e}}},$$

where $K_{o/w}$ is the octanol/water partition coefficient, $[X]_{o,e}$ is the concentration of solute in 1-octanol at equilibrium, and $[X]_{w,e}$ is the concentration of solute in water at equilibrium.

2.2.4 Sample Preparation for MALDI

A solution of CHCA matrix at 10 mg/mL (ca 50 mM) was freshly prepared by dissolving an appropriate amount of the compound in a mixture of acetonitrile and water (2:1,v/v) containing 0.1% TFA.[31] Solutions of AP at a concentration of 60 mM and the GUMBOS at a concentration of 40 mM were freshly prepared in methanol. MALDI samples were prepared by using a dried-droplet method.[39, 40]

2.2.5 MALDI-TOF-Mass Spectrometry Data Acquisition

All spectra were obtained using a MALDI-TOF mass spectrometer (UltrafleXtreme, Bruker, Bremen, Germany) in positive ion reflectron mode. A Nd:YAG laser at 355 nm wavelength with a pulse duration of 3 ns was used for ionization. The ion acceleration potential was 25 kV. One thousand laser shots were found to give an acceptable signal under nearly all conditions and were summed for each spectrum and 12 different positions were analyzed on each spot. Data were processed using FlexAnalysis 3.3 software (Bruker).

2.3 Results and Discussion

2.3.1 Preparation and Characterization of AP-based Materials

One major requirement for a MALDI matrix is that it should possess a sufficient molar absorption coefficient at the wavelength of the laser used.[41] Another basic requirement is that the matrix should act as a proton source for a given analyte.[41] An

important factor that affects the performance of MALDI matrices is the size of the matrix crystals. It has been reported that smaller crystals cause improved reproducibility, and resolution.[42-44] Smaller crystals also volatilize completely during laser irradiation.[42] Therefore, we have compared the sample morphology of our different matrices and all AP-based GUMBOS are found to be crystalline (See XRD graphs in Figures 2.1-2.3).

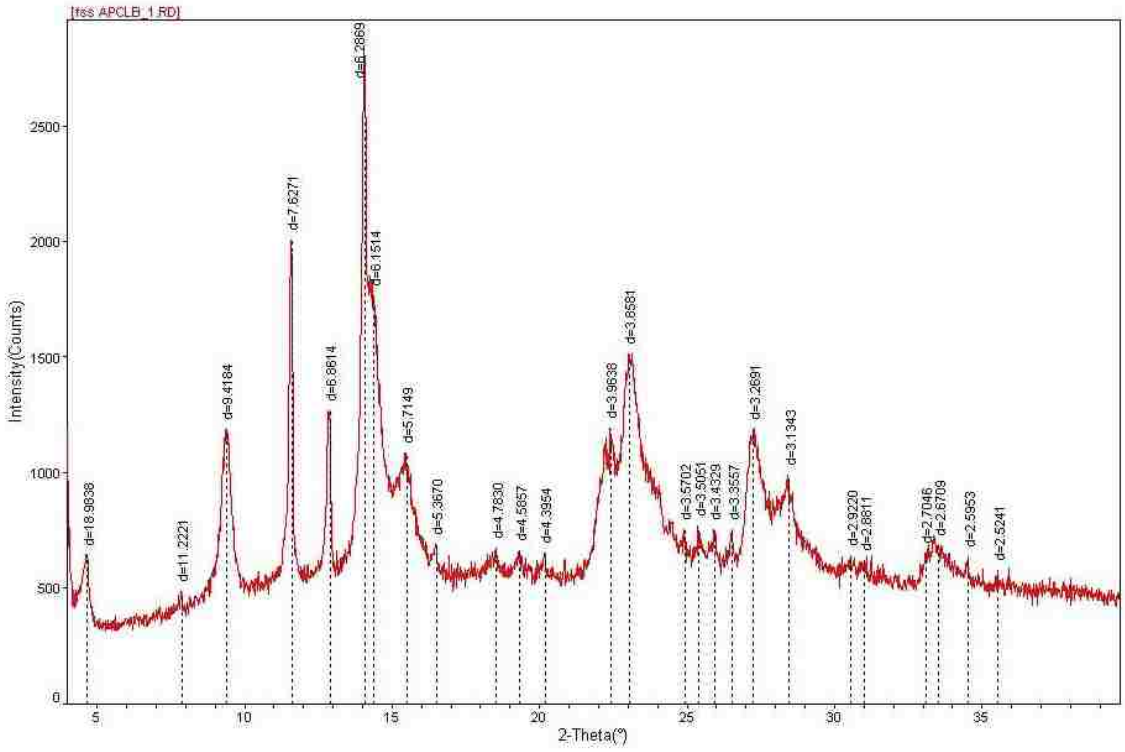

Figure 2.1. Powder X-ray diffraction pattern of [AP][Cl].

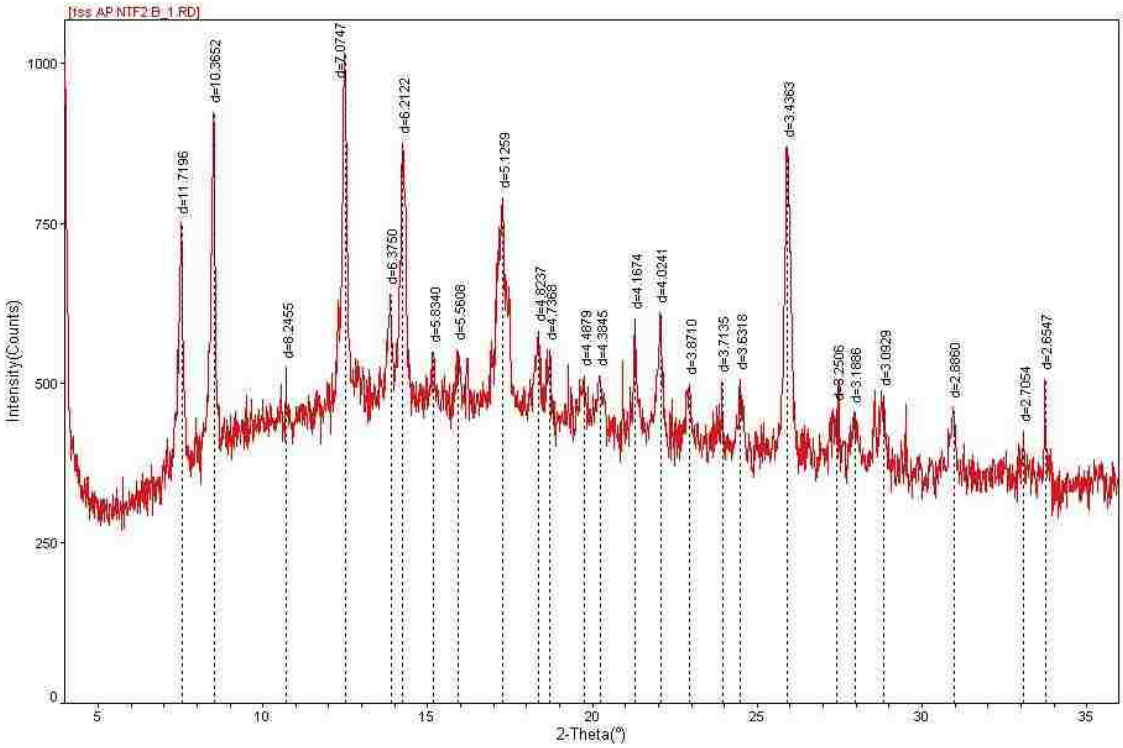

Figure 2.2. Powder X-ray diffraction pattern of [AP][NTF_2].

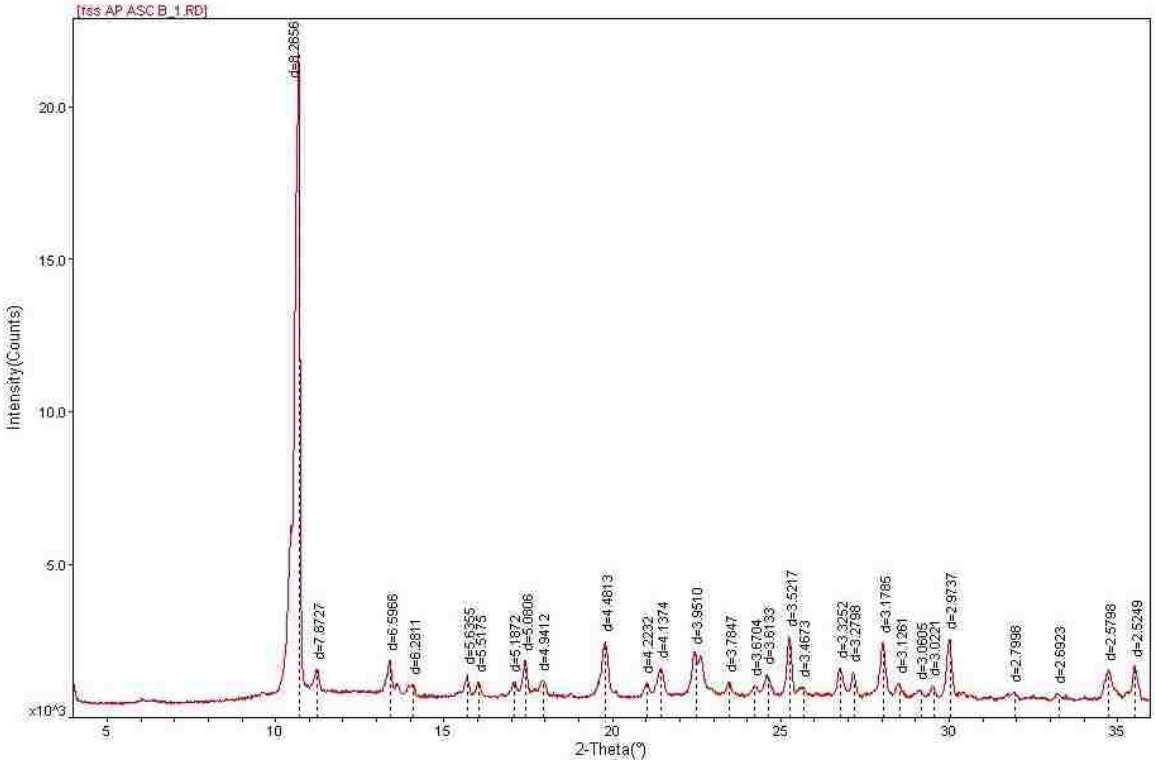

Figure 2.3. Powder X-ray diffraction pattern of [AP][Asc].

The sizes of the matrix crystals are shown in the images depicted in Figure 2.4. Microscopy was used to characterize the size of AP and AP-based GUMBOS on a MALDI target. Therefore, we have compared the sample morphology of our different compounds. The size of the matrix crystals are shown in the images depicted in (Figure 2.4). These images were taken by using a Zeiss steREO Lumar.V12. stereomicroscope at a magnification of 150x. All samples were prepared on the MALDI target by using the dried-droplet method as described above. AP and AP-based GUMBOS formed smaller crystals. These crystals had sizes between 5 and 20 µm. Thus, one of the reasons for the enhanced performance of AP and AP-based GUMBOS could be the formation of smaller crystals.

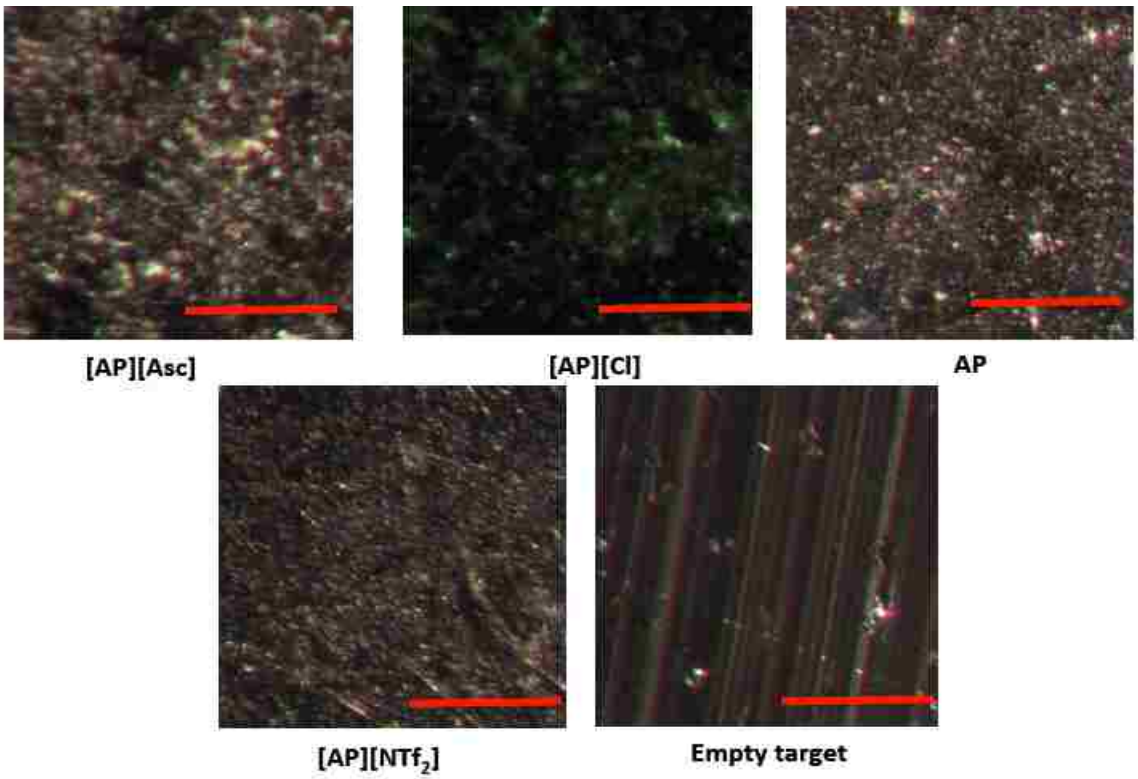

Figure 2.4. Images of different MALDI matrices in the presence of angiotensin II, The last image shows the empty target. The scale bar in each image represents 50 µm.

The hydrophobic compound, AP, was chosen as a matrix because it absorbs UV radiation, has the potential to donate a proton, and satisfies other requirements for a MALDI matrix. In addition, it can be easily converted to a GUMBOS compound such that its hydrophobicity can be tuned by changing the counter ion (the anion in this case). In this study, three different GUMBOS were prepared using 1-aminopyrene: [AP][Cl], [AP][Asc], and [AP][NTf_2]. All three compounds are solids with melting points above 100 ºC. These compounds were characterized by use of ^{1}H NMR (Figures 5-8). In addition, ^{9}F NMR was acquired for [AP][NTf_2] and characterization-using ESI-MS was used to corroborate the NMR data (data not shown).

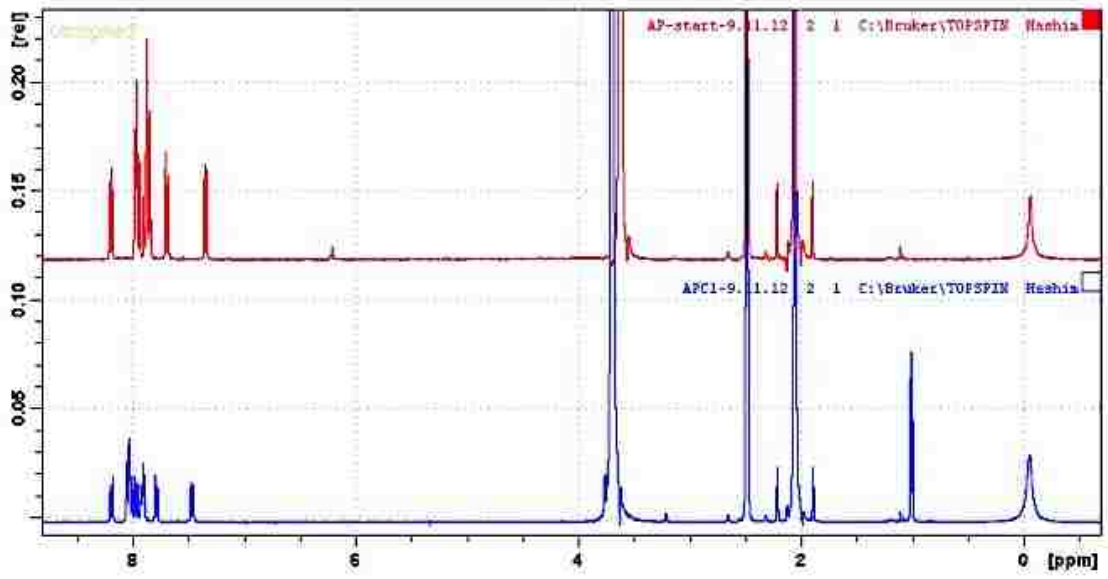

Figure 2.5. ^{1}H NMR spectrum of AP (upper) and [AP][Cl] (lower).

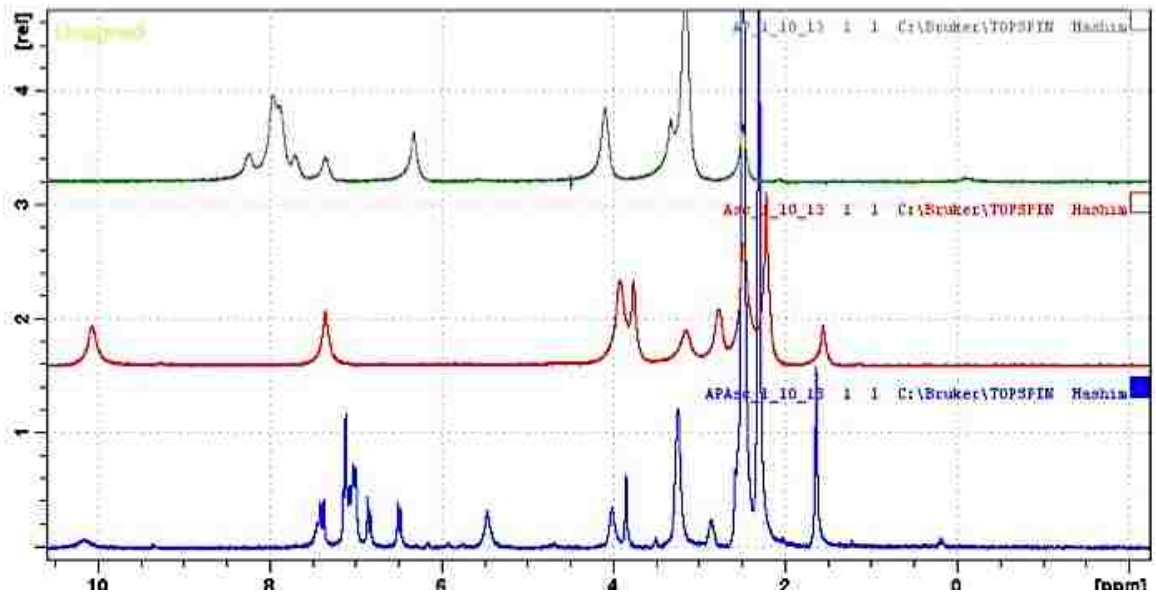

Figure 2.6. ^{1}H NMR Spectrum a) AP top (green). b) ascorbic acid in middle (red). c) [AP][Asc] bottom (blue).

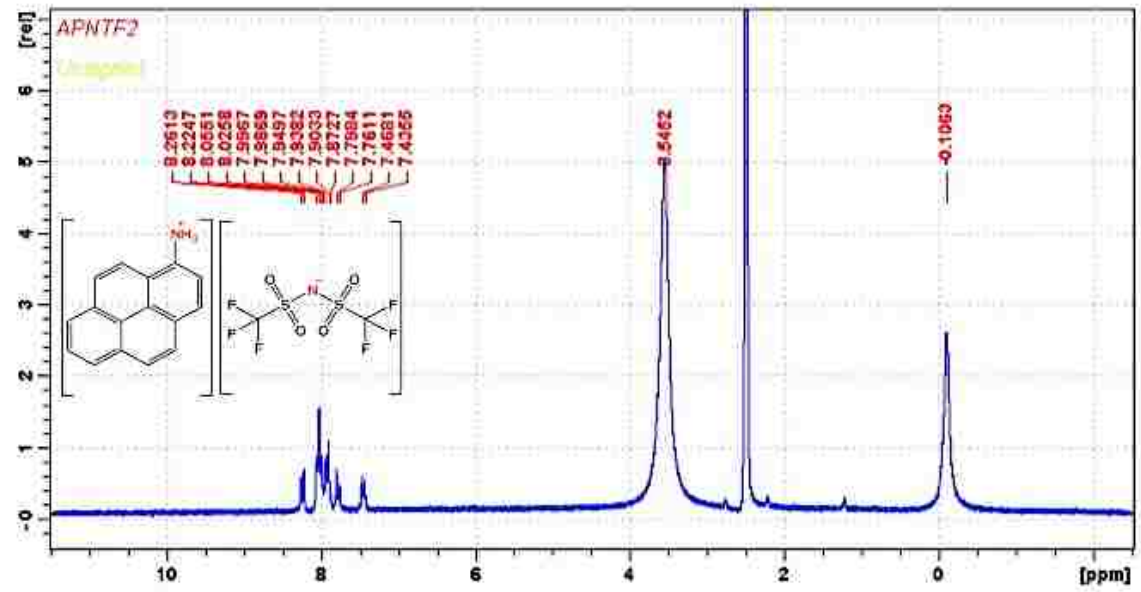

Figure 2.7. ^{1}H NMR spectrum of [AP][NTf_2].

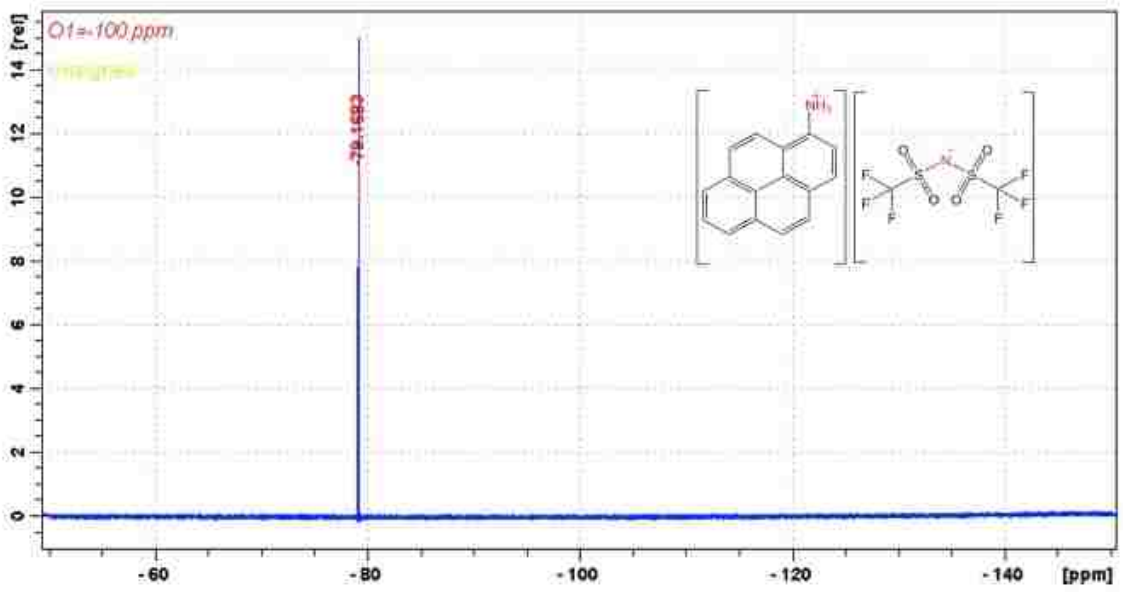

Figure 2.8. ^{19}F NMR spectrum of [AP][NTf_2].

The structures, molecular weights, and melting points of the compounds used in this study are shown in Table 2.1.

The absorption spectra of CHCA, AP, and AP-based GUMBOS in methanol are shown in Figure 2.9. The absorbance band lies between 300 to 400 nm for CHCA, and between 300 to 420 nm for AP and AP-based GUMBOS. All of these compounds absorb over a similar wavelength range as compared to a CHCA matrix. The performance of our materials as MALDI matrices, reported in the subsequent sections, is compared with that of CHCA because CHCA is a commonly used MALDI matrix for low molecular weight biomolecule applications.[12, 37] The molar absorptivities of all compounds at 355 nm are also listed in Table 2.1. It is observed that AP, [AP][Cl] and [AP][Asc] have lower molar absorptivities as compared to CHCA, and the molar absorptivity of [AP][NTf_2] is much lower than that of CHCA. Hence, the molar absorptivity is dependent on the counter ion.

Table 2.1. Structures, molecular weights, log $K_{(o/w)}$, molar absorptivity, and melting points of matrices used in this study.

Compounds	Structure	MP (ºC)	MW	Log $K_{(o/w)}$	Molar Absorptivity (M^{-1} cm^{-1})
α -CHCA	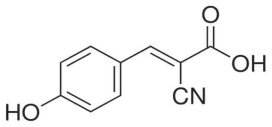	240[a]	189.17	-1.72	23500
AP	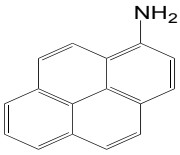	117[a]	217.27	1.42	20000
[AP][Asc]	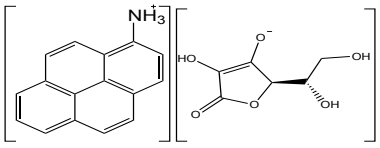	109[b]	394.13	0.81	18500
[AP][Cl]	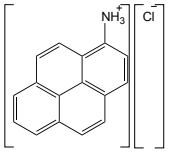	230[b]	253.73	1.02	15000
[AP][NTf_2]	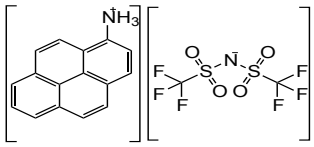	190[b]	498.42	1.54	9000

[a] Melting points reported by Sigma-Aldrich and verified by us.
[b] Melting points determined in this study.

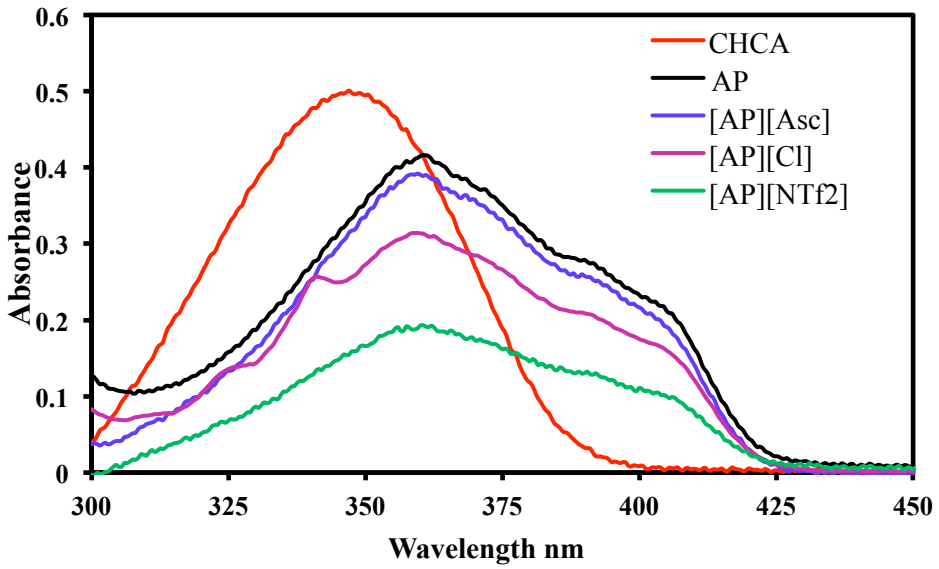

Figure 2.9. Absorbance spectra of CHCA, AP, and AP-based salts in methanol. The concentration of all these compounds is 50 μM.

In order to estimate the relative hydrophobicity of all these compounds, 1-octanol/ water partition coefficients ($K_{o/w}$) were determined. The logarithm of the partition coefficient (log $K_{o/w}$) for each compound is listed in Table 1. Hydrophobicity is directly related to the value of $K_{o/w}$. As seen from the values of log $K_{o/w}$, the relative hydrophobicity from lowest to highest increases as α-CHCA << [AP][Asc] < [AP][Cl] < AP < [AP][NTf_2]. This observation demonstrates that a significant change in the hydrophobicity of GUMBOS can be attained by a simple change of the counter ion.

2.3.2 Evaluation of the Performance of AP and AP-based GUMBOS as MALDI Matrices for Hydrophobic and Hydrophilic Peptide Detection

We have evaluated the performance of this new class of materials using two hydrophobic (valinomycin and gramicidin) and two hydrophilic peptides (bradykinin and angiotensin II). Initially, the effectiveness of these AP-based matrices was evaluated by acquiring individual MALDI spectra for all four peptides as shown in (Figures 2.10-2.29). A dried droplet method was used to prepare all MALDI samples. Briefly, 1 μL of

sample solution was spotted on the MALDI target and 1 μL of matrix was added and mixed, followed by drying under ambient conditions. Valinomycin and gramicidin, in all matrices including CHCA, showed a clear signal at *m/z* 1133.62 and 1904.06, respectively, which corresponds to the $[M+Na]^+$ peak. Similarly, the $[M+H]^+$ peak for bradykinin (1-7) and angiotensin II were observed at *m/z* 757.39 and *m/z* 1046.54, respectively, No matrix-derived peaks were observed in the spectral region of all peptides (Figures 2.11-2.14), indicating that these matrices do not interfere with peaks arising from the analytes.

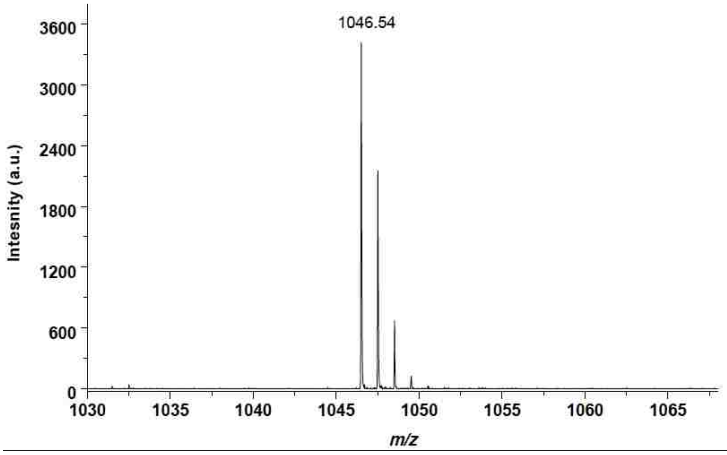

Figure 2.10. Positive ion mode MALDI-TOF mass spectra for angiotensin II with CHCA.

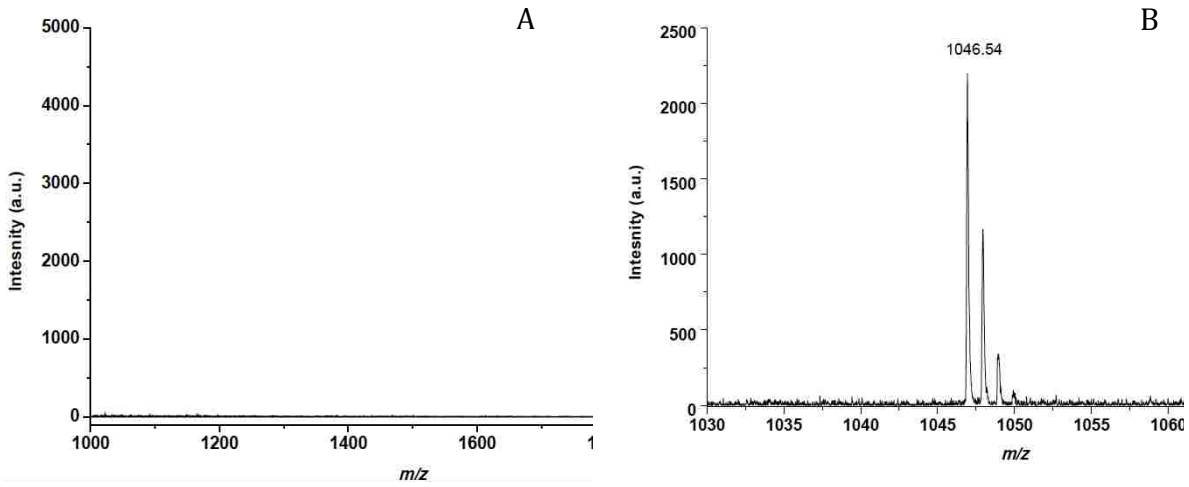

Figure 2.11. Positive ion mode MALDI-TOF mass spectra A) only AP. B) angiotensin II with AP.

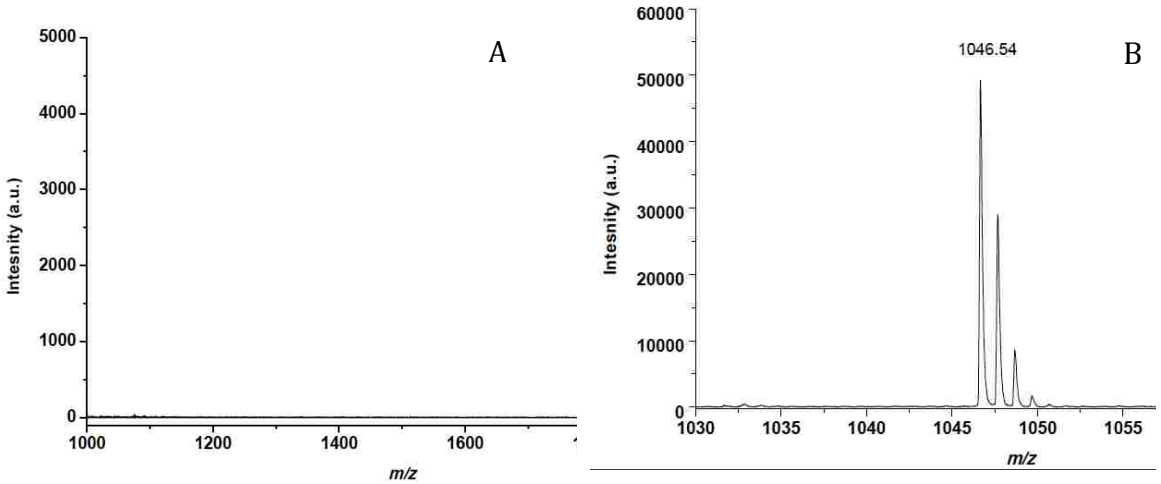

Figure 2.12. Positive ion mode MALDI-TOF mass spectra A) only [AP][Cl]. B) angiotensin II with [AP][Cl].

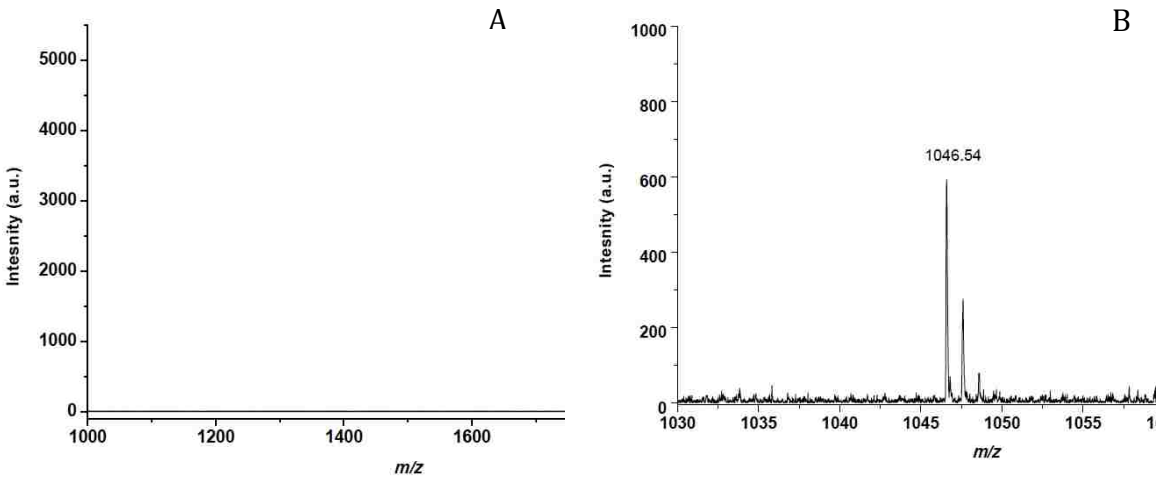

Figure 2.13. Positive ion mode MALDI-TOF mass spectra .A) only [AP][NTf_2]. B) angiotensin II with [AP][NTf_2].

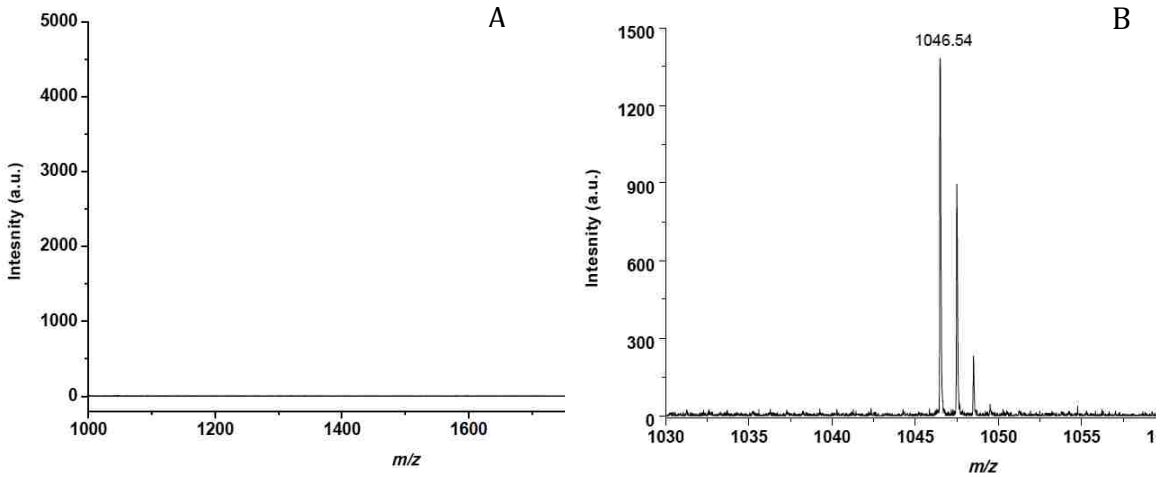

Figure 2.14. Positive ion mode MALDI-TOF mass spectra. A) only [AP][Asc]. B) angiotensin II with [AP][Asc].

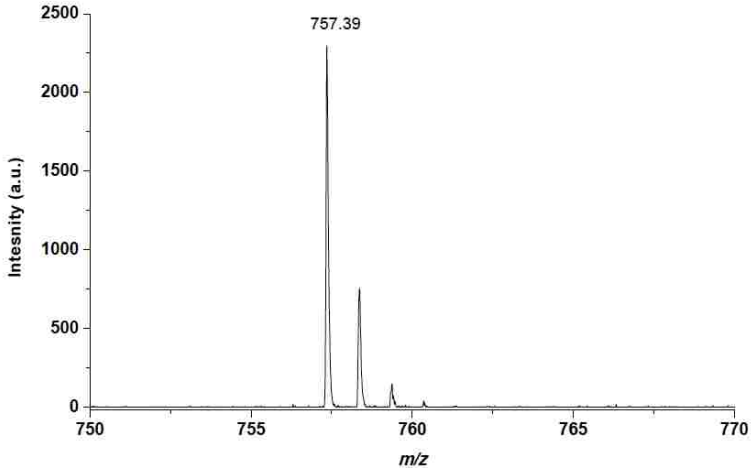

Figure 2.15. Positive ion mode MALDI-TOF mass spectra CHCA with bradykinin.

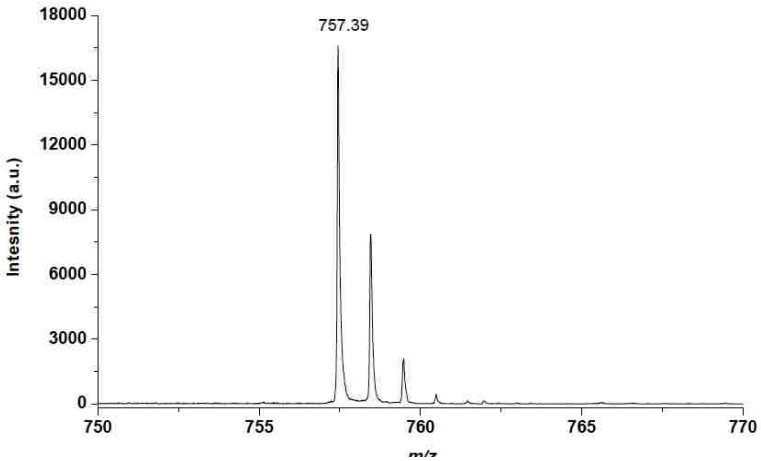

Figure 2.16. Positive ion mode MALDI-TOF mass spectra bradykinin with [AP][Asc].

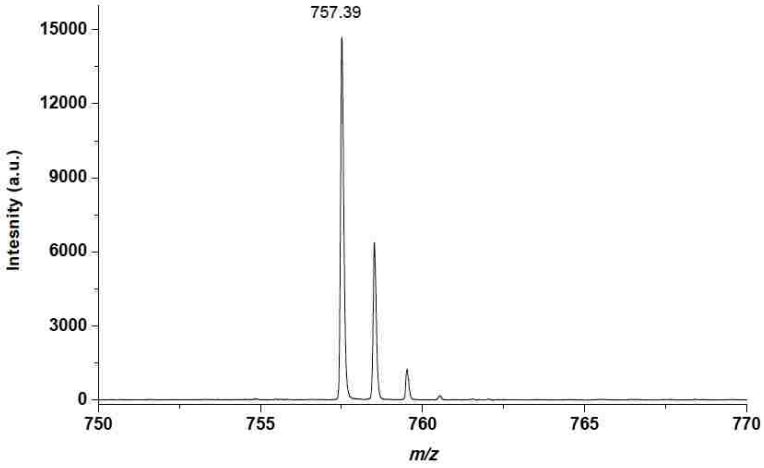

Figure 2.17. Positive ion mode MALDI-TOF mass spectra bradykinin with [AP][Cl].

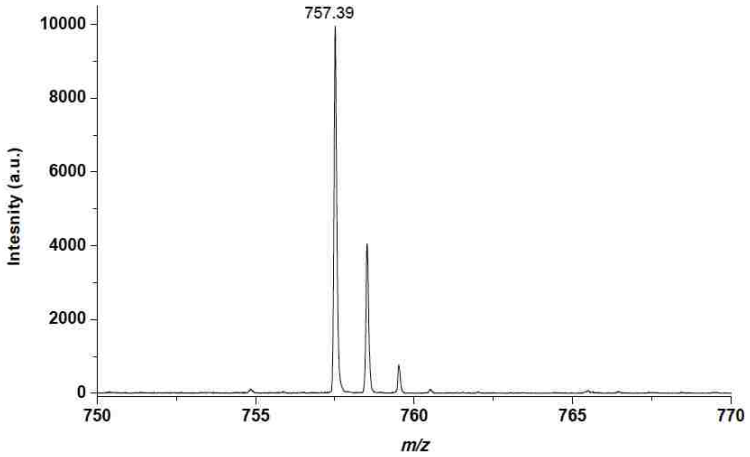

Figure 2.18. Positive ion mode MALDI-TOF mass spectra bradykinin with [AP].

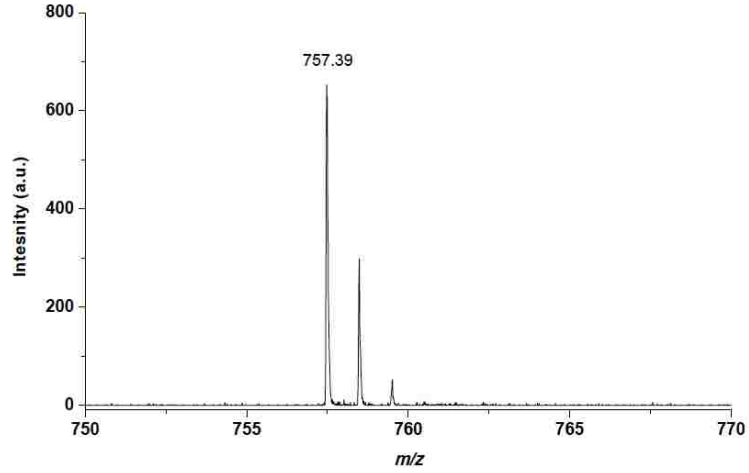

Figure 2.19. Positive ion mode MALDI-TOF mass spectra bradykinin with [AP][NTf_2].

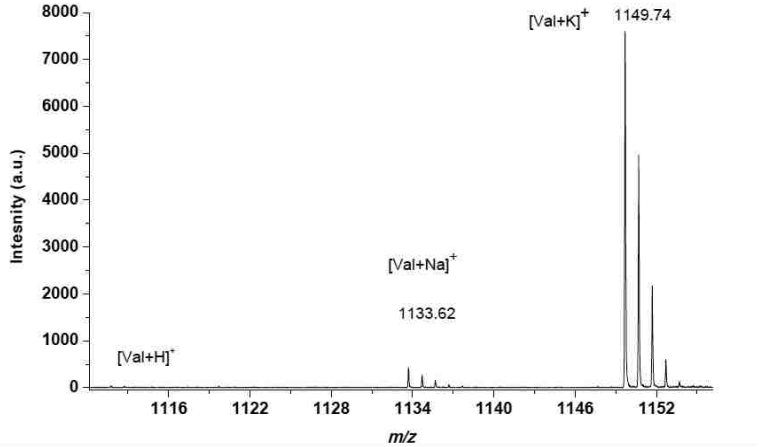

Figure 2.20. Positive ion mode MALDI-TOF mass spectra CHCA with valinomycin.

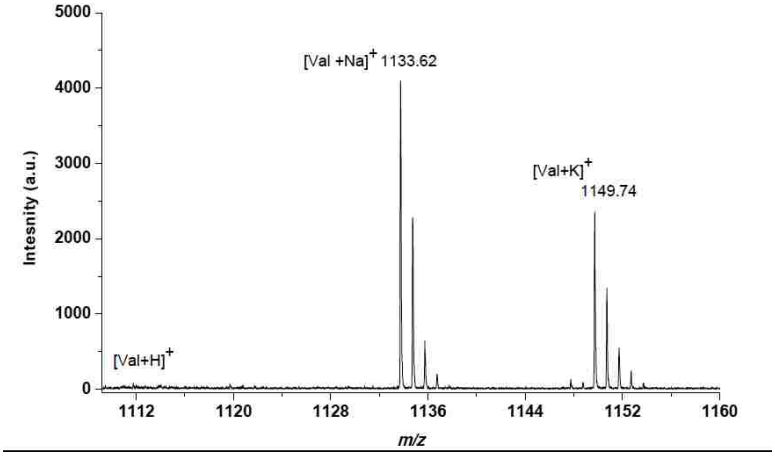

Figure 2.21. Positive ion mode MALDI-TOF mass spectra [AP][Asc] with valinomycin.

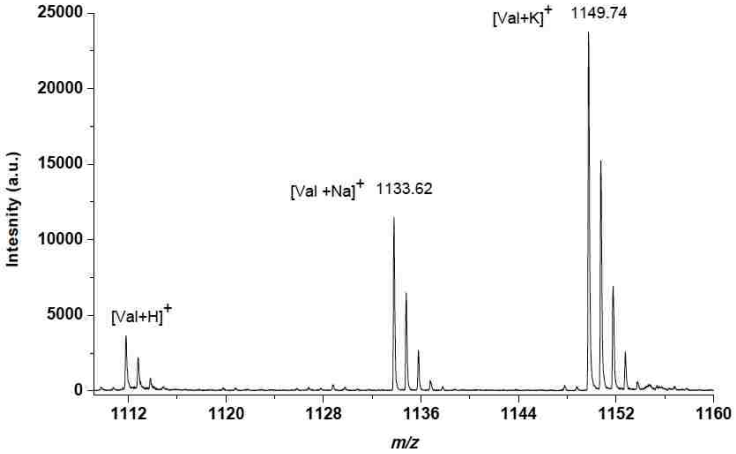

Figure 2.22. Positive ion mode MALDI-TOF mass spectra [AP][Cl] with valinomycin.

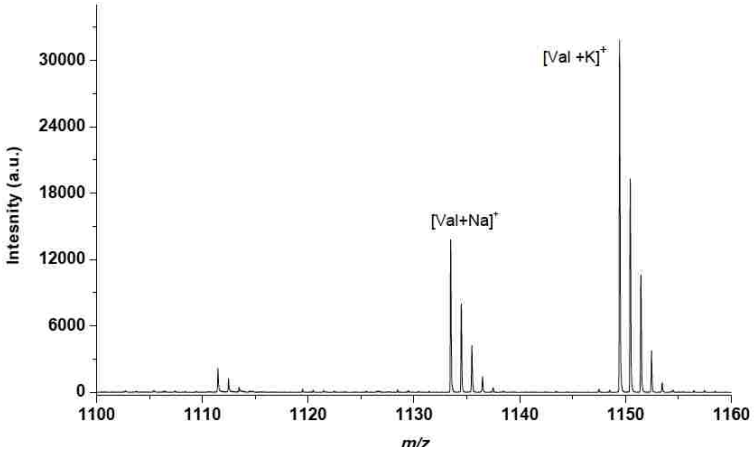

Figure 2.23. Positive ion mode MALDI-TOF mass spectra AP with valinomycin.

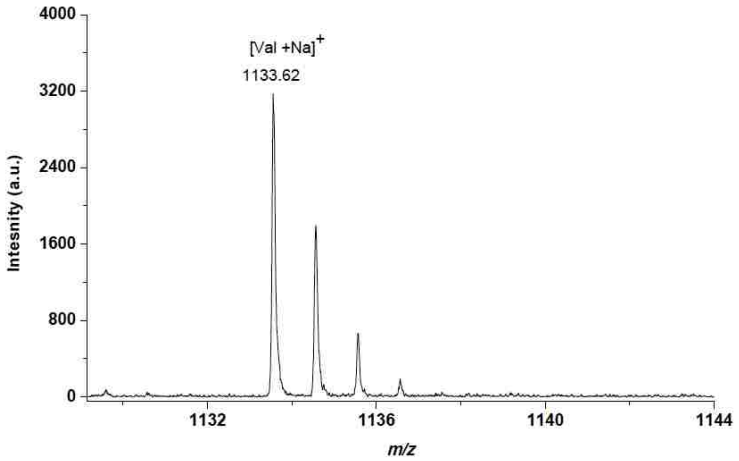

Figure 2.24. Positive ion mode MALDI-TOF mass spectra [AP][NTf_2] with valinomycin.

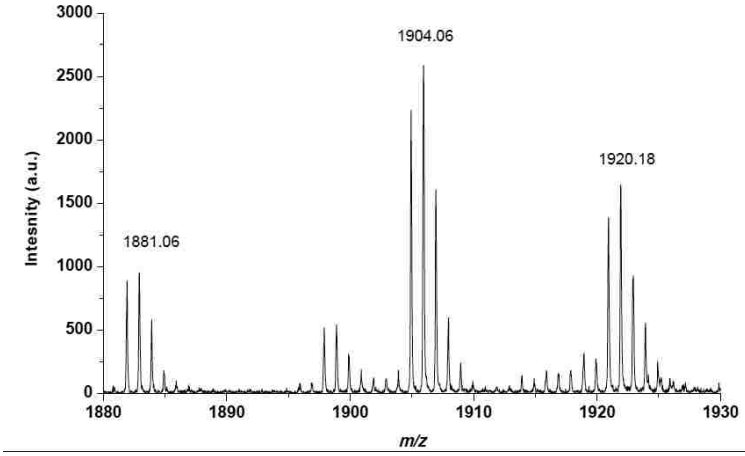

Figure 2.25. Positive ion mode MALDI-TOF mass spectra CHCA with gramicidin.

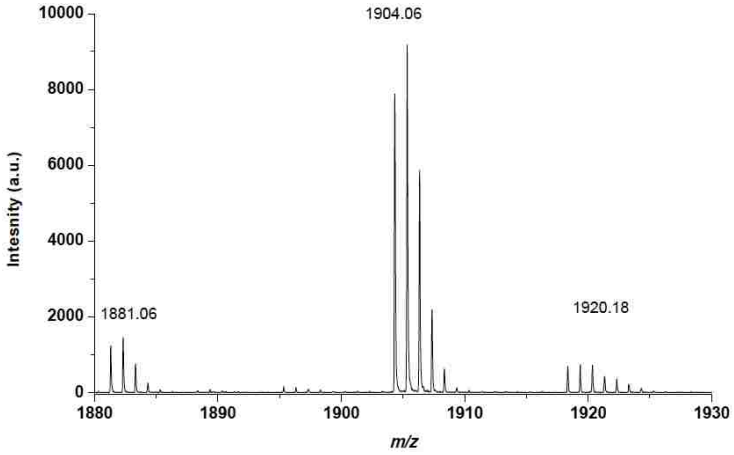

Figure 2.26. Positive ion mode MALDI-TOF mass spectra [AP][Asc] with gramicidin.

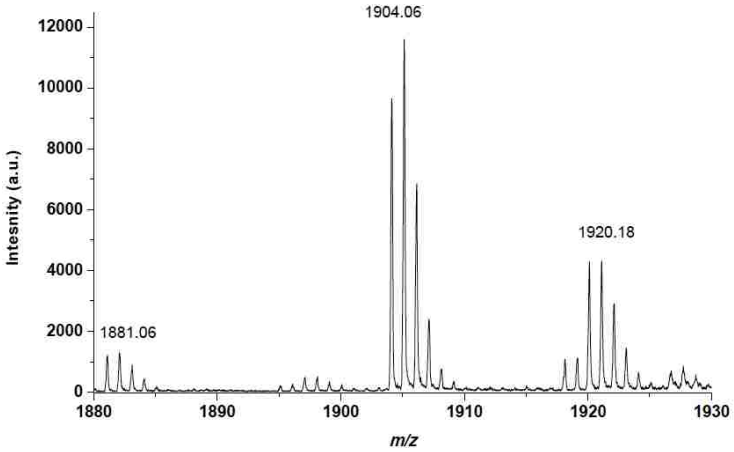

Figure 2.27. Positive ion mode MALDI-TOF mass spectra [AP][Cl] with gramicidin.

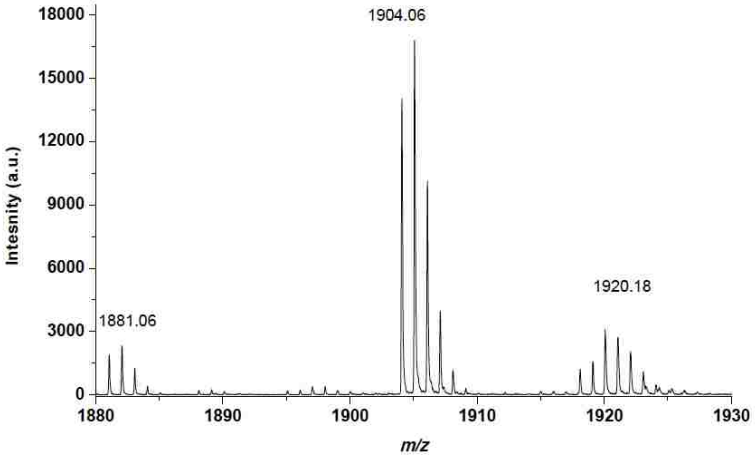

Figure 2.28. Positive ion mode MALDI-TOF mass spectra [AP] with gramicidin.

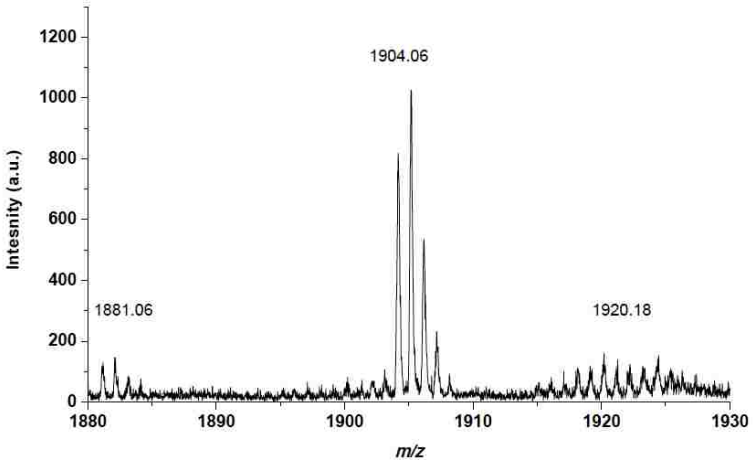

Figure 2.29. Positive ion mode MALDI-TOF mass spectra [AP][NTf_2] with gramicidin.

Table 2.2. Signal intensities and relative standard deviations for [bradykinin +H]$^+$, [angiotensin II +H]$^+$, [valinomycin + Na]$^+$ and [gramicidin + Na]$^+$ ions in the presence of CHCA, AP, and AP-based GUMBOS as matrices.

	Bradykinin		Angiotensin II		Valinomycin		Gramicidin	
Matrices	Average Intensity	RSD	Average Intensity	RSD	Average Intensity	RSD	Average Intensity	RSD
CHCA	2000	102	1200	63	1200	103	1100	90
[AP][Asc]	25000	16	9200	21	3300	29	2400	41
[AP][Cl]	25000	23	6724	26	7300	19	2900	6
AP	5000	41	5700	15	21000	36	7100	63
[AP][NTf_2]	2000	33	1800	16	5200	24	5500	13

The relative standard deviations (RSD), which is a measure of the spot-to-spot reproducibility, were evaluated by using the signal intensity measured at 12 different positions (Table 2.2). The laser settings used were the same for all matrices. In all measurements, only the spectra having a resolution greater than 10,000 were collected. Examination of Table 2.2 reveals that improved spot-to-spot reproducibility and significant enhancement (10-15 times) in signal intensity are obtained when using AP-based matrices as compared to the conventional CHCA matrix. The low signal intensity in the case of [AP][NTf_2] is attributed to the relatively low molar absorption coefficient of this salt as compared to AP and other AP-based GUMBOS. In addition, low signal intensity in [AP][NTf_2] could also be ascribed to formation of a hydrogen bonding network between the highly electronegative atoms in the $[NTf_2]^-$ anion and the AP cation. The hydrogen bonding between cation and anion in [AP][NTf_2] may also inhibit proton transfer from matrix to the analytes, thereby accounting for poor performance.[45, 46]

The results obtained using AP and AP-based GUMBOS matrices for hydrophilic (bradykinin, angiotensin II) and hydrophobic peptides, (valinomycin and gramicidin) are summarized in Figure 2. The results are consistent with relatively high signal intensity for

the hydrophobic peptides as compared to the hydrophilic peptides in the hydrophobic matrices (right hand side of Figure 2.30) and relatively high signal intensity for the hydrophilic peptides in the more hydrophilic matrices (left hand side of Figure 2.30). The propensity for hydrophobic/hydrophilic matrix favoring hydrophobic/hydrophilic analyte is not a strict rule. For example, angiotensin II and valinomycin have nearly the same intensity with [AP][Cl] and angiotensin and gramicidin have nearly the same intensity with [AP]. Nonetheless, the general trend of "like favors like" holds, when the results are taken in its entirety. Likewise, there is some variation in absolute signal intensity from matrix to matrix; for example, [AP][NTf_2] has a relatively low signal for all matrix compounds, most likely due to its low absorptivity. However, the hydrophobic [AP][NTf_2] matrix clearly favors the hydrophobic peptides in comparison to the hydrophilic peptides.

For all peptides, reproducibility is improved with GUMBOS matrices as compared to a conventional CHCA matrix. The improved reproducibility of the signal with these matrix materials likely results from a more homogeneous distribution of sample and matrix as compared to CHCA.

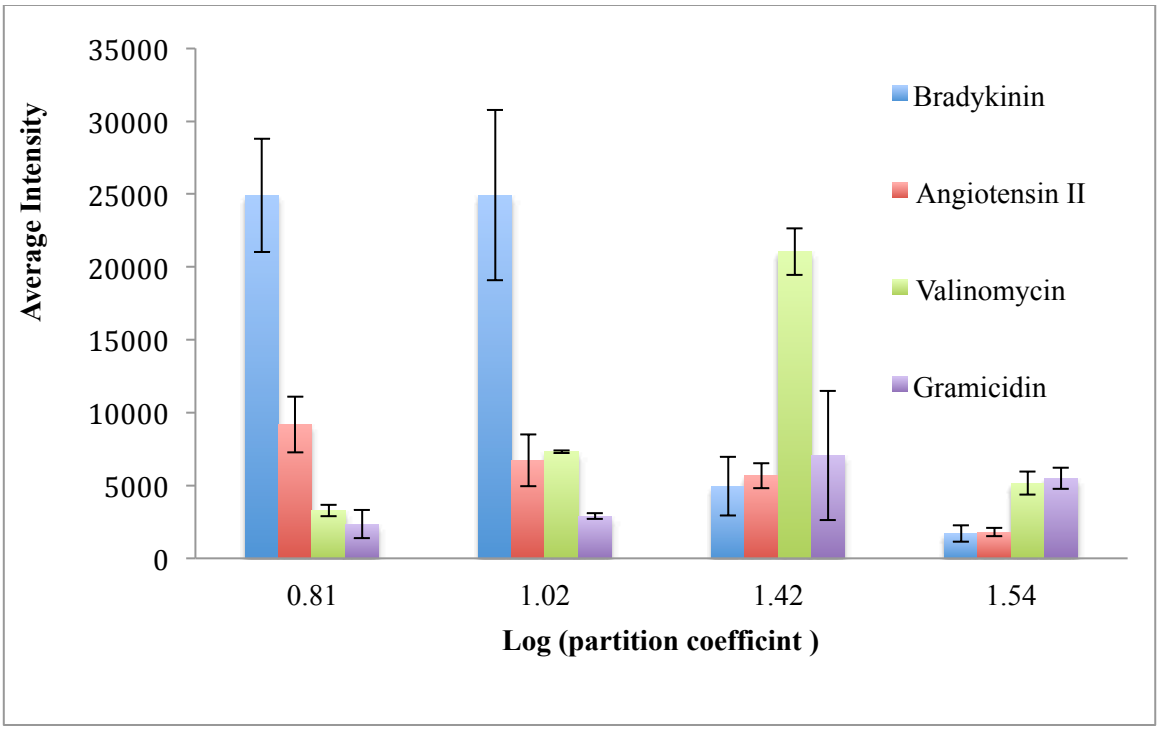

Figure 2.30. Average MALDI signal intensity as a function of the logarithm of the partition coefficient Log $K_{(o/w)}$ for (left to right) [AP][Asc], [AP][Cl], [AP], and [AP][NTF2]; a larger partition coefficient indicates a more hydrophobic matrix.

We also analyzed the data by obtaining the ratios of signal intensity of each hydrophilic peptide to each hydrophobic peptide (bradykinin/gramicidin, bradykinin/valinomycin, angiotensin II/valinomycin, and angiotensin II/gramicidin) in order to normalize the effect. A plot of the ratio of signal intensity against the logarithm of partition coefficient of AP and AP-based GUMBOS shows a clear trend with hydrophobicity (Figure 2.31). More specifically, the ratio of the signal intensity is found to decrease as the hydrophobicity of the matrix increases.

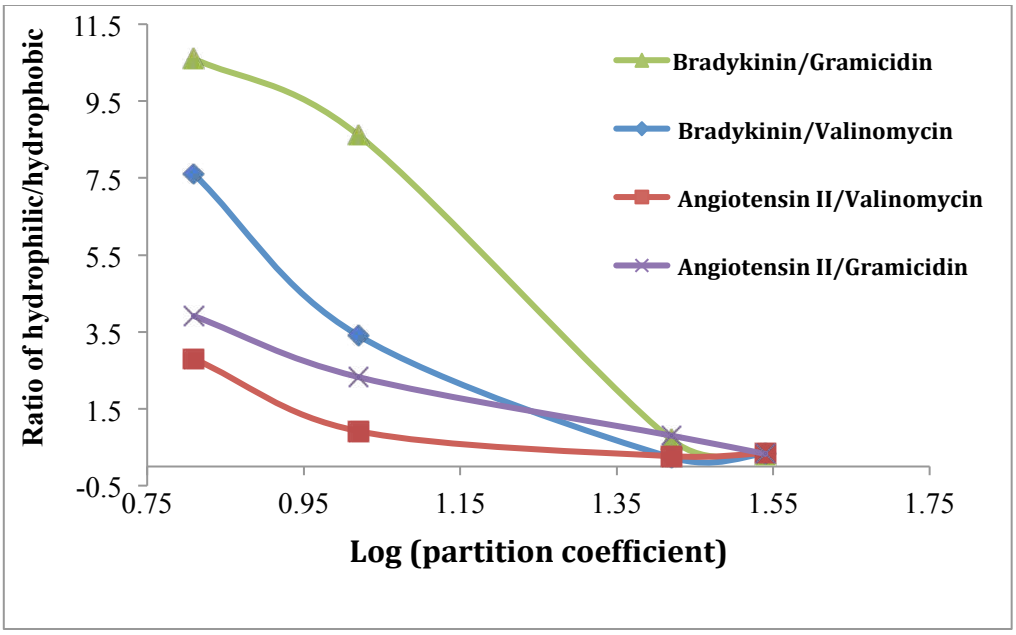

Figure 2.31. Intensity ratio for hydrophilic peptide/hydrophobic peptide as a function of log partition coefficient AP and AP-based GUMBOS.

2.3.3 Analysis of Hydrophobic and Hydrophilic Peptide Mixtures

Peptide mixtures were also analyzed using each matrix separately. An equimolar amount of hydrophobic (valinomycin) and hydrophilic (angiotensin II) peptide was mixed and the mixture was spotted on a MALDI target using a dried-droplet method. Each spot was analyzed at 12 different positions and the average intensity and the relative standard deviation were calculated. The resulting signal intensities of the mixtures obtained with different AP-based matrices were compared with a conventional CHCA matrix. In spite of the same concentration used for both peptides with the [AP][Asc] matrix, higher signal intensity was observed for angiotensin II than for valinomycin (Figure 2.32). This suggests that [AP][Asc], a hydrophilic matrix, exhibits a higher affinity for the hydrophilic peptide as compared to the hydrophobic peptide. Similarly, both CHCA and [AP][Cl], hydrophilic matrices, showed higher intensity for angiotensin

II and lower intensity for valinomycin (Figure 2.34 and 2.35). Thus, the hydrophilic matrices result in better signals for the hydrophilic peptides.

To investigate the hydrophobic peptides, a hydrophobic matrix was employed. Aminopyrene, a hydrophobic matrix, showed opposite results for a mixture of hydrophilic and hydrophobic peptides. In this case, higher signal intensity was observed for valinomycin as compared to the angiotensin II for the same molar concentration of peptides as shown in (Figure 2.33). Thus, it is likely that the enhanced signal for the hydrophobic peptide is due to its higher affinity for the hydrophobic matrix.

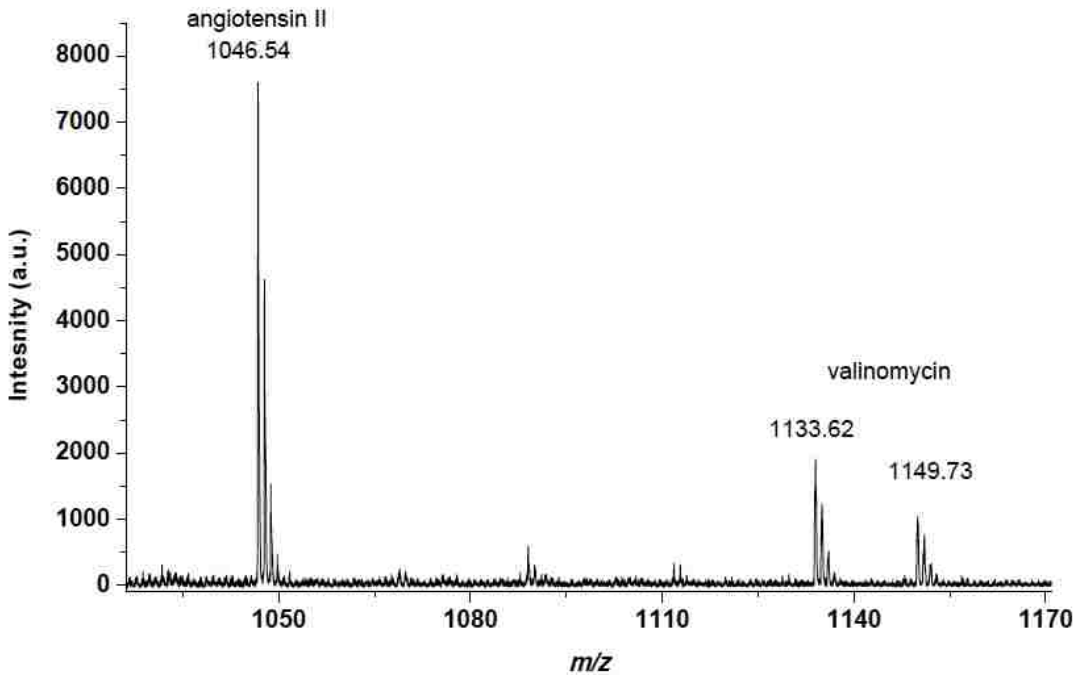

Figure 2.32. Positive ion mode. MALDI MS Spectrum of equimolar mixture of angiotensin II (hydrophilic) and valinomycin (hydrophobic) using [AP][Asc] matrix.

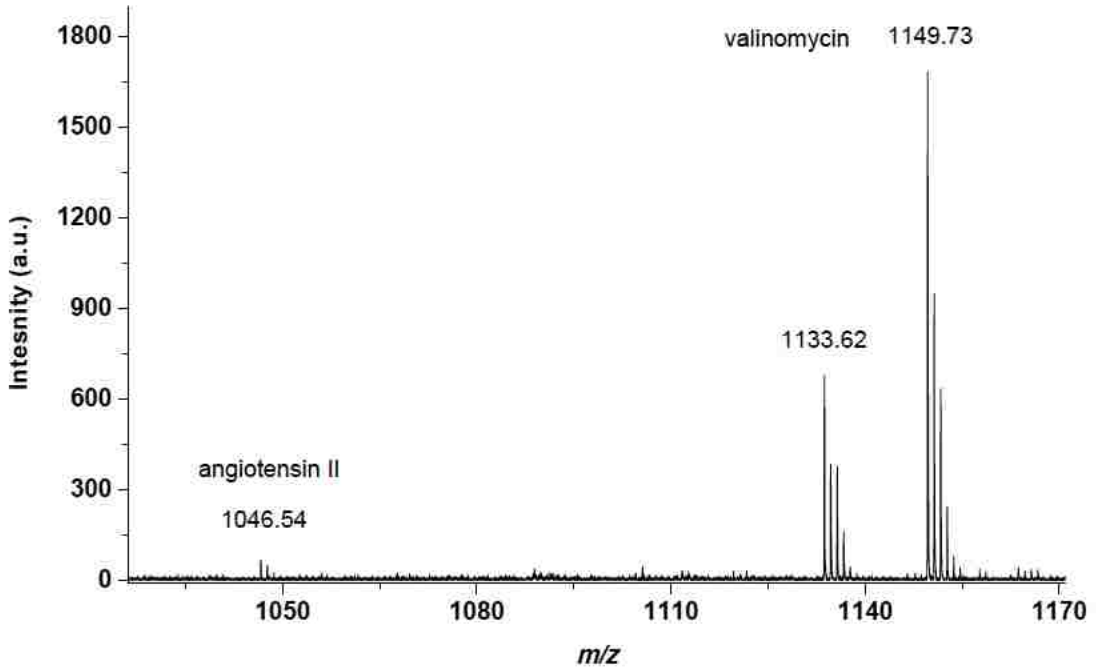

Figure 2.33. MALDI MS spectra for equimolar mixture of angiotensin II and valinomycin with AP matrix.

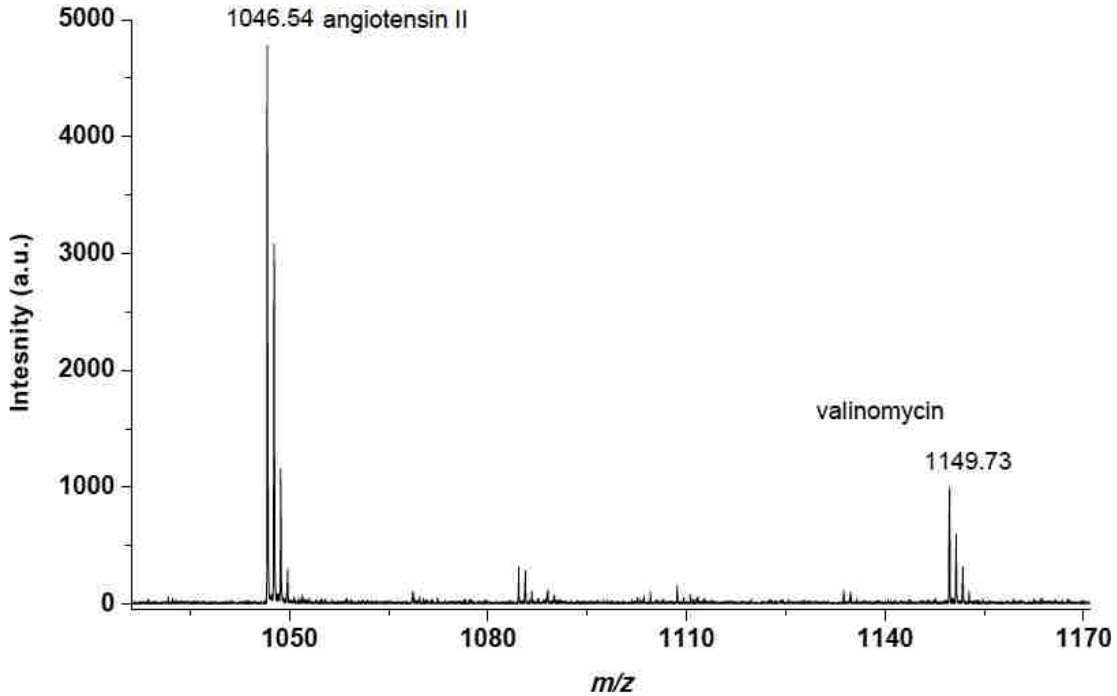

Figure 2.34. CHCA hydrophilic matrix detected higher intensity hydrophilic peptide (angiotensin II*)* compared with hydrophilic peptide (valinomycin).

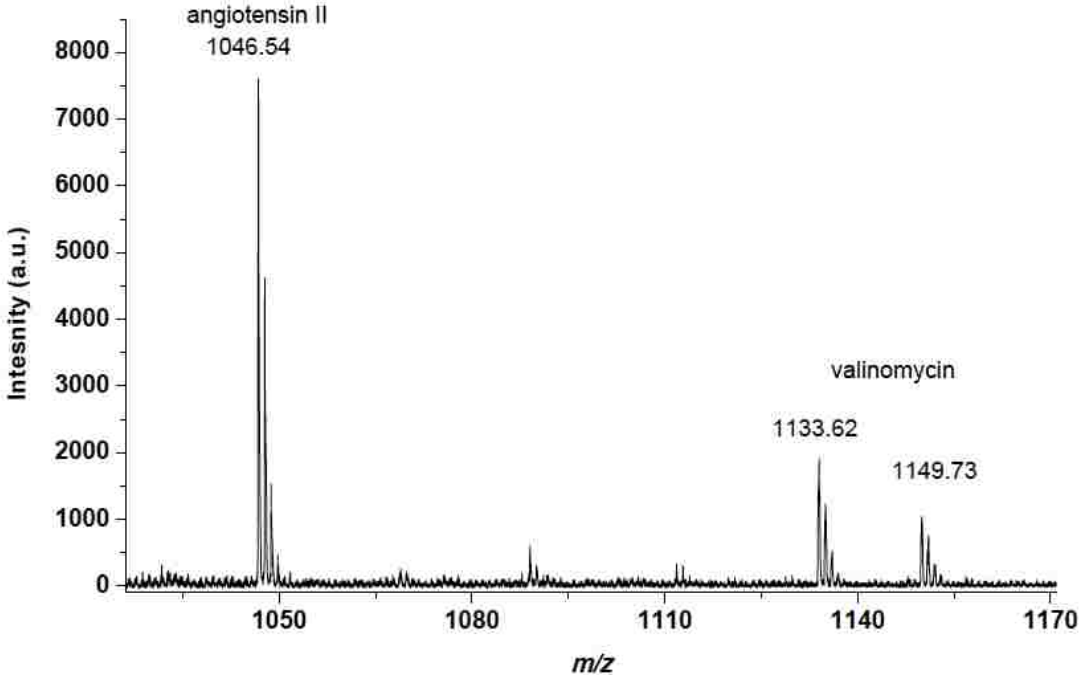

Figure 2.35. [AP][Cl] hydrophilic matrix detected higher intensity hydrophilic peptide (angiotensin II) compared with hydrophilic peptide (valinomycin).

The average signal intensity obtained for the mixture was plotted against the logarithm of the partition coefficient (log $K_{o/w}$) of different AP-based matrices (Figure 2.36). The relative standard deviation is highest in CHCA as compared to the AP and AP-GUMBOS matrices. In terms of reproducibility and signal intensity for both hydrophobic and hydrophilic peptides, AP-based matrices are better performing as compared with CHCA. In terms of relative intensity, the hydrophilic angiotensin II has approximately three times the signal intensity as the hydrophobic valinomycin for all but the most hydrophobic matrix [AP][NTf_2]. This supports the general trend of hydrophobic analytes requiring a hydrophobic matrix, but also suggests a nonlinear effect in which there is a threshold for matrix hydrophobicity above which ionization of the more hydrophobic components is favored. If this is the case, the ability to tune the matrix hydrophobicity

within a narrow range will be critical for selective ionization of the hydrophobic components in a sample.

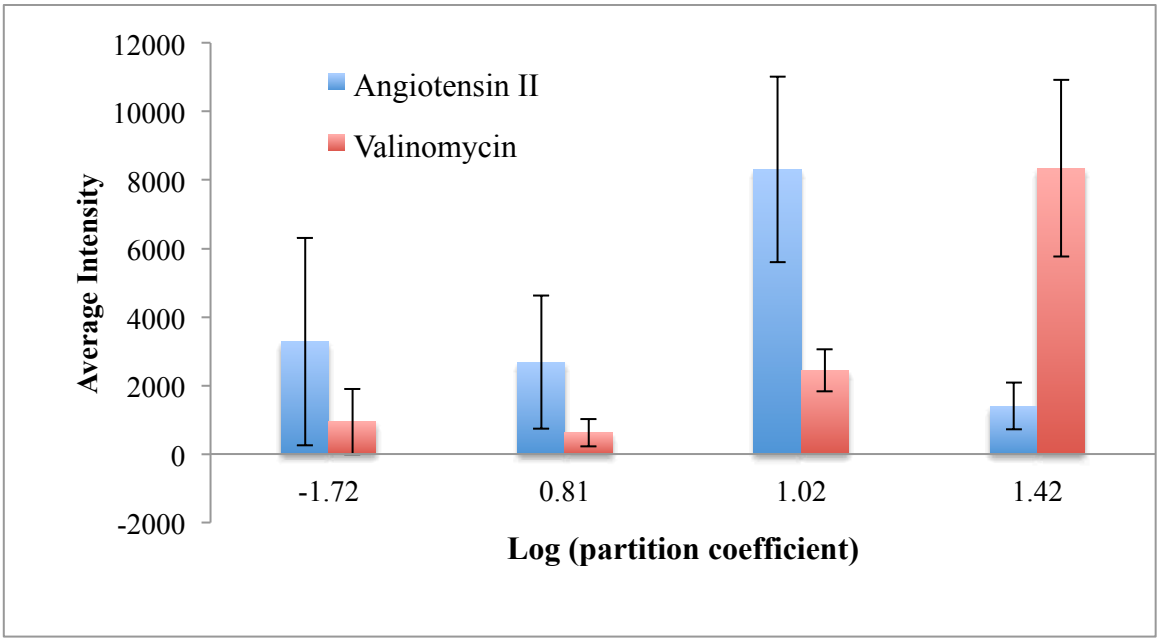

Figure 2.36. Signal intensities for a mixture of a hydrophilic (angiotension II) and hydrophobic (valinomycin) peptide at equimolar concentration in matrices of different hydrophobcities. (CHCA:-1.72), ([AP][Asc]:0.81), ([AP][Cl]:1.02) and (AP:1.42).

Table 2.3. Intensity for mixture of hydrophilic (angiotension II) and hydrophobic (valinomycin) peptides at equimolar concentration in different matrices of variable hydrophobcities.

	(Angiotensin II)		(Valinomycin)	
Matrices	Average Intensity	RSD	Average Intensity	RSD
CHCA	3300	92	1000	100
[AP][Asc]	2700	72	600	63
[AP][Cl]	8300	32	2500	25
AP	1400	48	8400	30

The result for the ratio of angiotensin II/ valinomycin as a function of the hydrophobicity of the matrices is shown in (Figure 2.37). A plot of the ratio signal intensity against the logarithm of partition coefficient of matrices shows a clear trend: as the hydrophobicity of the matrices increases, the ratio of the signal intensity of the

peptides decreases. This experiment was designed to normalize the effect of both hydrophobic and hydrophilic peptides at similar spots.

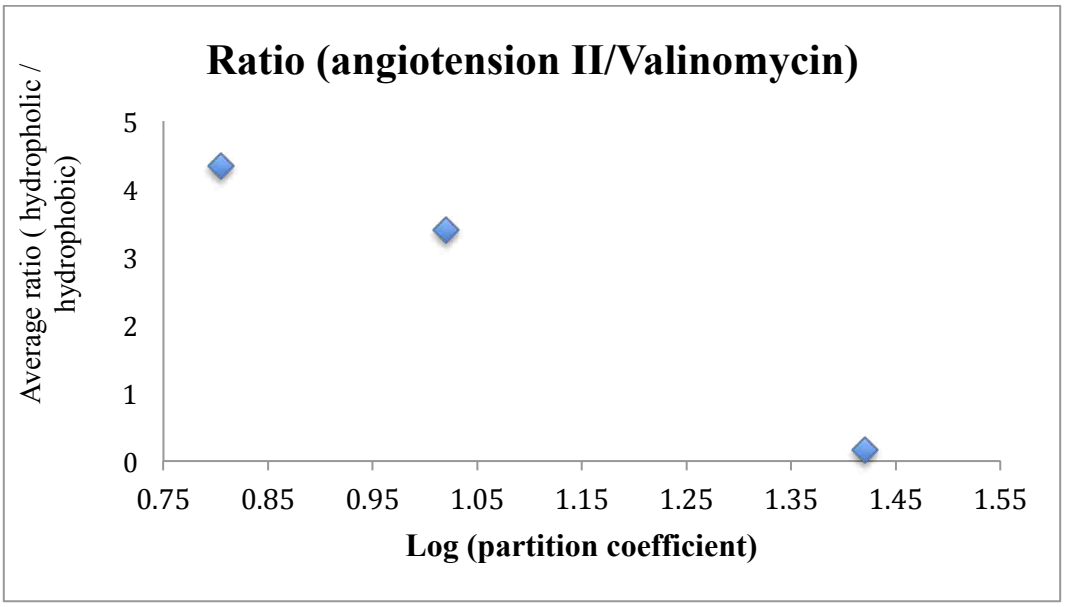

Figure 2.37. Ratio of average intensity (angiotensin II/ valinomycin) versus log ($K_{o/w}$) of matrices.

2.4 Conclusions

In this work, AP and AP-based GUMBOS of variable hydrophobicities were used as MALDI matrices. A series of AP-based GUMBOS were synthesized and characterized. A simple, facile and inexpensive approach was used to tune the hydrophobicity of AP based matrices. The performance of these salts, along with AP as MALDI matrices for detection of hydrophobic and hydrophilic peptides was evaluated. Tuning the hydrophobicity of the matrix by altering the counter ions in AP-based GUMBOS changes its performance with peptides. Hydrophilic and hydrophobic peptides were determined using AP and AP-based GUMBOS and compared with conventional MALDI matrices that are often used with peptides. As expected, the performance of these

matrices for different peptides depended on the matrix hydrophobicity. We have observed that increasing the hydrophobicity of a matrix increases the affinity to hydrophobic peptides after laser desorption. An increase in hydrophilicity of the matrix in the order of CHCA > [AP][Asc]> [AP][Cl]> AP led to a higher affinity for hydrophilic peptides. Likewise, the signal intensity for hydrophobic peptides increased when the hydrophobicity of the matrix was increased. A mixture of hydrophilic and hydrophobic peptides, demonstrated that these new matrices of variable hyrophobicities result in a similar trend in signal intensity, e.g. AP, a hydrophobic matrix, increased sensitivity of hydrophobic peptides, whereas the signal intensity for hydrophilic peptides were lower. Similarly, [AP][Cl] and [AP][Asc] and CHCA showed increased sensitivity for hydrophilic peptides and suppressed the detection of hydrophobic peptides. It was observed that CHCA, [AP][Asc], and [AP][Cl], showed good affinity for hydrophilic peptides. In ongoing work, these GUMBOS-based matrices and others are being used to enhance and selectively detect peptides in tissue samples for MALDI imaging.

2.5 References

[1] K. Dreisewerd. Recent methodological advances in MALDI mass spectrometry. *Anal. Bioanal. Chem.* **2014**, *406*, 2261.

[2] D. Ropartz, P. E. Bodet, C. Przybylski, F. Gonnet, R. Daniel, M. Fer, W. Helbert, D. Bertrand, H. Rogniaux. Performance evaluation on a wide set of matrix-assisted laser desorption ionization matrices for the detection of oligosaccharides in a high-throughput mass spectrometric screening of carbohydrate depolymerizing enzymes. *Rapid Commun. Mass Spectrom.* **2011**, *25*, 2059.

[3] E. Krause, H. Wenschuh, P. R. Jungblut. The dominance of arginine-containing peptides in MALDI-derived tryptic mass fingerprints of proteins. *Anal. Chem.* **1999**, *71*, 4160.

[4] L. K. Zhang, M. L. Gross. Matrix-assisted laser desorption/ionization mass spectrometry methods for oligodeoxynucleotides: Improvements in matrix, detection limits, quantification, and sequencing. *J. Am. Soc. Mass Spectrom.* **2000**, *11*, 854.

[5] J. Krause, M. Stoeckli, U. P. Schlunegger. Studies on the selection of new matrices for ultraviolet matrix-assisted laser desorption/ionization time-of-flight mass spectrometry. *Rapid Commun. Mass Spectrom.* **1996**, *10*, 1927.

[6] M. Towers, R. Cramer. Liquid matrices for analyses by UV-MALDI mass spectrometry. *Spectroscopy.* **2007**, *22*, 29.

[7] T. W. Jaskolla, W. D. Lehmann, M. Karas. 4-Chloro-alpha-cyanocinnamic acid is an advanced, rationally designed MALDI matrix. *Proc. Natl. Acad. Sci. U S A.* **2008**, *105*, 12200.

[8] D. W. Armstrong, L. K. Zhang, L. F. He, M. L. Gross. Ionic liquids as matrixes for matrix-assisted laser desorption/ionization mass spectrometry. *Anal. Chem.* **2001**, *73*, 3679.

[9] A. Tholey, E. Heinzle. Ionic (liquid) matrices for matrix-assisted laser desorption/ionization mass spectrometry-applications and perspectives. *Anal. Bioanal. Chem.* **2006**, *386*, 24.

[10] S. I. Snovida, V. C. Chen, H. Perreault. Use of a 2,5-dihydroxybenzoic acid/aniline MALDI matrix for improved detection and on-target derivatization of glycans: A preliminary report. *Anal. Chem.* **2006**, *78*, 8561.

[11] C. D. Calvano, S. Carulli, F. Palmisano. Aniline/alpha-cyano-4-hydroxycinnamic acid is a highly versatile ionic liquid for matrix-assisted laser desorption/ionization mass spectrometry. *Rapid Commun. Mass Spectrom.* **2009**, *23*, 1659.

[12] J. D. Leszyk. Evaluation of the new MALDI matrix 4-chloro-alpha-cyanocinnamic acid. *J. Biomol. Tech.* **2010**, *21*, 81.

[13] M. Rohmer, B. Meyer, M. Mank, B. Stahl, U. Bahr, M. Karas. 3-Aminoquinoline acting as matrix and derivatizing agent for MALDI MS analysis of oligosaccharides. *Anal. Chem.* **2010**, *82*, 3719.

[14] K. S. Lovejoy, G. M. Purdy, S. Iyer, T. C. Sanchez, A. Robertson, A. T. Koppisch, R. E. Del Sesto. Tetraalkylphosphonium-based ionic liquids for a single-step dye extraction/MALDI MS analysis platform. *Anal. Chem.* **2011**, *83*, 2921.

[15] N. Smargiasso, L. Quinton, E. De Pauw. 2-Aminobenzamide and 2-aminobenzoic acid as new MALDI matrices inducing radical mediated in-source decay of peptides and proteins. *J. Am. Soc. Mass Spectrom.* **2012**, *23*, 469.

[16] J. Jacksen, A. Emmer. Evaluation of 2,6-dihydroxyacetophenone as matrix-assisted laser desorption/ionization matrix for analysis of hydrophobic proteins and peptides. *Anal. Biochem.* **2012**, *425*, 18.

[17] Y. Fukuyama, R. Tanimura, K. Maeda, M. Watanabe, S. Kawabata, S. Iwamoto, S. Izumi, K. Tanaka. Alkylated dihydroxybenzoic acid as a MALDI matrix additive for hydrophobic peptide analysis. *Anal. Chem.* **2012**, *84*, 4237.

[18] K. B. Green-Church, P. A. Limbach. Matrix-assisted laser desorption/ionization mass spectrometry of hydrophobic peptides. *Anal. Chem.* **1998**, *70*, 5322.

[19] Y. Fukuyama, C. Nakajima, K. Furuichi, K. Taniguchi, S. I. Kawabata, S. Izumi, K. Tanaka. Alkylated trihydroxyacetophenone as a MALDI matrix for hydrophobic peptides. *Anal. Chem.* **2013**, *85*, 9444.

[20] J. L. Norris, R. M. Caprioli. Analysis of tissue specimens by matrix-assisted laser desorption/ionization imaging mass spectrometry in biological and clinical research. *Chem. Rev.* **2013**, *113*, 2309.

[21] G. A. Breaux, K. B. Green-Church, A. France, P. A. Limbach. Surfactant-aided, matrix assisted laser desorption/ionization mass spectrometry of hydrophobic and hydrophilic peptides. *Anal. Chem.* **2000**, *72*, 1169.

[22] P. Zollner, E. R. Schmid, G. Allmaier. K-4 Fe(CN)(6) /glycerol - A new liquid matrix system for matrix-assisted laser desorption/ionization mass spectrometry of hydrophobic compounds. *Rapid Commun. Mass Spectrom.* **1996**, *10*, 1278.

[23] S. Trimpin, S. Keune, H. J. Rader, K. Mullen. Solvent-free MALDI-MS: Developmental improvements in the reliability and the potential of MALDI in the analysis of synthetic polymers and giant organic molecules. *J. Am. Soc. Mass Spectrom.* **2006**, *17*, 661.

[24] S. Trimpin, M. L. Deinzer. Solvent-free MALDI-MS for the analysis of a membrane protein via the mini ball mill approach: Case study of bacteriorhodopsin. *Anal. Chem.* **2007**, *79*, 71.

[25] K. L. Schey, D. I. Papac, D. R. Knapp, R. K. Crouch. Matrix-assisted laser desorption mass-spectrometry of rhodopsin and bacteriorhodopsin. *Biophys. J.* **1992**, *63*, 1240.

[26] L. Przybilla, J. D. Brand, K. Yoshimura, H. J. Rader, K. Mullen. MALDI-TOF mass spectrometry of insoluble giant polycyclic aromatic hydrocarbons by a new method of sample preparation. *Anal. Chem.* **2000**, *72*, 4591.

[27] K. M. Ostermann, A. Luf, N. M. Lutsch, R. Dieplinger, T. P. Mechtler, T. F. Metz, R. Schmid, D. C. Kasper. MALDI orbitrap mass spectrometry for fast and simplified analysis of novel street and designer drugs. *Clin. Chim. Acta.* **2014**, *433C*, 254.

[28] H. N. Abdelhamid, M. S. Khan, H. F. Wu. Design, characterization and applications of new ionic liquid matrices for multifunctional analysis of biomolecules: A novel strategy for pathogenic bacteria biosensing. *Anal. Chim. Acta.* **2014**, *823*, 51.

[29] S. J. Gabriel, D. Pfeifer, C. Schwarzinger, U. Panne, S. M. Weidner. Matrix-assisted laser desorption/ionization time-of-flight mass spectrometric imaging of synthetic polymer sample spots prepared using ionic liquid matrices. *Rapid Commun. Mass Spectrom.* **2014**, *28*, 489.

[30] J. Yang, R. M. Caprioli. Matrix pre-coated targets for high throughput MALDI imaging of proteins. *J. Mass Spectrom.* **2014**, *49*, 417.

[31] S. Carda-Broch, A. Berthod, D. W. Armstrong. Ionic matrices for matrix-assisted laser desorption/ionization time-of-flight detection of DNA oligomers. *Rapid Commun. Mass Spectrom.* **2003**, *17*, 553.

[32] A. Berthod, J. A. Crank, K. L. Rundlett, D. W. Armstrong. A second-generation ionic liquid matrix-assisted laser desorption/ionization matrix for effective mass spectrometric analysis of biodegradable polymers. *Rapid Commun. Mass Spectrom.* **2009**, *23*, 3409.

[33] J. A. Crank, D. W. Armstrong. Towards a second generation of ionic liquid matrices (ILMs) for MALDI-MS of peptides, proteins, and carbohydrates. *J. Am. Soc. Mass Spectrom.* **2009**, *20*, 1790.

[34] Y. Fukuyama, N. Funakoshi, K. Takeyama, Y. Hioki, T. Nishikaze, K. Kaneshiro, S. Kawabata, S. Iwamoto, K. Tanaka. 3-Aminoquinoline/p-Coumaric acid as a MALDI matrix for glycopeptides, carbohydrates, and phosphopeptides. *Anal. Chem.* **2014**, *86*, 1937.

[35] P. K. S. Magut, S. Das, V. E. Fernand, J. Losso, K. McDonough, B. M. Naylor, S. Aggarwal, I. M. Warner. Tunable cytotoxicity of rhodamine 6G via anion variations. *J. Am. Chem. Soc.* **2013**, *135*, 15873.

[36] N. Siraj, F. Hasan, S. Das, L. W. Kiruri, K. E. S. Gall, G. A. Baker, I. M. Warner. Carbazole-derived group of uniform materials based on organic salts: Solid state

fluorescent analogues of ionic liquids for potential applications in organic-based blue light-emitting diodes. *J. Phys. Chem. C.* **2014**, *118*, 2312.

[37] N. Deng, M. Li, L. J. Zhao, C. F. Lu, S. L. de Rooy, I. M. Warner. Highly efficient extraction of phenolic compounds by use of magnetic room temperature ionic liquids for environmental remediation. *J. Hazard Mater.* **2011**, *192*, 1350.

[38] A. N. Jordan, S. Das, N. Siraj, S. L. de Rooy, M. Li, B. El-Zahab, L. Chandler, G. A. Baker, I. M. Warner. Anion-controlled morphologies and spectral features of cyanine-based nanoGUMBOS - an improved photosensitizer. *Nanoscale.* **2012**, *4*, 5031.

[39] S. Kjellstrom, O. N. Jensen. In situ liquid-liquid extraction as a sample preparation method for matrix-assisted laser desorption/ionization MS analysis of polypeptide mixtures. *Anal. Chem.* **2003**, *75*, 2362.

[40] A. Poetsch, D. Schlusener, C. Florizone, L. Eltis, C. Menzel, M. Rogner, K. Steinert, U. Roth. Improved identification of membrane proteins by MALDI-TOF MS/MS using vacuum sublimated matrix spots on an ultraphobic chip surface. *J. Biomol. Technol.* **2008**, *19*, 129.

[41] X. J. Chen, J. A. Carroll, R. C. Beavis. Near-ultraviolet-induced matrix-assisted laser desorption/ionization as a function of wavelength. *J. Am. Soc. Mass Spectrom.* **1998**, *9*, 885.

[42] M. Sadeghi, A. Vertes. Crystallite size dependence of volatilization in matrix-assisted laser desorption ionization. *Appl. Surf. Sci.* **1998**, *127*, 226.

[43] T. Jaskolla, M. Karas, U. Roth, K. Steinert, C. Menzel, K. Reihs. Comparison between vacuum sublimed matrices and conventional dried droplet preparation in MALDI-TOF mass spectrometry. *J. Am. Soc. Mass Spectrom.* **2009**, *20*, 1104.

[44] O. Vorm, P. Roepstorff, M. Mann. Improved resolution and very high-sensitivity in MALDI TOF of matrix surfaces made by fast evaporation. *Anal. Chem.* **1994**, *66*, 3281.

[45] D. O'Hagan. Understanding organofluorine chemistry. An introduction to the C-F bond. *Chem. Soc. Rev.* **2008**, *37*, 308.

[46] L. Goodman, H. B. Gu, V. Pophristic. Gauche effect in 1,2-difluoroethane. Hyperconjugation, bent bonds, steric repulsion. *J. Phys. Chem. A.* **2005**, *109*, 1223.

CHAPTER 3: SELECTIVE BINDING AFFINITIES OF AP AND AP-BASED GUMBOS FOR HYDROPHOBIC AND HYDROPHILIC PEPTIDES IN MALDI MS

3.1 Introduction

With advantages such as rapid analysis, mass accuracy, good resolution, and high sensitivity, matrix assisted laser desorption ionization (MALDI) mass spectrometry has been widely used to determine the molecular weight of both hydrophobic and hydrophilic biomolecules.[1-4] Moreover, MALDI, unlike other techniques, can be used to detect mixtures of analytes on samples, such as tissues.[5, 6]

Matrix is one of the key components of the MALDI analysis. Here, we have introduced new matrices with variable hydrophobicity. A clear understanding of the interaction between MALDI matrix and analytes is imperative to obtain good performance. Biomolecules possess both hydrophobic and/or hydrophilic properties depending on the amino acids they are composed of. Those biomolecules that mostly have hydrophobic amino acids are hydrophobic; however, some biomolecules exhibit both properties, which enable amphiphilic molecules to interact with them. [7-10] Various methods, such as confocal laser scanning microscopy,[11] MALDI imaging,[12] scanning electron microscopy,[13, 14] and X-ray crystallography[15] have been used to study the incorporation of analytes within the matrix. Dai *et al*[16] demonstrated that confocal microscopy could be used to provide information on the distribution and incorporating analyte within a matrix by using either different sample preparation techniques or morphologies of MALDI crystals. Additionally, MALDI imaging was used to study the distribution of analyte on the matrix.[1, 13, 16]

Hydrophobic biomolecules are difficult to detect using MALDI-MS because of their poor solubility in polar solvents.[2] As a result, surfactants have been used to improve the solubility of hydrophobic biomolecules in aqueous media.[2] However, binding of the biomolecules to the surfactant may occur depending on the properties of the surfactant used.[4, 8] Although surfactants can be beneficial, they have limitations and can adversely affect both mass accuracy and signal to noise ratio.[17]

The function of the group and structure present in biomolecules can be understood by their interaction with surfactants, which have been studied using various model proteins and properties of surfactant.[18-21] The hydrophobic bulky moieties of surfactants have been used to attract hydrophobic moieties of analytes.[22] Anionic surfactants, for example, sodium dodecyl sulfate (SDS) bind strongly with the protein bovine serum albumin (BSA), causing denaturation.[23, 24] However, anionic and cationic surfactants show a lower tendency to interact with proteins because the electrostatic interaction based on the pH is used. Both cationic and anionic surfactants show similar binding isotherm shapes when used with the same protein. [7]

The Warner research group has recently introduced a new class of materials defined as a ***g***roup of ***u***niform ***m***aterials ***b***ased on ***o***rganic ***s***alts (GUMBOS) that have melting points between 25 °C to 250°C.[25-27] They have similar physical and chemical properties as frozen ionic liquids, but have melting points from 25 to 100°C. GUMBOS are frequently composed of bulky organic anions and cations: however, similar to ionic liquids, the properties of GUMBOS can be tuned by changing one of the ions.[28]

In order to overcome the challenges faced with matrix–analyte combinations in MALDI in the present study, we have developed a series of AP and AP-based GUMBOS

using various counter anions in order to tune their hydrophobicities for use as MALDI matrices. The interaction of the MALDI matrices with gramicidin, a hydrophobic peptide, and angiotensin II, a hydrophilic peptide, was studied using absorbance and fluorescence spectroscopy. Scatchard analysis and fluorescence anisotropy studies were then performed to compare the behavior of hydrophobic and hydrophilic peptides with the matrices. The results showed that the interaction between the matrices and the analytes varied with the hydrophobicity of both components. Decreasing the hydrophobicity of the matrix resulted in an increased interaction with hydrophilic analytes. Binding studies between matrices and peptides were used to better understand the mechanism of interaction between peptides and matrices. In this study, α-cyano-4-hydroxycinnamic acid (CHCA) was used as a control.

3.2 Experimental

3.2.1 Materials

The reagents (CHCA), acetonitrile, acetone, methanol, ethanol, trifluoroacetic acid (TFA, 99%), bis(trifluoromethane) sulfonimide ($HNTf_2$, 99.95%), ascorbic acid (Asc,99%), and 1-aminopyrene (AP, 98%) were purchased from Sigma-Aldrich. Gramicidin, valinomycin, and angiotensin II, were purchased from Sigma-Aldrich. All chemicals were received and used without further purification.

3.2.2 Instrumentation

3.2.2.1 MALDI-TOF-MS Analysis

All mass spectrometry experiments were performed using an UltrafleXtreme (Bruker, Bremen, Germany), equipped with a frequency tripled Nd: YAG laser at (355

nm) and pulse duration of 3 ns was used for ionization. All the experiments were obtained using positive ion reflectron mode with the ion acceleration potential of 25 kV. Finally, laser shots amounted to one thousand shots for each spectrum; data were processed using Flex Analysis 3.3 software (Bruker); and the matrix solution consisted of 10 mg/mL CHCA in 2:1 acetonitrile and 0.1% TFA which was prepared in water.

3.2.2.2 Fluorescence Spectra

Fluorescence emission spectra were obtained using a Spex Fluorolog-3 (Jobin Yvon, Edison, NJ) at room temperature equipped with a 450-W xenon lamp and R928P photomultiplier tube (PMT) emission detector. A 0.4 cm quartz cuvette was used. An excitation at a wavelength of 280 nm was used due to the presence of tryptophan. Emission spectra were collected between 290 – 400 nm.

3.2.2.3 Determination of Binding Parameters of CHCA, AP, and AP-based GUMBOS to Peptides

A titration procedure was used to estimate the strength of binding of CHCA, AP, and AP-based GUMBOS with the two peptides employed in this study. The concentration of the peptides was 10 μM and the concentration of the matrices ranged from 0 to 100 μM. The data of the Scatchard analysis was employed to determine the binding isotherms, stoichiometries, and dissociation constants.[29-31] In biological systems, there is a receptor for the binding of ligands, L. The number of ligands binding per site, the binding constants, and the regions of binding were determined using Scatchard plots. The various parameters used to interpret the resulting Scatchard plot are described below;

The fraction of matrix bound is given by

$$\alpha = (I-I_o)/(I_m-I_o)\ , \qquad (1)$$

and the concentration of the bound matrix is

$$M_b = \alpha\ [\text{total concentration}]\ , \qquad (2)$$

where I_o is the fluorescence intensity of the peptide without matrix, I is fluorescence intensity when the peptide and matrix are in equilibrium, and I_m represents fluorescence intensity when the peptide is completely saturated with the matrix. Free matrix concentration was determined by 1-[bound matrix]. The parameter, ν, is defined as α[total matrix]/[total peptide], and free matrix concentration C was obtained from [total matrix](1-α). Equilibrium binding constant, (k), was determined by the linear portion of scatchard plot ($\frac{\nu}{C}$ vs ν). Binding sites (n) were quantified using different regions of concentrations.

3.2.2.4 Determination of Fluorescence Anisotropy of CHCA, AP, and AP-based GUMBOS to Peptides

Fluorescence anisotropy, r, measures the average angular displacement of the fluorophore and can be calculated using the following equation:

$$r = \frac{I_{vv}-GI_{vh}}{I_{vv}+2GI_{vh}}\ , \qquad (3)$$

where I_{vv} and I_{vh} are the fluorescence emission intensity measured parallel or perpendicular to the vertically polarized excitation, respectively. *G* represents the grating factor, which is included to correct for the wavelength dependent response of the polarization of the emission, the detector, and optics. [26]

3.3 Results and Discussion

3.3.1 MALDI Analysis

MALDI-MS detection of hydrophobic biomolecules remains difficult due to the inherent hydrophilicity of most MALDI matrices. In this study, 1-aminopyrene (AP) and AP-based GUMBOS were investigated as MALDI matrices for hydrophobic peptides, then their performance was evaluated in terms of selectivity towards two peptides, gramicidin, a hydrophobic peptide, and the angiotensin II, a hydrophilic peptide. AP was selected specifically for these studies because it exhibits strong absorption at the appropriate laser wavelength; as well, it displays hydrophobic characteristics and the ability to protonate the analytes. In this study, we synthesized and tested a series of AP-based GUMBOS including [AP][ascorbate] ([AP][Asc]), and [AP][bis(trifluoromethane) sulfonamide] ([AP][NTf_2]).[27] The relative hydrophobicity of these compounds and conventional MALDI matrix, CHCA, was estimated by measuring their 1-octanol/water partition coefficients ($K_{o/w}$). The relative hydrophobicity occurs in the following order CHCA=(-1.72) << [AP][Asc]=(0.81)< AP < [AP][NTf_2]=(1.54). The compounds were then evaluated as MALDI matrices for analysis of hydrophobic (gramicidin) as well as hydrophilic (angiotensin II) peptides. An equimolar amount of hydrophobic and hydrophilic peptide were mixed and analyzed using AP and AP-based GUMBOS in comparison with CHCA, a conventional matrix for peptides. Angiotensin II and gramicidin showed peaks at *m/z* 1046.54 and 1904.06, respectively, which corresponds to the sodiated adduct $[M+Na]^+$. Figure 3.1 and 3.2 show the MALDI mass spectra of angiotensin II and gramicidin mixture as analyzed using AP and [AP][Asc] as matrices. The positive ion mode mass spectra of a mixture containing the same concentration of

peptides using AP and [AP][Asc] as matrices reveal a clear difference in signal with variation in signal intensity due to the hydrophobicity of matrices. In (Figure 3.2), the matrix [AP][Asc], which is less hydrophobic than AP, detected angiotensin II, a hydrophilic peptide, with higher intensity than gramicidin. Conversely, when AP was used as a matrix, gramicidin was detected with higher signal intensity than angiotensin II (Figure 3.1). When CHCA, the most hydrophilic matrix, was used, angiotensin II was detected with higher intensity than gramicidin,(Figure 3.3). When [AP][NTf_2], the most hydrophobic matrix, was used gramicidin detected with higher intensity than angiotensin II (Figure 3.4). These results reveal that AP improved the signal of hydrophobic peptides. The selective detection of hydrophobic or hydrophilic peptides by variation of hydrophobicities of the matrix materials implies some specific interactions between the matrix and analyte, such as cooperative binding, which will be investigated in the later sections of this study.

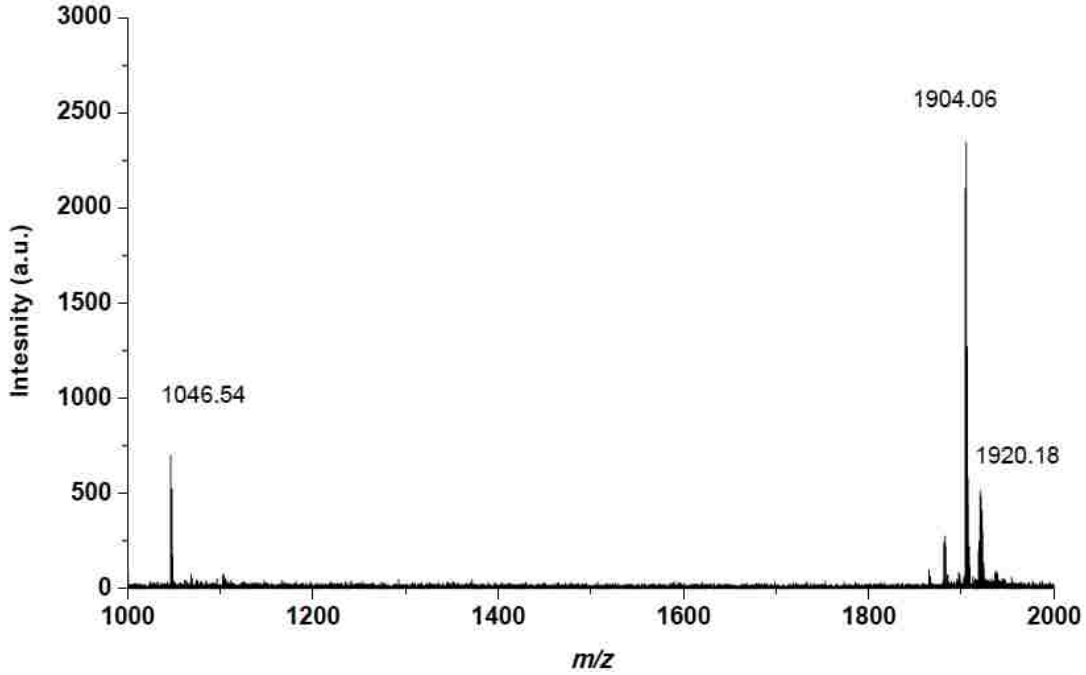

Figure 3.1. MALDI mass spectra of a mixture of gramicidin (hydrophobic) and angiotensin II (hydrophilic) with (AP Log $K_{(o/w)}$=1.42).

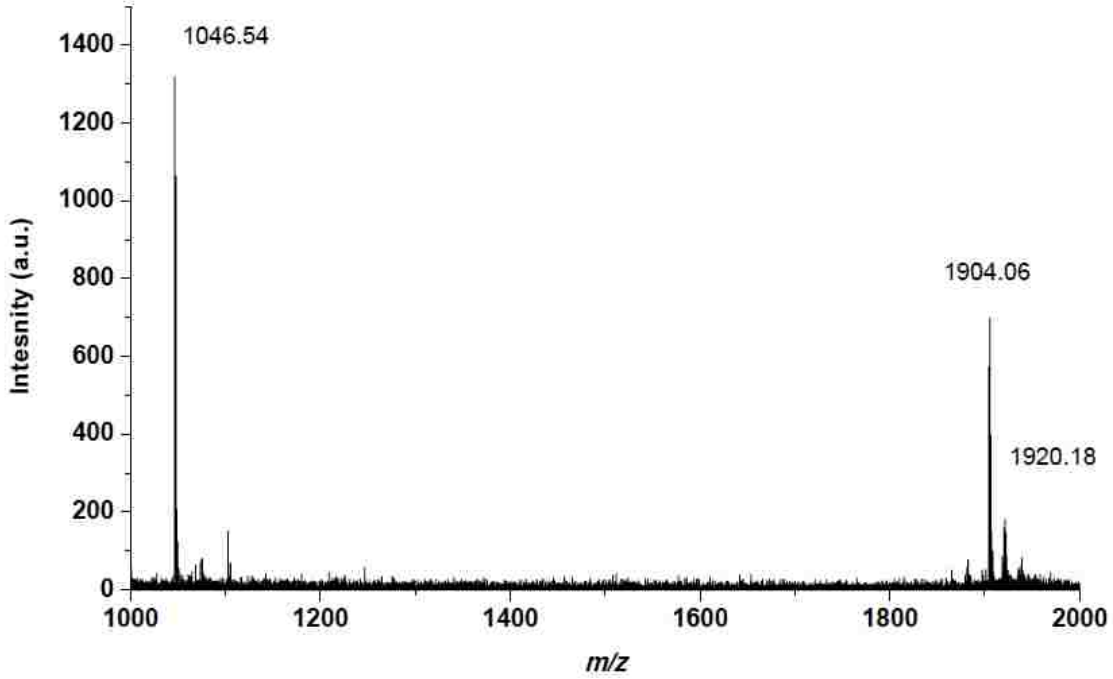

Figure 3.2. MALDI mass spectra of a mixture of gramicidin (hydrophobic) and angiotensin II (hydrophilic) with [AP][Asc] Log $K_{(o/w)}$ =0.81.

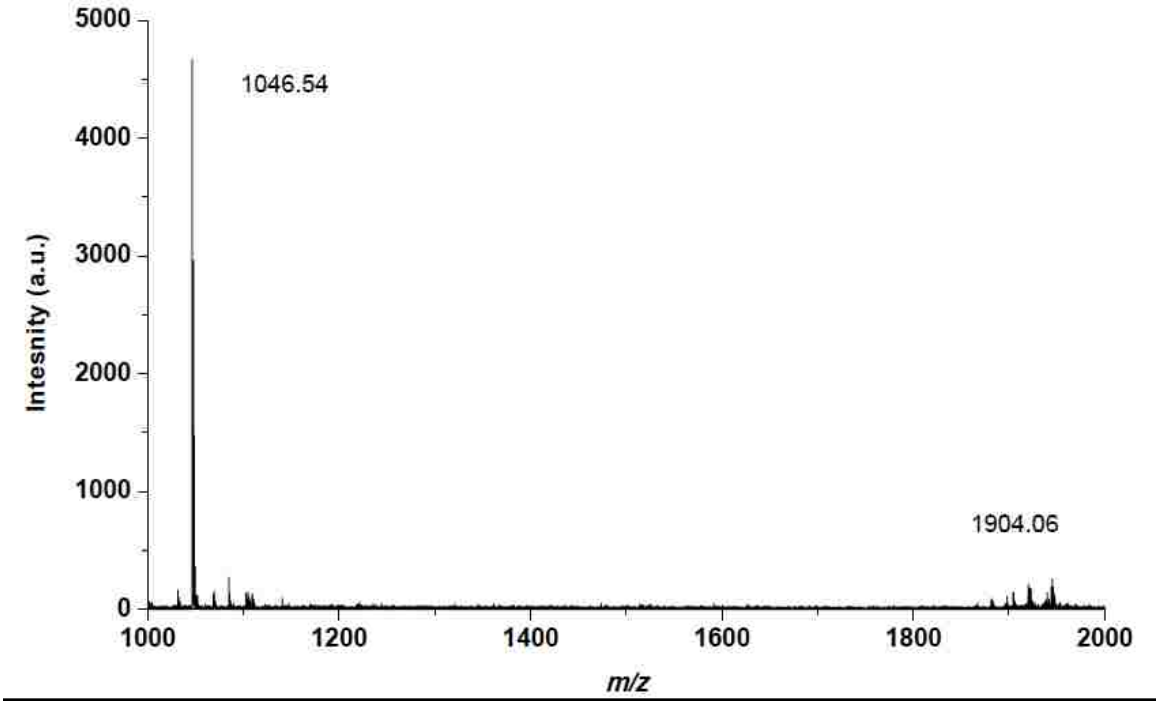

Figure 3.3. MALDI mass spectra of a mixture of gramicidin (hydrophobic) and angiotensin II (hydrophilic) with A) CHCA Log $K_{(o/w)}$ =(-1.72).

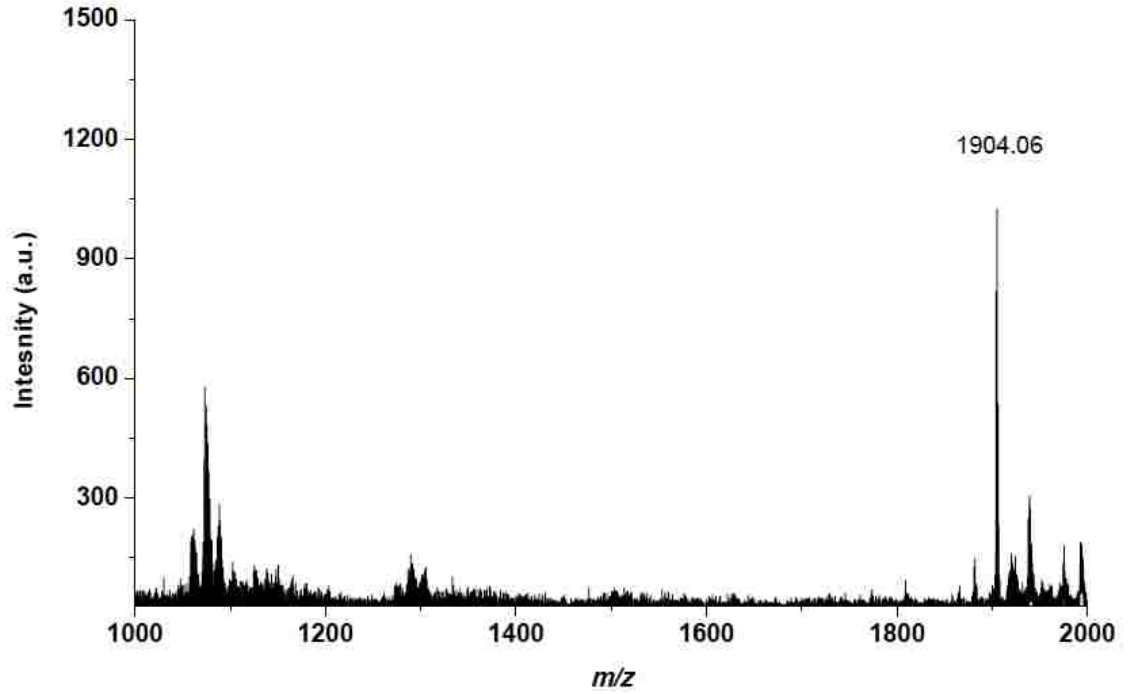

Figure 3.4. MALDI mass spectra of a mixture of gramicidin (hydrophobic) and angiotensin II (hydrophilic) with [AP]NTf_2] Log $K_{(o/w)}$ =1.54.

3.3.2 Spectral Studies of AP and AP-based GUMBOS

3.3.2.1 Absorbance and Fluorescence

The use of AP and AP-based GUMBOS as matrices in MALDI to detect biomolecules requires investigation of their affinity with the analyte, which can be studied using spectral behavior. Methanol solutions of AP and AP-based GUMBOS had similar absorbance spectra with a λ_{max} near 360 nm (Figure 3.5). Generally, the absorbance spectra of AP and each AP-based GUMBOS at 20 µM revealed that anion variations have an effect on the shape of the spectra. However, the absorbance varied slightly with anion. In the case of [AP][NTf_2], the spectrum had an absorption shoulder in the blue region relative to the main peak.

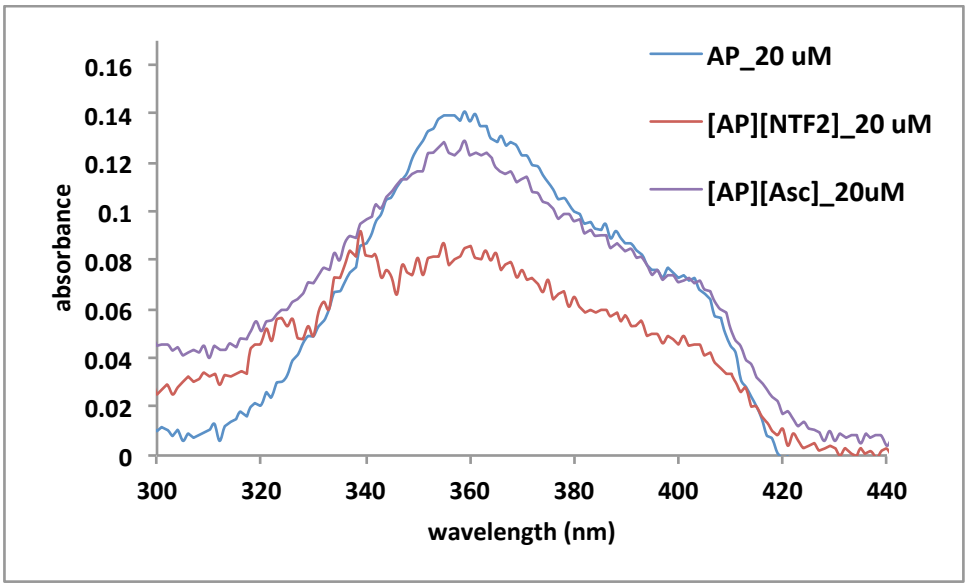

Figure 3.5. Absorbance spectra of 20 µM AP and AP-based GUMBOS. The solvent is methanol.

An intense emission signal from AP and AP-based GUMBOS appears at 426 nm with an excitation of 290 nm. The fluorescence excitation and emission spectra followed

the expected mirror-image rule (Figure 3.6). The Stokes shifts were similar regardless of the anion and ranged from 66 to 69 nm (Table 3.1). Thus, the anion didn't affect the fluorescence excitation and emission properties of these compounds significantly.

Table 3.1. Stokes shift for AP and AP-based GUMBOS.

Compounds	Absorbance (nm)	Emission (nm)	Stokes shift nm
AP	357	426	69
[AP][Asc]	360	426	66
[AP][NTf_2]	360	426	66

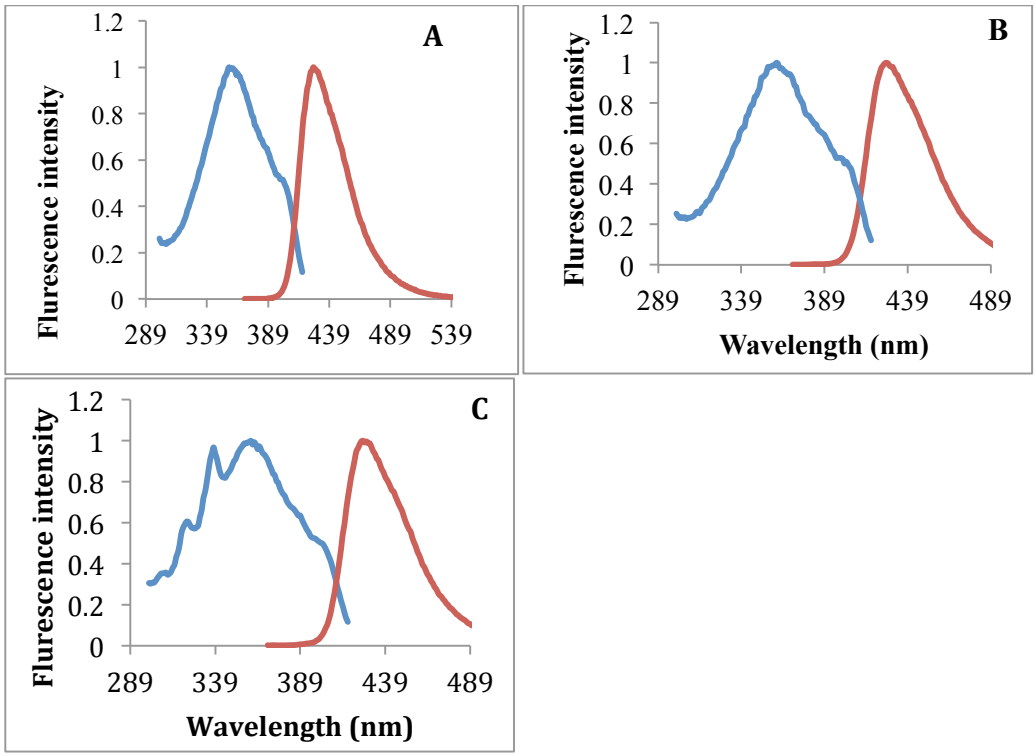

Figure 3.6. Normalized absorbance (Blue) and fluorescence emission (red) spectra of (A) AP, (B) [AP][Asc]and (C) [AP][NTf_2].

3.3.2.2 Binding Studies and Scatchard Analysis

The mechanism of ligand, in this case the GUMBOS matrix, binding to peptides was studied through excitation of tryptophan (trp), tyrosine (tyr), and phenylalanine (phe) amino acids by fluorescence.[31, 32] In this study, angiotensin II and gramicidin were chosen to study the binding between matrix and peptide. Both peptides have tryptophan (trp) residues, which absorb at 280 nm. In the absence of matrix, the fluorescence of angiotensin II and gramicidin had an emission band between 290 to 400 nm (Figure 3.7). The maximum emission wavelength was 328 nm for angiotensin II and 345 nm for gramicidin.

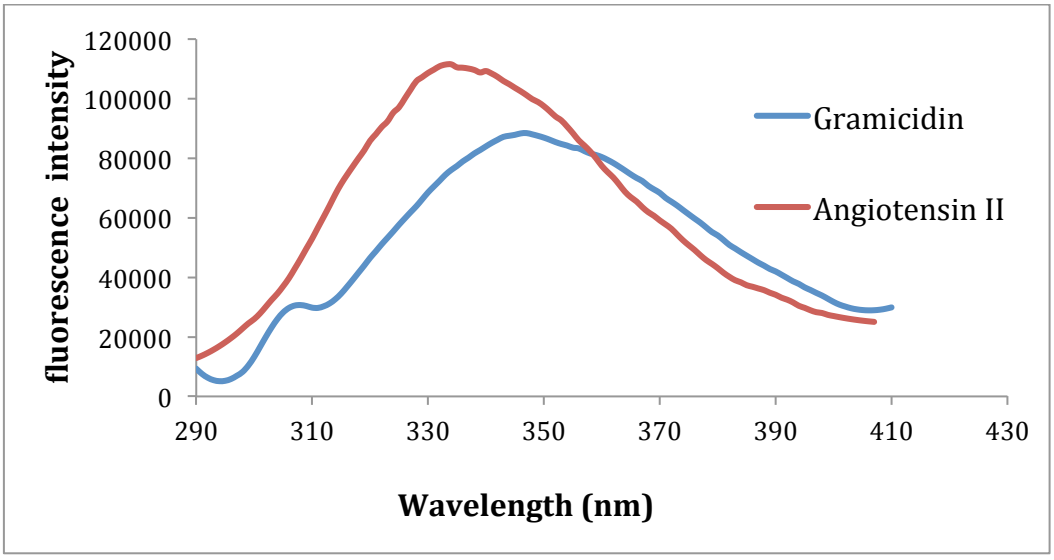

Figure 3.7. The fluorescence spectra of gramicidin and angiotensin II without the use in the absence of a matrix.

The fluorescence of both peptides was gradually quenched and red-shifted as the concentration of the matrix increased (Figure 3.8- 3.15).

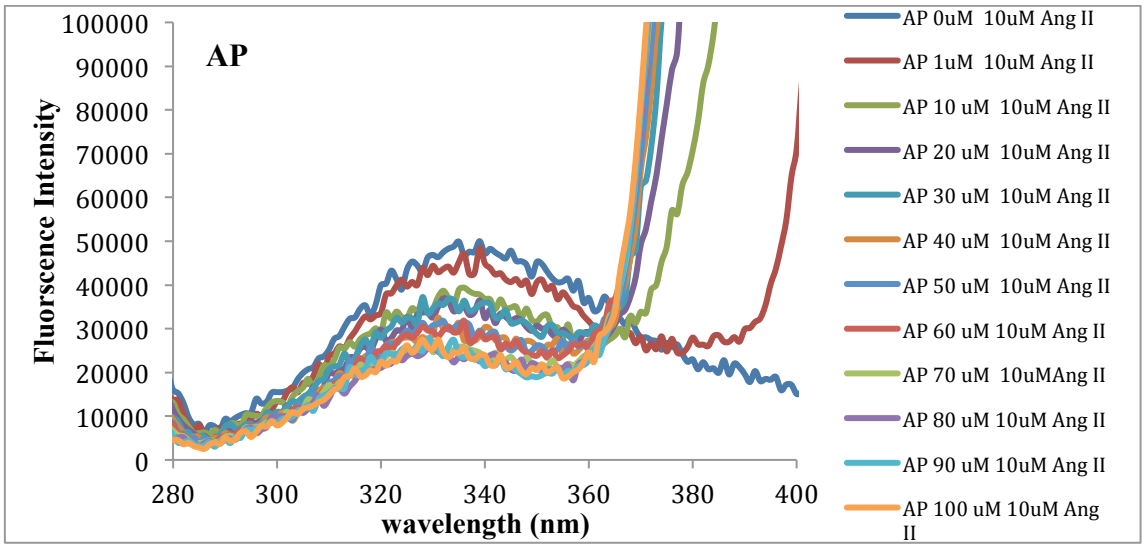

Figure 3.8. AP with 10 µM angiotensin II.

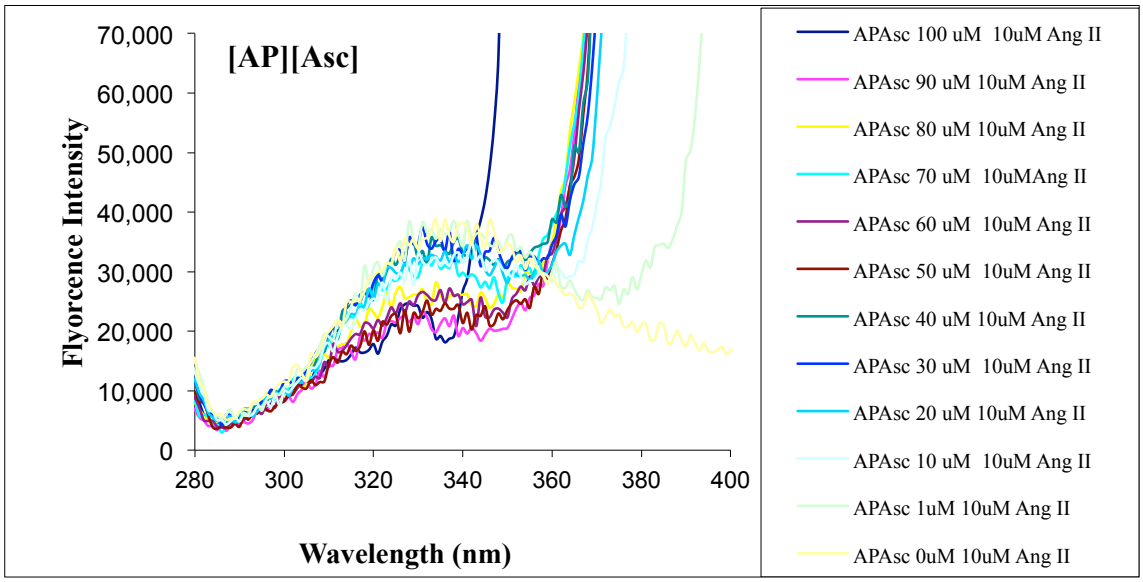

Figure 3.9. [AP][Asc] with 10 µM angiotensin II.

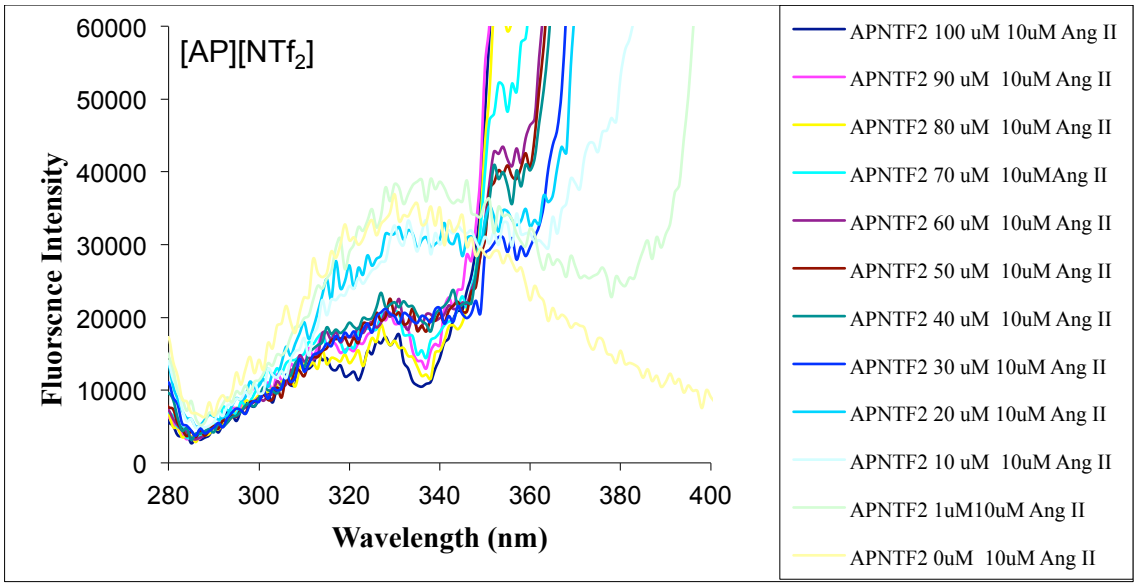

Figure 3.10. [AP][NTf_2] with 10 µM angiotensin II.

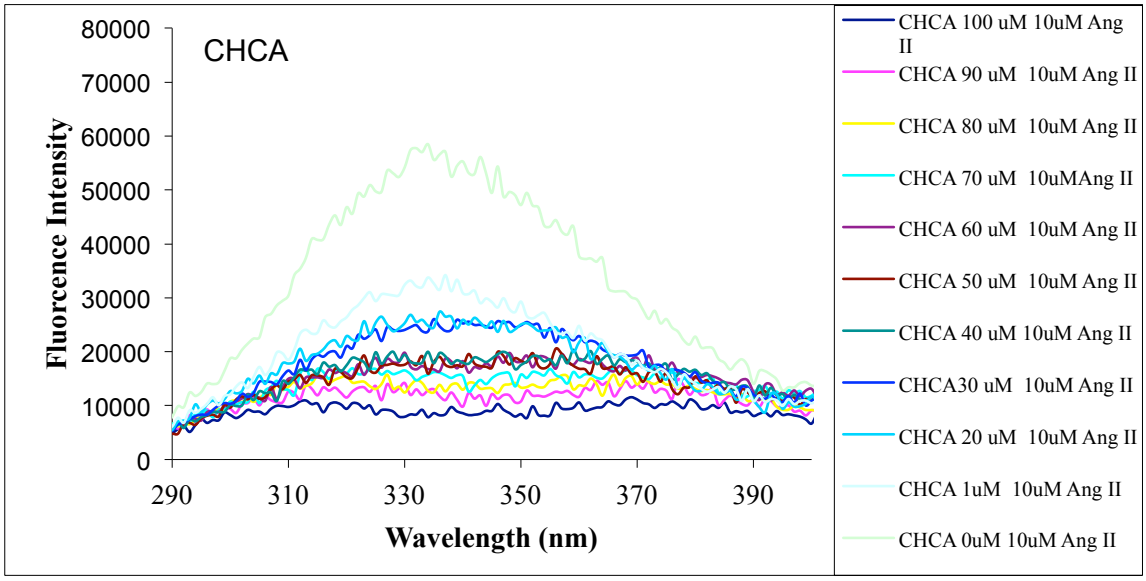

Figure 3.11. CHCA with 10 µM angiotensin II.

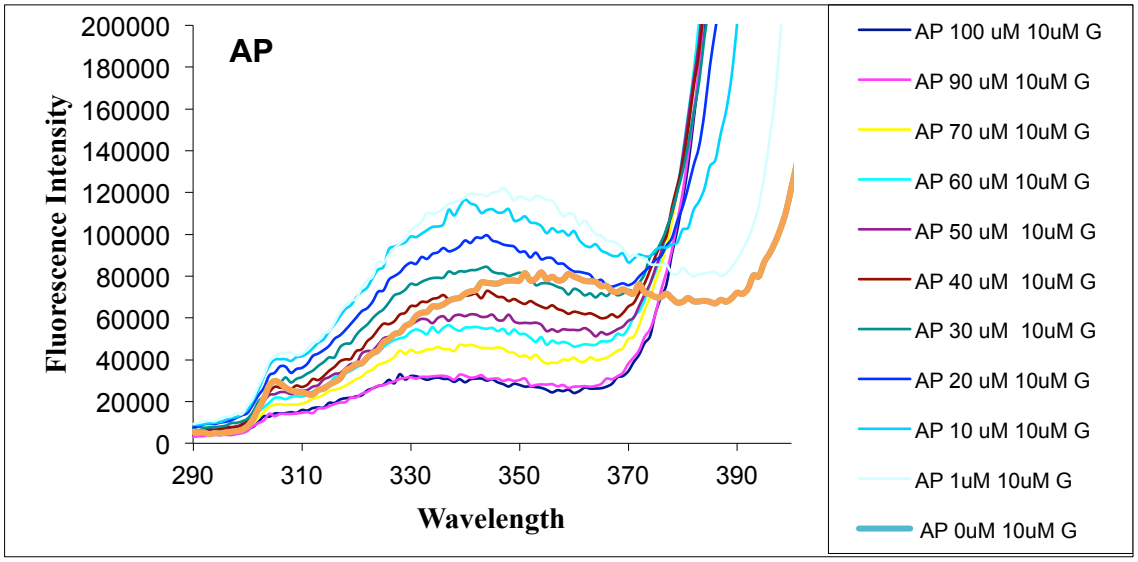

Figure 3.12. AP 10 µM Gramicidin.

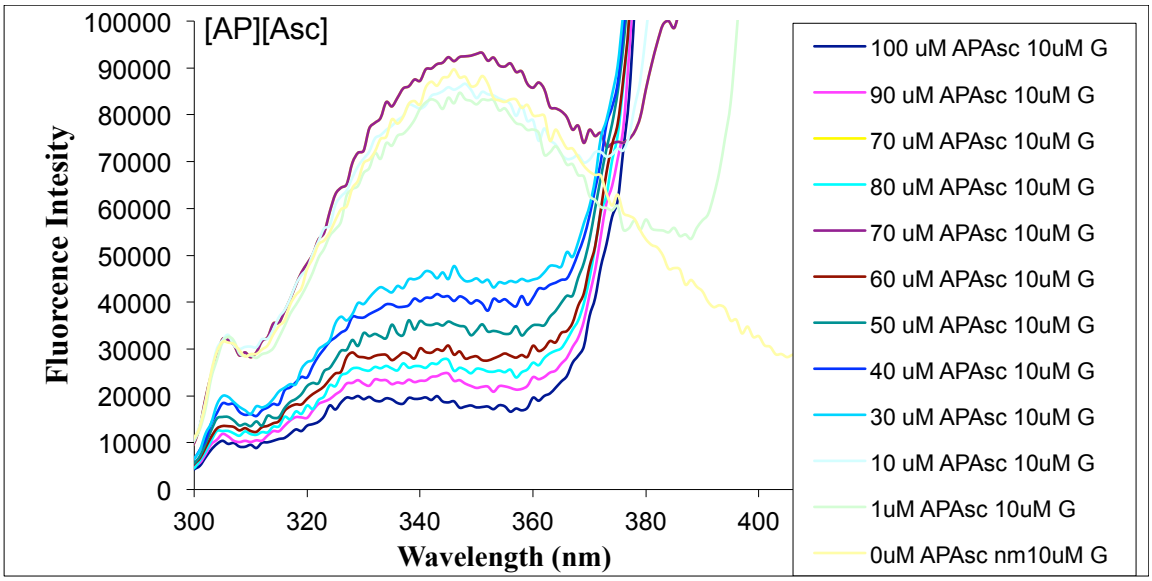

Figure 3.13. [AP][Asc] 10 µM Gramicidin.

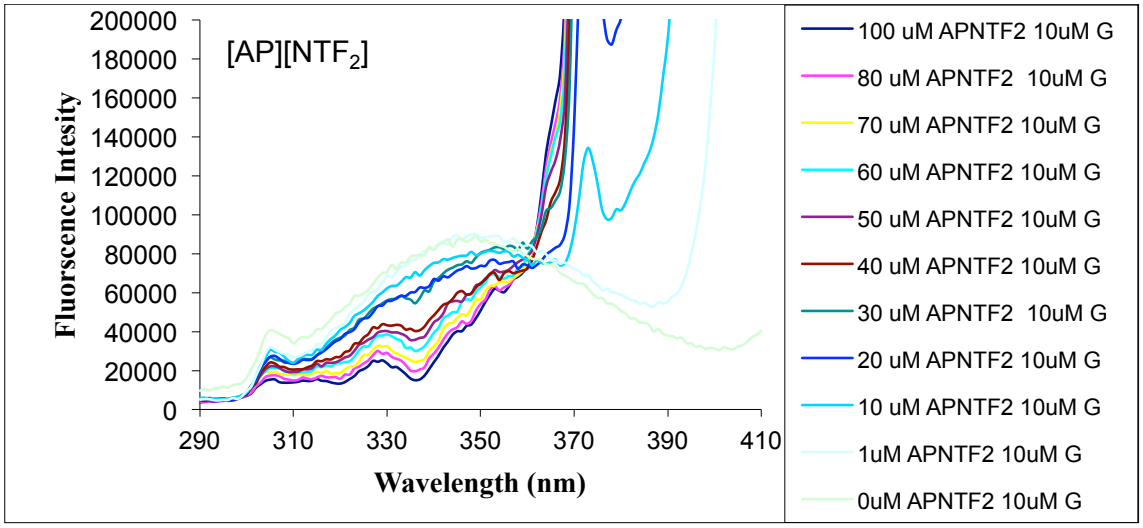

Figure 3.14. [AP][NTf_2] 10 µM Gramicidin.

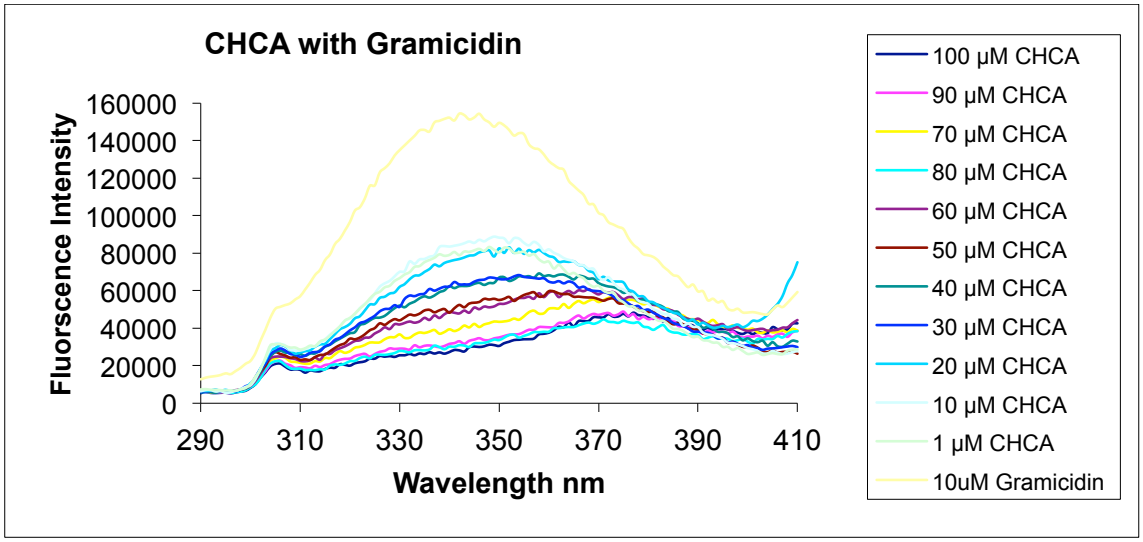

Figure 3.15. CHCA 10 µM Gramicidin.

Scatchard analysis was used in order to study the binding between matrices and peptides, which displayed four characteristic regions with increasing concentrations: specific binding, non-specific binding, negative cooperative binding, and positive binding.[33] There are four characteristic regions in the binding isotherm of an analyte with matrices as the concentration of matrices increases. Specific binding occurs when the interaction is electrostatic in nature and is associated with binding of matrix

monomers to the specific high-energy sites of the analytes. Non-cooperative binding occurs when the isotherm slowly increases and a plateau region may occur. Within this boundary the binding of matrices to biomolecules is unaffected. Another region is called the cooperative binding region where a massive increase in binding occurs due to allosteric binding effects. The last region occurs when the matrices become saturated, resulting in a plateau in the binding isotherm. This means the excess matrix is not binding to analyte.[9, 20, 31, 33]

The observed binding of angiotensin II with AP in the concentration range of 1 to 50 μM demonstrated several types of interactions. The first region was specific binding indicating strong interaction between the matrix and analyte whereas the second region was negative cooperative binding. The plot for AP with gramicidin also demonstrated two linear regions in the first region, from 1 to 30 μM, being the specific binding region and the second region, from 40 to 100 μM, being negative-cooperative binding suggesting similar type of interaction with both peptides. However, the binding constant for the binding of AP to the hydrophobic peptide gramicidin was 10 times higher than for the binding to the hydrophilic peptide angiotensin II (Table 3.2) and see appendix (Figure A1 to Figure A8). Table 3.2 shows the observations of the peptides binding with various matrices. Based on the binding constants, the hydrophobic matrix [AP][NTf_2] also exhibited strong binding with the hydrophobic peptide compared to the hydrophilic peptide. [AP][Asc] demonstrated a non-cooperative followed by negative cooperative binding with angiotensin II, whereas it demonstrated a specific, positive cooperative, and finally negative cooperative binding with gramicidin. The binding constant for this hydrophilic matrix binding to the hydrophilic peptide was much higher as compared to

the hydrophobic peptide, suggesting its capability of distinguishing the peptides in terms of hydrophobicities. The conventional MALDI matrix CHCA was found to exhibit a positive followed by a negative cooperative binding region with angiotensin II whereas with gramicidin the binding was mostly non-cooperative. However, the binding constant for binding with hydrophilic angiotensin and hydrophobic gramicidin was comparable. At low concentrations, AP displayed non-specific binding while AP based GUMBOS displayed specific binding with angiotensin II. Thus, similar to AP, [AP][NTf_2] had higher binding with gramicidin than angiotensin II. [AP][Asc] behaved differently from the hydrophobic matrices AP and [AP][NTf_2].

3.3.2.3 Fluorescence Anisotropy of CHCA, AP and AP-based GUMBOS

Results from fluorescence anisotropy studies of CHCA, AP, and AP-based GUMBOS are presented in (Figure 3.16-3.17). The anisotropy studies suggest the hydrophobic peptide (gramicidin) tends to bind more strongly to hydrophobic matrices (AP, and [AP][NTf_2]) and the greater the hydrophobicity of the matrices, the greater the strength of binding, as indicated by greater differences in anisotropies between bound and unbound states. In contrast, the same hydrophobic matrices show no specific tendency of binding to the hydrophilic peptide (angiotensin II), which is clearly indicated by the overlapping anisotropy values for both bound and unbound states. Similarly, the hydrophilic GUMBOS [AP][Asc] and conventionally used MALDI matrix, CHCA, which is very hydrophilic as observed from $K_{o/w}$, exhibited greater tendency of binding to the hydrophilic peptide angiotensin II and no specific binding to the hydrophobic peptide gramicidin. Thus, the result shows from these studies peptides can be differentiated based on their hydrophobicities by varying the hydrophobicities of matrices through careful

tuning of the GUMBOS counter anion. These results also help explain the performance of these GUMBOS as matrices in MALDI in order to distinguish between hydrophilic and hydrophobic peptides,

Table 3.2. Scatchard analysis data for the interaction of the hydrophobic peptide (gramicidin) and hydrophilic peptide (angiotensin II) with MALDI matrices (CHCA, AP and AP-based GUMBOS)

Peptide	Abbreviation	Concentration Range		Binding Constant (μM^{-1})
Angiotensin II	AP	1-50 µM	Specific Binding	9.49
		60-100 µM	- Cooperative Binding	
Gramicidin	AP	1-30 µM	Non-Specific Binding	19.05
		40-100 µM	Specific Binding	
Angiotensin II	[AP][Asc]	1-30µM	Specific Binding	7.52
		40 – 60 µM	+ Cooperative Binding	
		70 – 100 µM	-Cooperative Binding	
Gramicidin	[AP][Asc]	1-40µM	Specific Binding	0.12
		50-100 µM	Specific binding	
Angiotensin II	[AP][NTf_2]	1-60 µM	+ Cooperative Binding	8.33
		70- 100 µM	-Cooperative	
Gramicidin	[AP][NTf_2]	1-30µM	Specific	12.27
		40-90 µM	- Cooperative Binding	
Angiotensin II	CHCA	1-40	Non specific	12.72
		50-100 µM	- Cooperative Binding	
Gramicidin	CHCA	1-30 µM	- Cooperative binding	10.00
		40 – 80 µM	- Cooperative binding	

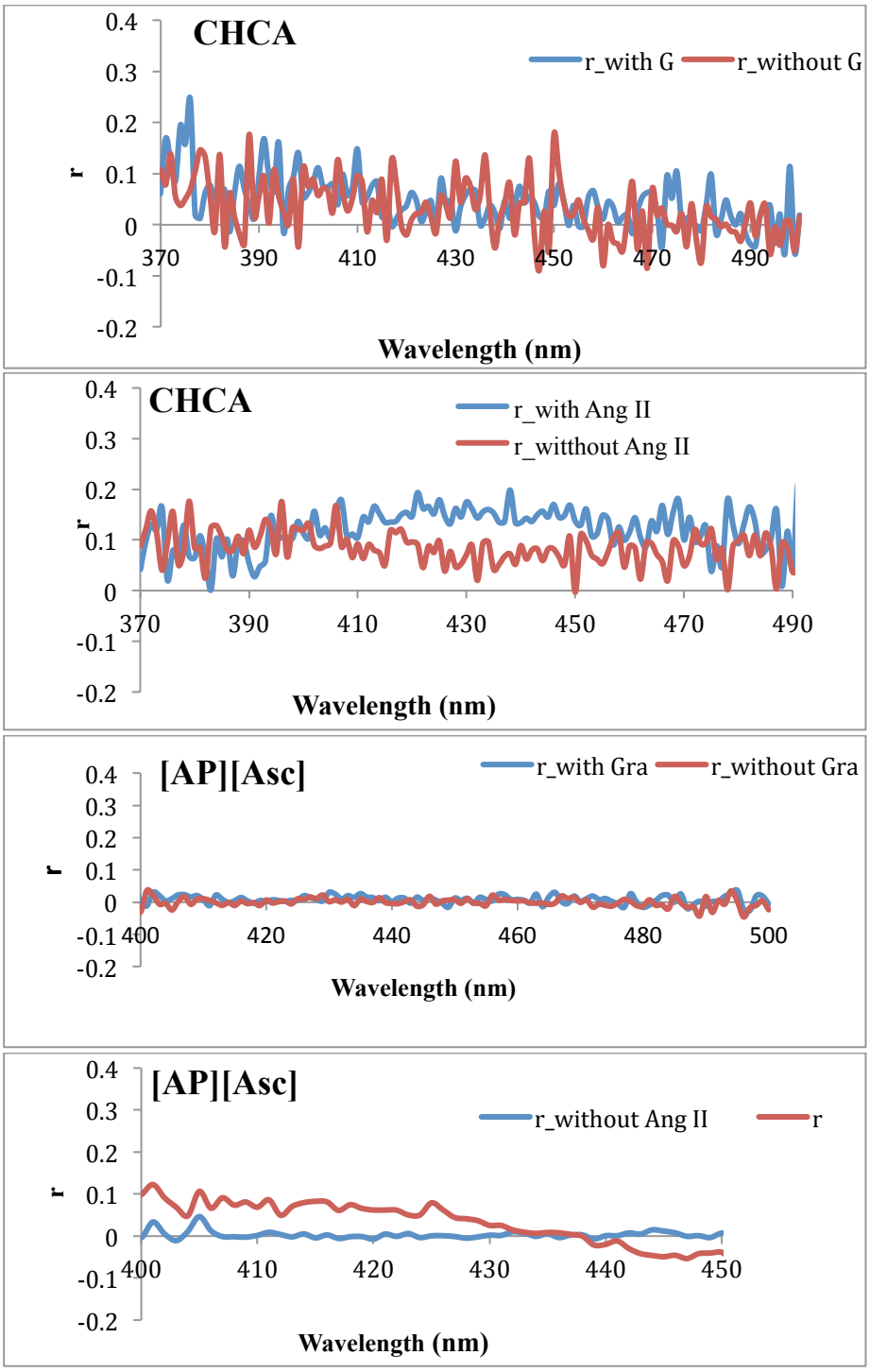

Figure 3.16. Fluorescence anistropy studies using a hydrophobic (gramicidin) and hydrophilic (angiotensin II) peptide with MALDI matrices (CHCA and [AP][Asc].

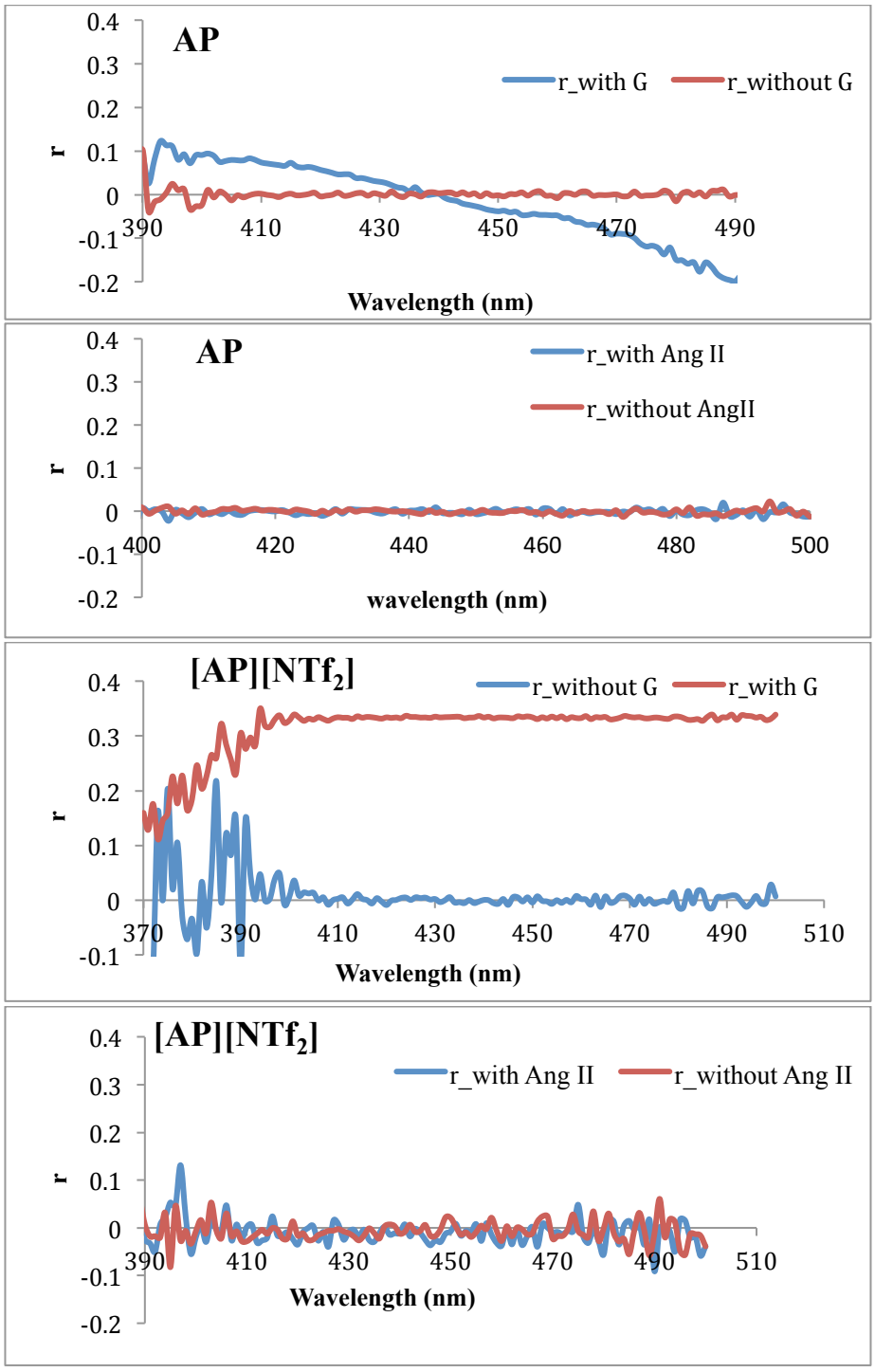

Figure 3.17. Fluorescence anistropy studies using a hydrophobic (gramicidin) and hydrophilic (angiotensin II) peptide with MALDI matrices (AP and [AP][NTf_2].

3.4 Conclusions

In this work we have demonstrated that AP and AP-based GUMBOS matrices selectively interact with both hydrophilic and hydrophobic peptides, even when mixed, based on their hydrophobicities. The hydrophilic matrices were selective to hydrophilic peptides while hydrophobic matrices were selective to hydrophobic peptides. AP and [AP][NTf_2] were more selective to hydrophobic analytes when hydrophilic and hydrophobic analytes were mixed at the same concentration. CHCA and [AP][Asc] showed good affinity for hydrophilic peptides. The binding studies demonstrated the binding between the matrix (hydrophobic or hydrophilic) and analyte was different in each case. The binding type and the binding constant were both found to be specific to the matrix/analyte combination. In ongoing work, these GUMBOS based matrices are being used to enhance and selectively detect hydrophobic compounds in tissue samples for MALDI imaging.

3.5 References

[1] Y. Fukuyama, R. Tanimura, K. Maeda, M. Watanabe, S. Kawabata, S. Iwamoto, S. Izumi, K. Tanaka. Alkylated dihydroxybenzoic acid as a MALDI matrix additive for hydrophobic peptide analysis. *Anal. Chem.* **2012**, *84*, 4237.

[2] G. A. Breaux, K. B. Green-Church, A. France, P. A. Limbach. Surfactant-aided, matrix assisted laser desorption/ionization mass spectrometry of hydrophobic and hydrophilic peptides. *Anal. Chem.* **2000**, *72*, 1169.

[3] K. B. Green-Church, P. A. Limbach. Matrix-assisted laser desorption/ionization mass spectrometry of hydrophobic peptides. *Anal. Chem.* **1998**, *70*, 5322.

[4] V. Mainini, P. M. Angel, F. Magni, R. M. Caprioli. Detergent enhancement of on-tissue protein analysis by matrix-assisted laser desorption/ionization imaging mass spectrometry. *Rapid Commun. Mass Spectrom.* **2011**, *25*, 199.

[5] R. M. Caprioli, T. B. Farmer, J. Gile. Molecular imaging of biological samples: Localization of peptides and proteins using MALDI-TOF MS. *Anal. Chem.* **1997**, *69*, 4751.

[6] B. Chatterji, A. Pich. MALDI imaging mass spectrometry and analysis of endogenous peptides. *Expert. Rev. Proteomics.* **2013**, *10*, 381.

[7] A. V. Few, R. H. Ottewill, H. C. Parreira. The interaction between bovine plasma albumin and dodecyltrimethylammonium bromide. *Biochim. Biophys. Acta.* **1955**, *18*, 136.

[8] A. Helenius, K. Simons. Solubilization of membranes by detergents. *Biochim. Biophys. Acta.* **1975**, *415*, 29.

[9] Y. J. Li, X. Y. Wang, Y. L. Wang. Comparative studies on interactions of bovine serum albumin with cationic gemini and single-chain surfactants. *J. Phys. Chem. B.* **2006**, *110*, 8499.

[10] P. D. McCrea, J. L. Popot, D. M. Engelman. Transmembrane topography of the nicotinic acetylcholine receptor delta subunit. *Embo. J.* **1987**, *6*, 3619.

[11] V. Horneffer, A. Forsmann, K. Strupat, F. Hillenkamp, U. Kubitscheck. Localization of analyte molecules in MALDI preparations by confocal laser scanning microscopy. *Anal. Chem.* **2001**, *73*, 1016.

[12] S. J. Gabriel, D. Pfeifer, C. Schwarzinger, U. Panne, S. M. Weidner. Matrix-assisted laser desorption/ionization time-of-flight mass spectrometric imaging of synthetic polymer sample spots prepared using ionic liquid matrices. *Rapid Commun. Mass Spectrom.* **2014**, *28*, 489.

[13] R. Tummala, K. B. Green-Church, P. A. Limbach. Interactions between sodium dodecyl sulfate micelles and peptides during matrix-assisted laser desorption/ionization mass spectrometry (MALDI-MS) of proteolytic digests. *J. Am. Soc. Mass Spectrom.* **2005**, *16*, 1438.

[14] A. Poetsch, D. Schlusener, C. Florizone, L. Eltis, C. Menzel, M. Rogner, K. Steinert, U. Roth. Improved identification of membrane proteins by MALDI-TOF MS/MS using vacuum sublimated matrix spots on an ultraphobic chip surface. *J. Biomol. Tech.* **2008**, *19*, 129.

[15] J. Kampmeier, K. Dreisewerd, M. Schurenberg, K. Strupat. Investigations of 2,5-DHB and succinic acid as matrices for IR and UV MALDI. Part I: UV and IR laser ablation in the MALDI process. *Int. J. Mass Spectrom.* **1997**, *169*, 31.

[16] Y. Q. Dai, R. M. Whittal, L. Li. Confocal fluorescence microscopic imaging for investigating the analyte distribution in MALDI matrices. *Anal. Chem.* **1996**, *68*, 2494.

[17] B. Rosinke, K. Strupat, F. Hillenkamp, J. Rosenbusch, N. Dencher, U. Kruger, H. J. Galla. Matrix-assisted laser desorption/ionization mass spectrometry (MALDI-MS) of membrane proteins and non-covalent complexes. *Eur. J. Mass Spectrom.* **1995**, *30*, 1462.

[18] L. Tofani, A. Feis, R. E. Snoke, D. Berti, P. Baglioni, G. Smulevich. Spectroscopic and interfacial properties of myoglobin/surfactant complexes. *Biophys. J.* **2004**, *87*, 1186.

[19] T. Chakraborty, I. Chakraborty, S. P. Moulik, S. Ghosh. Physicochemical and conformational studies on BSA-surfactant interaction in aqueous medium. *Langmuir.* **2009**, *25*, 3062.

[20] N. Gull, P. Sen, R. H. Khan, D. Kabir ud. Interaction of bovine (BSA), Rabbit (RSA), and Porcine (PSA) Serum Albumins with cationic single-chain/gemini surfactants: A comparative study. *Langmuir.* **2009**, *25*, 11686.

[21] G. Vignesh, S. Nehru, Y. Manojkumar, S. Arunachalam. Spectroscopic investigation on the interaction of some surfactant-cobalt(III) complexes with serum albumins. *J. Lumin.* **2014**, *145*, 269.

[22] B. K. Paul, S. P. Moulik. Uses and applications of microemulsions. *Current Science.* **2001**, *80*, 990.

[23] D. Kelley, D. J. McClements. Interactions of bovine serum albumin with ionic surfactants in aqueous solutions. *Food Hydrocolloid.* **2003**, *17*, 73.

[24] A. Wangsakan, P. Chinachoti, D. J. McClements. Maltodextrin-anionic surfactant interactions: Isothermal titration calorimetry and surface tension study. *J. Agric. Food Chem.* **2001**, *49*, 5039.

[25] A. N. Jordan, S. Das, N. Siraj, S. L. de Rooy, M. Li, B. El-Zahab, L. Chandler, G. A. Baker, I. M. Warner. Anion-controlled morphologies and spectral features of cyanine-based nanoGUMBOS - an improved photosensitizer. *Nanoscale.* **2012**, *4*, 5031.

[26] S. Das, D. Bwambok, B. El-Zahab, J. Monk, S. L. de Rooy, S. Challa, M. Li, F. R. Hung, G. A. Baker, I. M. Warner. Nontemplated approach to tuning the spectral properties of cyanine-based fluorescent nanoGUMBOS. *Langmuir.* **2010**, *26*, 12867.

[27] H. Al Ghafly, N. Siraj, S. Das, B. P. Regmi, P. K. S. Magut, W. I. S. Galpothdeniya, K. K. Murray, I. M. Warner. GUMBOS matrices of variable hydrophobicity for matrix-assisted laser desorption/ionization mass spectrometry. *Rapid Commun. Mass Spectrom.* **2014**, *28*, 2307.

[28] I. M. Warner, B. El-Zahab, N. Siraj. Perspectives on moving ionic liquid chemistry into the solid phase. *Anal. Chem.* **2014**, *86*, 7184.

[29] A. C. Notides, N. Lerner, D. E. Hamilton. Positive cooperativity of the estrogen receptor. *Proc. Natl. Acad. Sci.* **1981**, *78*, 4926.

[30] B. Perlmutterhayman. Cooperative binding to macromolecules. A formal approach. *Acc. Chem. Res.* **1986**, *19*, 90.

[31] S. Das, M. R. Sylvain, V. E. Fernand, J. N. Losso, B. El-Zahab, I. M. Warner. Positive cooperative mechanistic binding of proteins at low concentrations: A comparison of poly (sodium N-undecanoyl sulfate) and sodium dodecyl sulfate. *J. Colloid Interface Sci.* **2011**, *363*, 585.

[32] X. J. Chen, J. A. Carroll, R. C. Beavis. Near-ultraviolet-induced matrix-assisted laser desorption/ionization as a function of wavelength. *J. Am. Soc. Mass Spectrom.* **1998**, *9*, 885.

[33] N. J. Turro, X. G. Lei, K. P. Ananthapadmanabhan, M. Aronson. Spectroscopic probe analysis of protein-surfactant interactions: The BSA/SDS system. *Langmuir.* **1995**, *11*, 2525.

CHAPTER 4: OLEYLAMINE α-CYANO-4-HYDROXYCINNAMIC ACID [OA][CHCA] AS A MATRIX FOR MALDI IMAGING MASS SPECTROMETRY OF LIPIDS

4.1 Introduction

Lipids can be classified into phospholipids, glycerolphospholipids, cholesterols, and fatty acids. These molecules are the fundamental building blocks of biological membranes.[1, 2] There are many types of lipids, each with different chemicals and/or physical properties depending on the variety of functional groups present. Lipids are divided into simple and complex classes based on structure and function. Simple lipids include cholesterols and fatty acids, while complex lipids include glycerolphospholipids. In general, lipids have one or more long chain hydrophobic tails connected with various groups of different polarity and hydrophobicity. Phospholipids, lipids with a phosphate group, are important structural components of cell membranes and they are a major component of the cell. Localization studies of lipids in brain tissue are important, because a change in the phospholipid distribution in the brain tissue can indicate the presence of diseases such as Alzheimer's.[3-5]

Phospholipids in tissues can be analyzed by mass spectrometry after extraction and purification; however, these methods are tedious and labor-intensive. Various imaging methods such as fluorescence spectroscopy,[6] infrared spectroscopy,[7, 8] as well as mass spectrometry are used to measure lipids directly on tissues.[9] Matrix assisted laser desorption ionization imaging mass spectrometry (MALDI IMS)[10, 11], has become a powerful technique for direct analysis of biological compounds such as lipids, peptides, and proteins. MALDI IMS is used for detecting, identifying, and characterizing analytes in complex mixtures such as tissues because of its high sensitivity and high tolerance for

salts and other contaminants.[12, 13] MALDI IMS is a particularly useful technique for biomolecules analysis in tissues since it can be performed directly on tissues, eliminating the need of extraction or purification steps.[14] Additionally, the use of mass spectrometry allows the detection of all biomolecules in the sample as opposed to other techniques like fluorescence microscopy where intrinsic fluorescence or fluorescent labeling is required.[6, 15] MALDI IMS has also been developed for biological, medical, pharmaceutical, and biomarker applications because it can be used over a wide mass range that includes many biomolecules.[16-18]

Recently, the development of MALDI has enabled the exploration of complex lipids and drugs in biological tissues for use in cancer or neuroscience studies.[19] This method helps detect drugs and biomarkers on tissues.[20] MALDI IMS has been used for detecting and studying lipids such as phospholipids and sphingolipids, which are the most abundant ions observed by the MALDI IMS in the brain [14] or liver[21].

The requirements of matrices used in MALDI IMS include providing protons to analytes, absorbing at the wavelength of the laser, and mixing well with analytes in tissues. When synthesizing a new matrix, it is important that the matrix gives good spectral quality (in regard to sensitivity, resolution, and intensity) and stability in vacuum. Crystallization of the matrix on tissue is another important factor to achieve homogeneity. When a uniform layer of the matrix crystallizes on the tissues, the homogeneity and signal are improved [20, 22] Various matrices have been used for MALDI IMS. For example, 2,5-dihydroxybenzoic acid (DHB) and 2,4,6-trihydroxyacetophenone (THAP) are commonly used for detecting lipids in both negative and positive mode. However, 2,5-DHB and THAP have been shown to form large crystals, causing poor

sample-to-sample reproducibility and molecular delocalization.[23-27] Other matrices that have been used for detecting lipids are 2-mercaptobenzothiazole (MBT) and 9-aminoacrine (9-AA). MBT yields high reproducibility from spot to spot due to the formation of small crystals, which increases the homogeneity of the matrix deposit.[21, 28] A drawback of using MBT as a matrix is that it forms a large amount of fragments below 500 Da, which can interfere with the analysis of analytes in that region.[21, 29] 9-AA is used to detect low molecular weight metabolites and it has been used for detecting lipids in negative ion mode. Some matrices perform well in only a particular polarity mode.[9, 26, 30, 31]

Ionic liquids (ILs) have been used as matrices for imaging and detecting biomolecules.[32] ILs are composed of bulky organic ions and have melting points less than or equal to 100 °C. IL matrices are divided into two categories: those that have melting points less than 25 °C and frozen ionic liquids (FILs), which have melting points between 25 to 100 °C. ILs have several advantages over conventional matrices such as stability under the high vacuum. Furthermore, they give high signal intensity, good signal to noise ratio, and a large number of compounds can be detected on tissues. A Group of Uniform Materials Based on Organic Salts (GUMBOS) have melting points between 25 and 250 °C and their properties are similar to those of ILs, with the exception of their physical state. Like ionic liquids, the counter ions used to make GUMBOS can be changed to tune the materials for specific applications.[33]

In the present study, we have synthesized and applied a new long-chain alkyl GUMBOS, [OA][CHCA], as a MALDI matrix for the detection of lipids. The use of this matrix has been found to yield a homogeneous mixture of analyte and matrix. This

homogeneity is in part due to the hydrophobic tail, which aids in dissolving hydrophobic proteins. The performance of [OA][CHCA] was found to be equal to or better than 2,5-dihydroxylbenzoic acid (DHB). Specifically, a significant improvement in signal and sensitivity were observed when [OA][CHCA] was used for detecting hydrophobic proteins. When [OA][CHCA] was used as a matrix, better shot-to-shot reproducibility, desorption properties, increase of signal/noise ratio, and increased stability under vacuum were observed. Herein, we report [OA][CHCA] as a matrix for the detection of hydrophobic and hydrophilic lipids, peptides, and proteins on tissue samples. Rat brain tissue sections were imaged to demonstrate the use of [OA][CHCA] in direct analysis of tissues. We evaluated shot-to-shot reproducibility, vacuum stability, homogeneity, and signal intensity in positive ion mode MS. In molecular imaging applications, [OA][CHCA] shows enhanced performance over DHB.

4.2 Experimental

4.2.1 Materials

α-Cyano-4-hydroxycinmic acid (CHCA), oleylamine (OA), 2,5-dihydroxybanzoic acid (2,5-DHB), sinapinic acid (SA), methanol, [GLU^{1}] Fibrino peptide B human, gramicidin, 2,5-dihydroxybenzoic acid (DHA), bacteriorhodopsin (BR) from *Haloobacterium salinarum*, *acetonitrile* (CH_3CN), trifluoroacetic acid (TFA), and methanol were purchased from Sigma and used as received. MTP 384 massive target T was obtained from Bruker Daltonics. ITO coated conduction glass slides for MALDI imaging were purchased from Bruker.

4.2.2 Synthesis and Characterization of GUMBOS

The GUMBOS matrix was prepared as in previous studies [34]. Briefly, 0.5 g of OA was dissolved in 10 mL of methanol to yield a 0.187 M solution. An equimolar amount of CHCA was prepared and dissolved in methanol. The CHCA solution was added to the OA solution and stirred for 24 hours. Methanol was removed using rotary evaporation. The melting point of [OA][CHCA] was determined using a melting point apparatus (Digit Melt MPA 160, Stanford Research Systems).

4.2.3 NMR Analysis

For ^{1}H analysis of CHCA and [OA][CHCA] were dissolved in deuterated dimethyl sulfoxide-d6 (DMSO) (Figure 4.1). The red trace represents CHCA and the blue trace represents [OA][CHCA]. The carboxylic acid group on CHCA has a proton with a chemical shift around 11 ppm. The disappearance of this proton indicates the reaction between oleylamine and CHCA is complete. In addition to the NMR characterization, the compound was also characterized by electrospray ionization and this data is shown in figure A11.

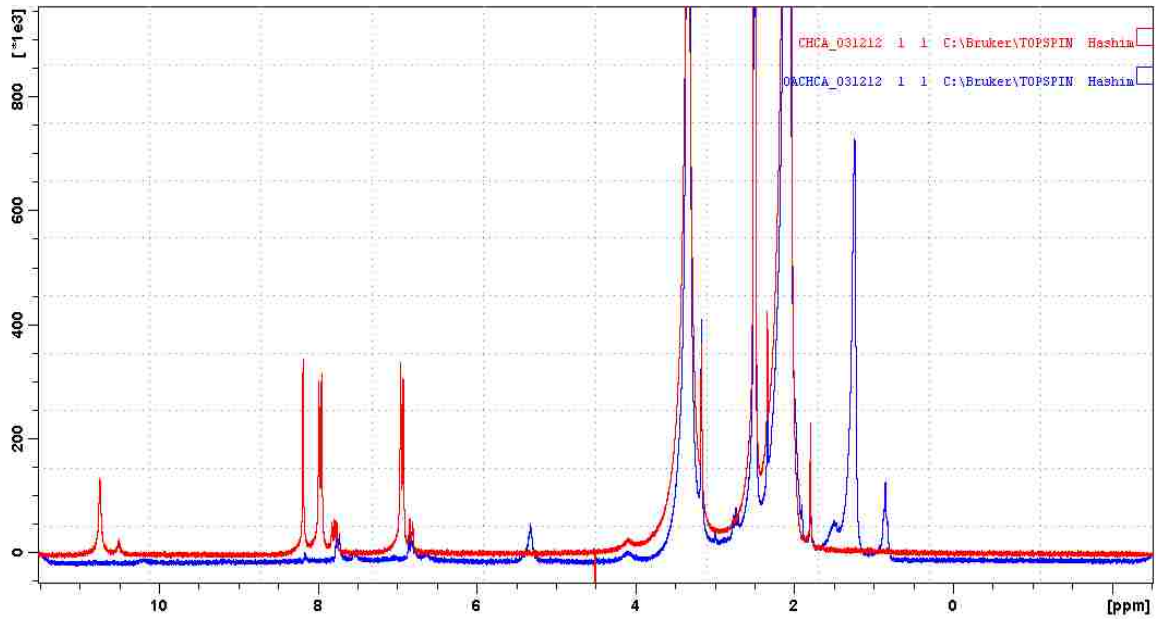

Figure 4.1. ^{1}H NMR for [OA][CHCA]. The red spectrum corresponds to CHCA while the blue corresponds to [OA][CHCA]. Disappearance of a peak at 11 ppm indicates a complete reaction.

4.2.4 Tissue Preparation

A rat was sacrificed by decapitation by Louisiana State University School of Veterinary Medicine (13-075) and immediately dissected to remove the brain. The rat brain section was covered with liquid nitrogen and foil to keep the sample below -80 °C in order to prevent protein and peptide degradation. Rat tissue sections of 10 µm were mounted on indium tin oxide (ITO) coated glass slides. The samples were used without washing and were stored at -80°C. Before being used in MALDI, the slides were stored in a desiccator for 15 minutes. These samples were then coated with matrix and transferred to stainless steel MALDI plates for imaging.

4.2.5 Sample Preparation for MALDI TOF MS

Matrix solutions were prepared fresh daily with CHCA at a concentration of 10 mg/mL acetonitrile and H_2O with 0.1% TFA in a ratio of 2:1. A 10 mg aliquot

[OA][CHCA] was dissolved in 1 mL of acetonitrile and H_2O with 0.1% TFA in a ratio of 2:1. The dried droplet method was used for sample preparation, in which 1 μL of the matrix and 1 μL of the analyte were mixed on the target. The sample was then allowed to dry at room temperature. For MALDI IMS analysis, both matrices DHB and [OA][CHCA], were dissolved in a mixture of methanol and water at a ratio of 70:30 and 0.1% TFA. The concentration of both matrices was 20 mg DHB and 10 mg [OA][CHCA] in 1 mL of methanol and water with TFA mixture.

4.2.6 MALDI-TOF MS

IMS spectra were acquired using a MALDI-TOF mass spectrometer (Ultra fleXtreme, Bruker, Bremen, Germany) in positive ion reflectron mode. The ion acceleration potential was 25 kV with 500 laser shots. A frequency tripled Nd: YAG laser at a wavelength of 355 nm with a pulse duration of 3 ns was used for ionization. Data were processed using Flex Analysis 3.3 software (Bruker).

4.3 Results and Discussion

4.3.1 Characterization of [OA][CHCA]

Oleylamine α-cyano-4-hydroxycinnamic acid, ([OA][CHCA]) was synthesized as described above at a 1:1 molar ratio in methanol. The cation, OA was used here to significantly enhance the solubility of hydrophobic peptides and proteins due to the long alkyl chain. [OA][CHCA] was characterized using ^{1}H NMR (Figure 1). Disappearance of the carboxylic acid proton present in CHCA indicates that the reaction between OA and CHCA went to completion to form [OA][CHCA]. The melting point was observed at 122°C.

Table 4.1. Structure, molecular weight, melting point, and molar absorptivity of tested matrices.

Compounds	Structure	MW	MP °C	Molar Absorptivity (M^{-1} cm^{-1})
CHCA	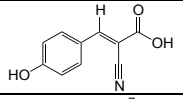	189.17	240	11708
[OA][CHCA]	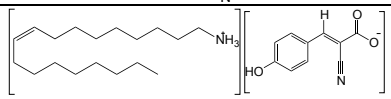	456.34	122	6594

The ultraviolet visible absorbance spectra of CHCA and [OA][CHCA] is shown in Figure 2. Both compounds have a broad absorption from 380 to 260 nm (Figure 4.2). The absorbance maximum of the parent compound, CHCA, occurs at 330 nm, whereas the maximum of [OA][CHCA] is blue shifted to 328 nm. The molar absorptivity of CHCA is almost twice as large as that of the CHCA-based GUMBOS at a wavelength 355 nm, which was used for MS analysis (Table 4.1).

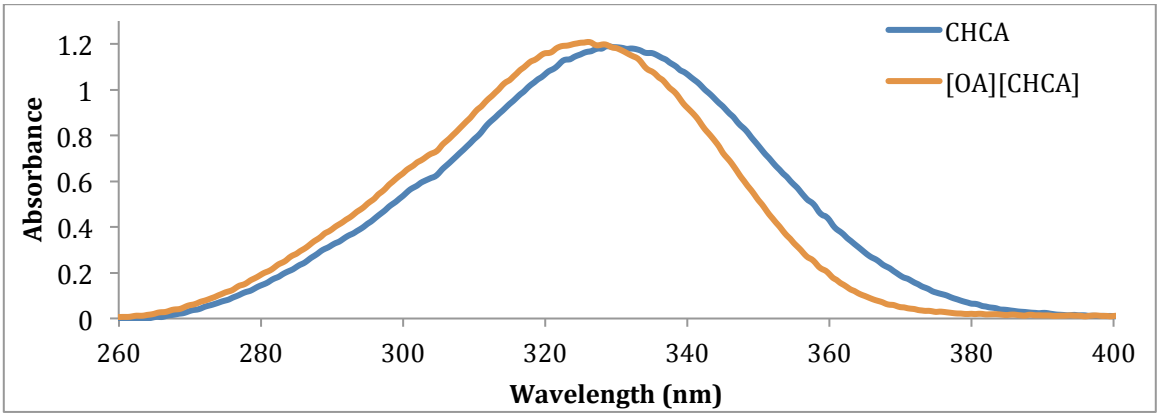

Figure 4.2. Absorbance spectra of 50 µM solutions CHCA and [OA][CHCA] in methanol.

Figure 4.3 shows the laser desorption ionization (LDI) mass spectrum for [OA][CHCA] in the mass range of 100 to 600 Da. The most prominent peaks observed

for [OA][CHCA] are *m/z* 178 corresponding to [M- OA-CN+H]$^+$, *m/z* 268 corresponding to [oleylamine]$^+$, *m/z* 300 corresponding to [oleylamine + O_2]$^+$, and *m/z* 483 corresponding to [OACHCA+H_2O]$^+$. Electrospray ionization was used to show the positive ion and negative ions, which resulted in *m/z* 268 and 189, respectively.

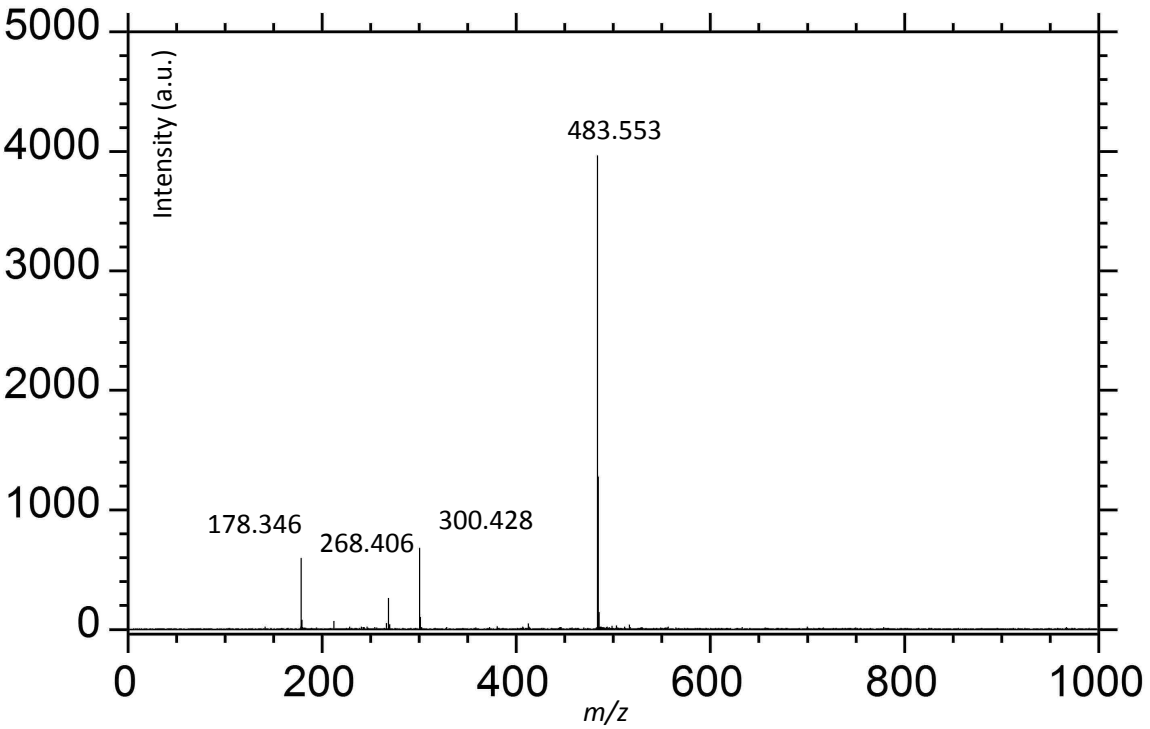

Figure 4.3. Laser desorption ionization spectra of [OA][CHCA] matrix (no analyte present).

4.3.2 GUMBOS as a MALDI Matrix for Detection of Peptides and Proteins

We evaluated [OA][CHCA] as a matrix for MALDI analysis of hydrophilic peptides (angiotensin II, [GLU^1] fibrinopeptide B) and the hydrophobic protein (bacteriarhodopsin). The primary reason oleylamine was chosen as the cation was to increase the hydrophobicity of CHCA and increase the interaction of the matrices with both hydrophobic and hydrophilic analytes. The synthesized GUMBOS was successfully used as matrices for MALDI. The hydrophobic tail of OA can increase the interaction of hydrophobic proteins, as observed in this study, as well as function as a matrix for

MALDI. The CHCA head group is polar and can protonate the analyte making it a good matrix. [OA][CHCA] is not soluble in water, so methanol was used as the solvent. The dried droplet method was used for sample preparation because it is rapid and simple.

First [OA][CHCA] was evaluated alone without analytes (Figure 4.3) as a control to determine the background signal of the matrix. Then, the selected proteins and peptides were evaluated with the matrices. Angiotensin II and [GLU^1] Fibrinopeptide B showed clear signals at *m/z* 1046.54 and *m/z* 1570.57, respectively, which corresponds to the $[M+H]^+$ peak. Bacteriorhodopsin showed a clear signal at *m/z* 26,225, which also corresponds to the $[M+H]^+$ peak. MALDI spectra for angiotensin II and bacteriorhodopsin are shown in Figures 4.4 and 4.5. Figure 4.4 is a mass spectrum of 0.1 fmol angiotensin II with [OA][CHCA] as a matrix. Figure 4.5 is the mass spectrum of the hydrophobic protein bacteriorhodopsin (BR) with [OA][CHCA] as a matrix. The results obtained using [OA][CHCA] and DHB as matrices to detect hydrophilic peptide [GLU^1] Fibrinopeptide B at a concentration of 1 pmol is summarized in (Figure 4.6) and (see the appendix table 1 and Figure A9 and A10). The relative standard deviation (RSD) was calculated to determine spot-to-spot reproducibility. RSD was evaluated by calculating the average signal intensity at 12 different positions. Figure 4.6 reveals that improved spot to spot reproducibility was obtained and also [OA][CHCA] showed higher signal intensity than DHB. In addition, [OA][CHCA] was very stable under high vacuum and yields homogenous mixtures with hydrophobic peptides or proteins, thereby overcoming deficiencies in typical systems.

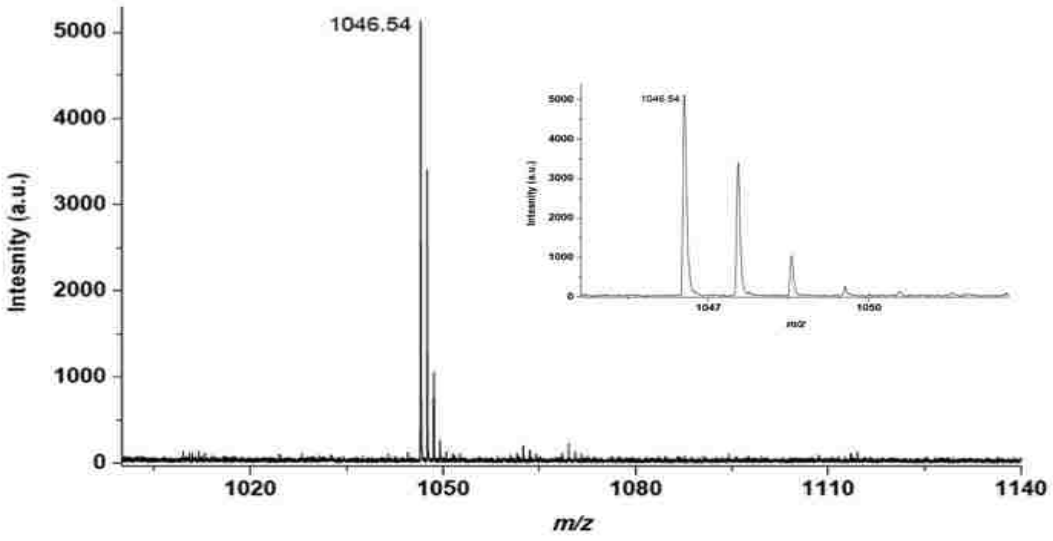

Figure 4.4. Mass spectrum reflectron mode of 0.1 fmol angiotensin II with [OA][CHCA] matrix and inside the spectra zoomed area.

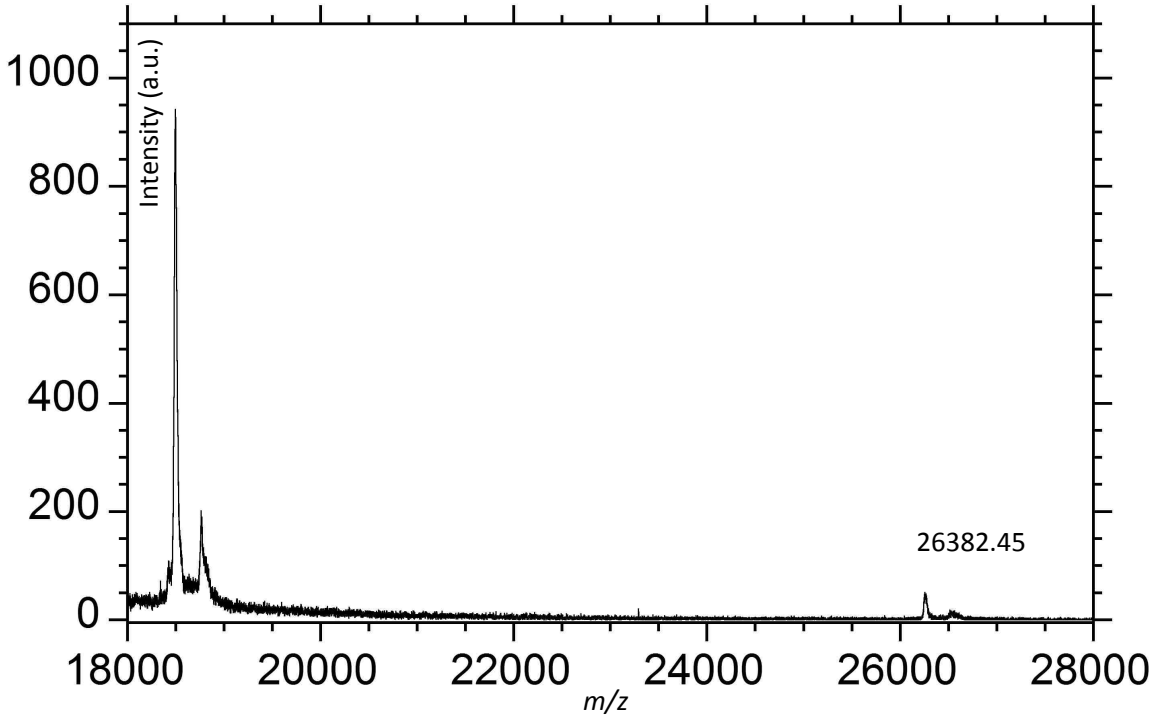

Figure 4.5. Mass spectrum linear mode [OA][CHCA] with bacteriorhodopsin (BR) hydrophobic protein.

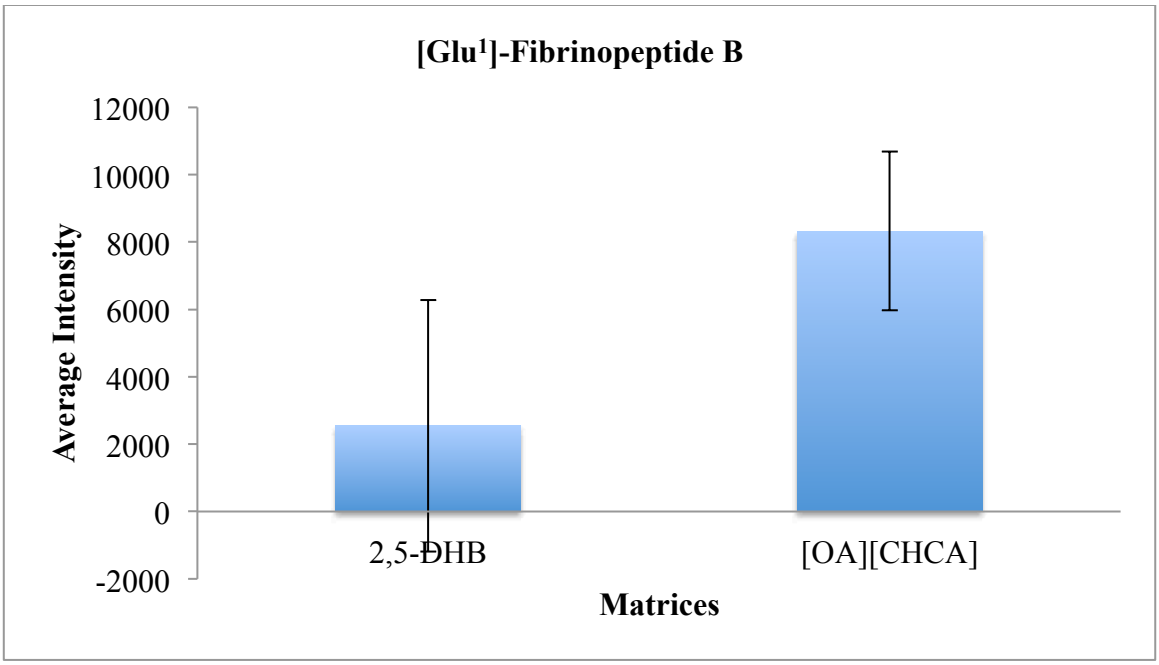

Figure 4.6. Average MALDI of signal intensity for hydrophilic peptide GLU1 Fibrinopeptide (1 pmol) with DHB and [OA][CHCA] matrices.

4.3.3 Direct Detection of Lipids in Rat Tissue

Lipids are the most prevalent biomolecules in the brain where they are the major component after water. They are the building block of cellular membranes and energy storage units in the body; further, they aid in signal transduction for biological processes, playing an important role in immunology. Lipids interact with proteins and are studied for drug use.[12]. Imaging mass spectrometry (IMS) has been used to visualize and identify biomolecules on rat brain tissue. IMS of lipids can provide information about the identity of phospholipids (PLs) and spatial distribution of PLs on tissues. In order to study lipids *in situ*, we first had to optimize the tissue section thickness to give the best signal intensity. To do this we studied tissues ranging in thickness from 5 to 20 µm. We found the best thickness was 10 µm of tissue, because that thickness gave the best signal to noise ratio. In the second part of this study the optimum matrix composition and the

proper solvent was determined. [OA][CHCA] GUMBOS and DHB, a commonly employed matrix for detecting lipids on tissue, were used as matrices. Methanol and water with 0.1% TFA at a ratio of (70:30) was used as a solvent. Concentrations of 20 mg/mL DHB and 10 mg/mL GUMBOS were used. The corresponding spectra comparing the two matrices were collected in positive ion mode and are shown in Figures 4.7 and 4.8. [OA][CHCA] showed higher signal intensity compared to DHB. The *m/z* region between 734 and 820 showed high intensity for lipids. Some important phospholipids, such as, phophotidylcholine (PC) and sphingomyeline (SM), were detected with [OA][CHCA]. For example the following peaks were detected *m/z* 734.5(PC 32:0), *m/z* 760.5 (PC 34:1), *m/z* 782.5 (PC 34:1 +Na), 788 (PC 36:1). Most of the peaks generated in positive mode are PC and SM because they are the major constituents of cell membranes.[24, 28] The most abundant species of phosphatidylcholine (PC) found in the spectra were 16:0/ 16:0 PC ($[M+H]^+$ *m/z* 734.5, $[M+Na]^+$ *m/z* 756.5, $[M+ K]^+$ *m/z* 772.5), and 16:0/18:1 PC ($[M+H]^+$ *m/z* 760.5, $[M+Na]^+$ *m/z* 782.6, $[M+K]^+$ *m/z* 798.6). Phospholipids detected by [OA][CHCA] showed two times higher intensity than when the matrix DHB was used. During imaging it was found that [OA][CHCA] is stable at high vacuum and improved the signal intensity for phospholipids on the rat brain tissue as compared with DHB. Identities of these species were confirmed by previous studies in the literature.[30, 35] The most abundant species of phosphatidylcholine (PC) found in the spectra were 16:0/ 16:0 PC ($[M+H]^+$ *m/z* 734.5, $[M+Na]^+$ *m/z* 756.5, $[M+ K]^+$ *m/z* 772.5), and 16:0/18:1 PC ($[M+H]^+$ *m/z* 760.5, $[M+Na]^+$ *m/z* 782.6, [M+K]+ *m/z* 798.6). These phospholipids detected by [OA][CHCA] showed two times higher intensity than with DHB. During imaging it was found that [OA][CHCA] is stable at high vacuum. The

identities of these species were confirmed by papers in the literature.[30, 35] There are few peaks shown above *m/z* 1000.

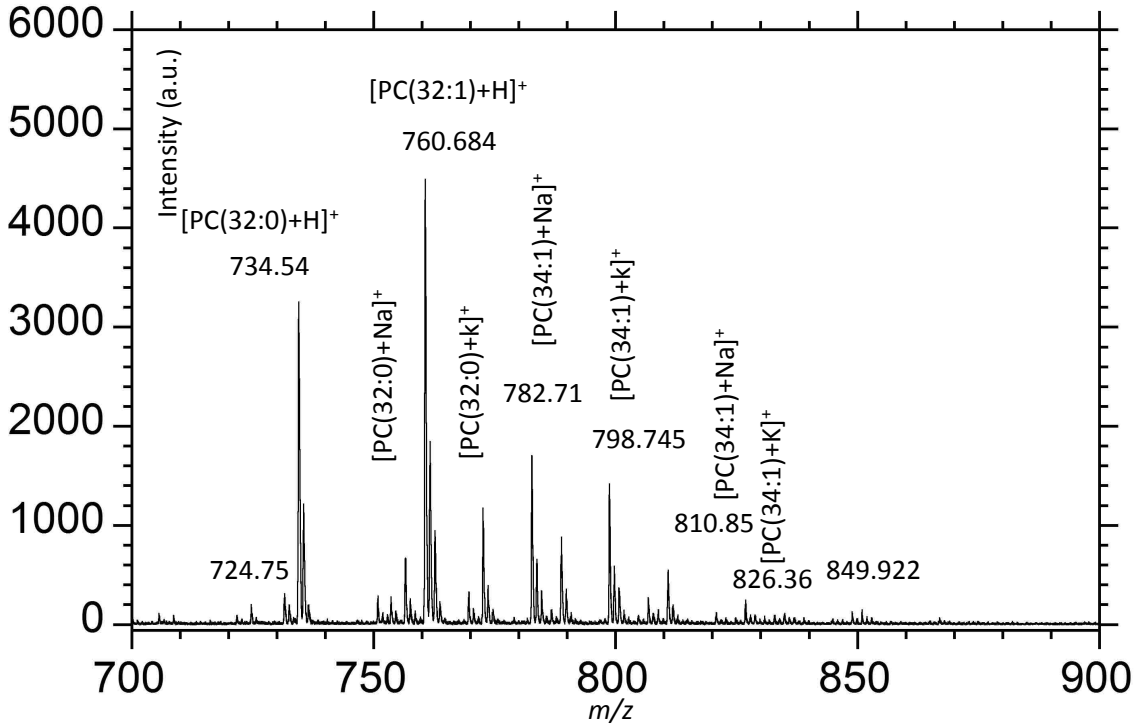

Figure 4.7. MALDI mass spectrum of rat brain tissue in positive ion reflectron mode with DHB matrix.

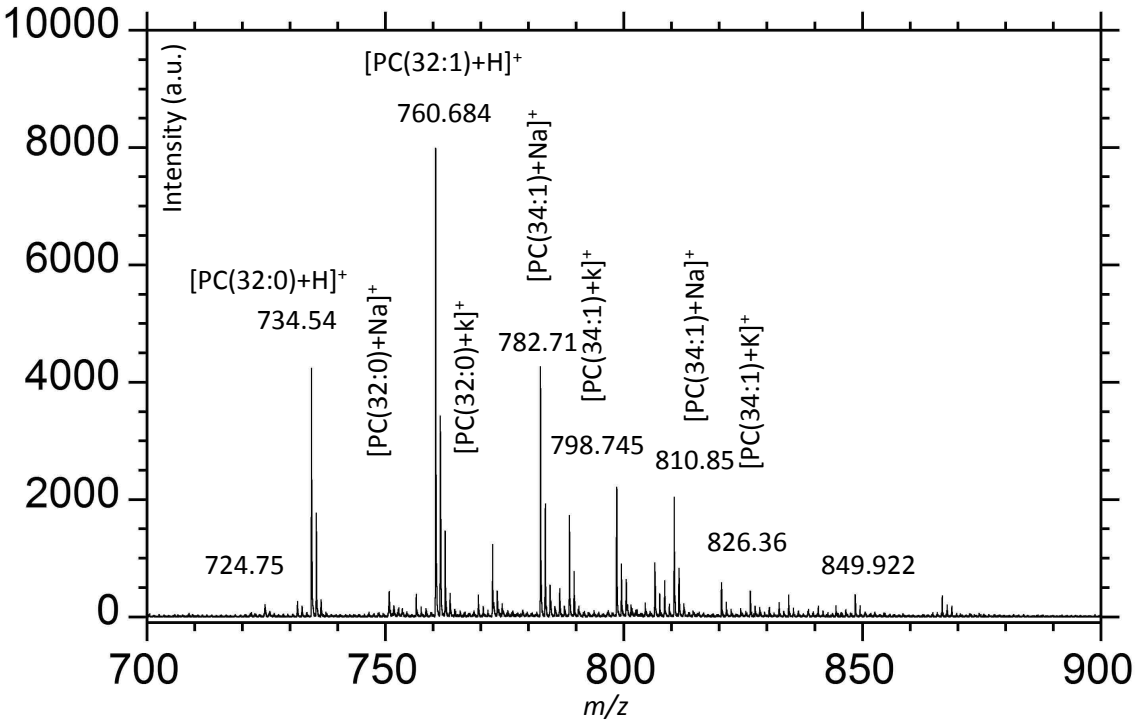

Figure 4.8. MALDI spectrum obtained from a rat brain tissue in positive ionization mode. The tissue section was coated with GUMBOS [OA][CHCA]. Inset: Zoom from *m/z* 600 to *m/z* 875.

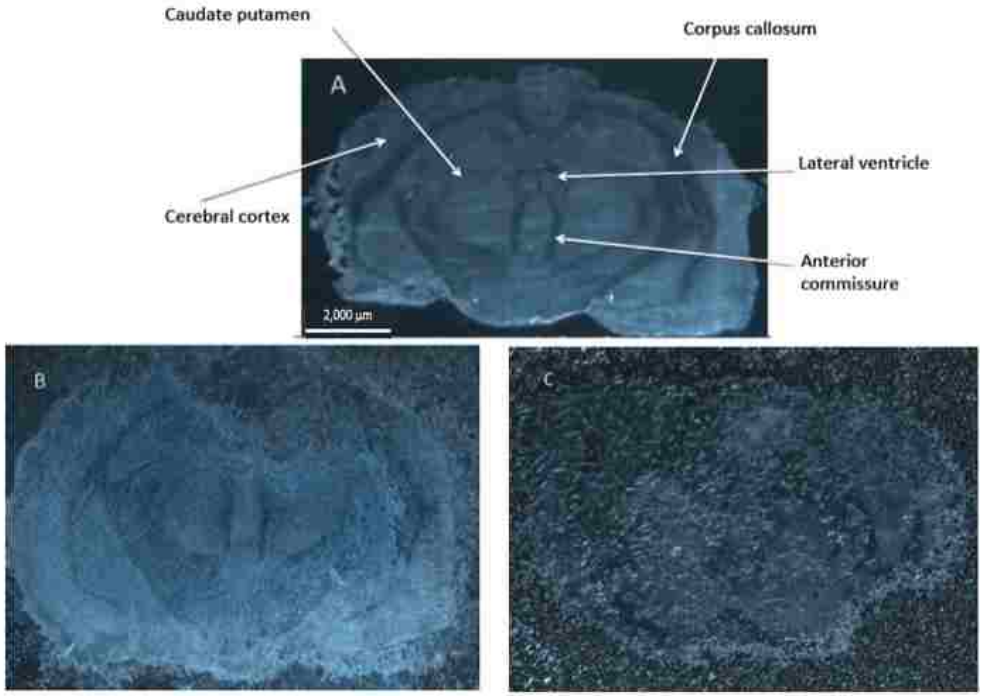

Figure 4.9. Optical imaging: A) 10 µm thick rat brain tissue. B) Tissue coated with [OA][CHCA] C) Tissue coated with DHB.

Microscopy was used to characterize the size of DHB and [OA][CHCA] crystals formed on the tissue sections. These images were taken by using a Zeiss steREO Lumar. Figure 4.9A shows a rat brain tissue section in the absence of a matrix coating. Rat brain tissue sections after coating with the matrices [OA][CHCA] and DHB are shown in Figures 4.9 B and 4.9 C, respectively. A nebulizer was used to spray the matrices on the tissue sections and approximately 3 mL of the matrix solution was used to cover the tissue. A flow rate of 100 μL/min was utilized and the distance between the tissue and nebulizer was around 12 cm. Morphology of the matrix is the most important factor for desorption and ionization of lipids. DHB has been shown to form large crystals (Figure 4.9 C) and [OA][CHCA] was found to form smaller crystals as compared to DHB. The homogeneity of the matrix [OA][CHCA] on the sample is increased as compared to DHB, since [OA][CHCA] forms smaller crystals (Figure 4.9 B). Formation of smaller crystals provides an explanation for the higher signal intensity and better shot-to-shot reproducibility compared with DHB.[36] Matrices that formed smaller crystals were completely volatilized after irradiation by the laser. However, matrices that formed larger crystals were not completely volatilized after irradiation by the laser. It is also notable that [OA][CHCA] remained stable under vacuum through the duration of the imaging experiments.

Phospholipids can be classified into different groups.[14] Thus, some phospholipids can be identified using positive ion mode, while others require negative ion mode. For some phospholipids, either mode can be used. Common phospholipids from tissues include phosphatidylcholine (PC), phosphatidylinositol (PI), phosphoric acid (PA), phosphatidylethanolamine (PE), sulfa tides (ST), and sphingomyeline (SM).

Normally, the peaks for these phospholipids appear between *m/z* 500 to 1000, with few above *m/z* 1000. They typically have low intensity and little fragmentation (Table 4.2).

Table 4.2. Detected *m/z* values corresponding to phospholipids in positive ion mode.

Phospholipids ID	M+H	M+Na	M+K
PC24:3	616.17		
SM 16:0		724.898	
SM18:0	731.619		
PC32:1	734.594	756.566	772.55
PC 34:1	760.575	782.557	798.528
PC34:0	762.595	784.73	
PC36:1	788.615	810.604	826.565
PC36:3		806.565	822.542
PC36:4			820.512
PC38:4		832.629	848.637
PC40:6	834.627		
PC40:5	*		
PC40:4	838.773		
PC38:6			844.503
PS36:1			850.67
GlcCer 24:0 OH			866.711
ST 38:4			868.487
PC 32:0 (2M+H)	1468.104		
SM 16:0		724.898	
SM18:0	731.619		
PC32:1	734.594	756.566	772.55
PC 34:1	760.575	782.557	798.528
PC34:0	762.595	784.73	
PC36:1	788.615	810.604	826.565
PC36:3		806.565	822.542
PC36:4			820.512
PC38:4		832.629	848.637
PC40:6	834.627		
PC40:5	*		
PC40:4	838.773		
PC38:6			844.503
PS36:1			850.67

The heterogeneous distribution of several phospholipids in the brain tissue can be studied and identified by MALDI IMS. Figure 4.10 shows the results of MALDI IMS

acquired with [OA][CHCA] as a matrix from rat brain tissue sections in positive ion mode. Figures 4.10 A-D display the different disruption of phospholipids such as PC 32:OK (*m/z* 772.5), PS 36:1K (*m/z* 850.6), PC 36:1K (*m/z* 826.5). For example, *m/z* 772 PC32:0K is found mostly in the caudate putamen and lateral ventricle regions of the brain; conversely, it is low in corpus callosum (Figure 4.10A). However, *m/z* 850 PS36:1K is high in corpus callosum and is low in caudate putamen and lateral ventricle (Figure 4.10B). Furthermore, the use of MALDI IMS can distinguish the presence of two different phospholipids within the same tissue section (Figure 4.10D and 4.10E). The distribution of *m/z* 734 PC 32:0. *m/z* 734 PC 32:0 was primarily found in the cerebral cortex and lateral ventricle, whereas *m/z* 826.5 PC 36:1K was distributed throughout the corpus callosum (Figure 4.10D). From Figure 4.10F it is strongly suggested that both *m/z* 734 PC 32:0 and *m/z* 826.5 PC 36:1K have different distributions in rat brain tissue.

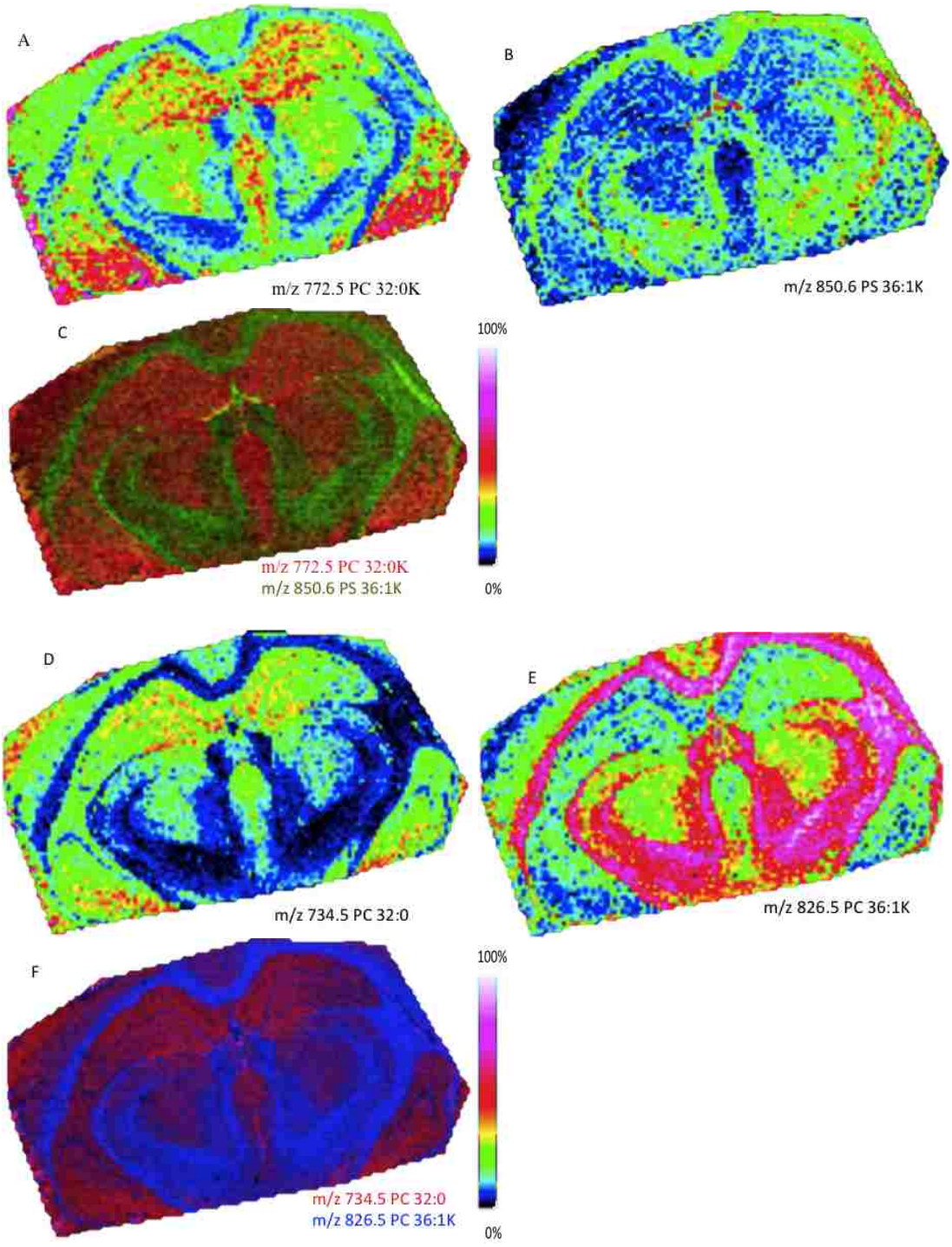

Figure 4.10. [OA][CHCA] was as matrix for MALDI IMS for detecting different lipids on the rat brain tissue.A) *m/z* 772.5 PC 32:0K, (B) *m/z* 850.6 PS 36:1K, (C) Represent different distribution of two *m/z* 772.5 and PC 32:0K and *m/z* 550.6 PS 36:1K. (D) *m/z* 734.5 PC 32:0, (E) 826.5 PC 36:1K on the rat of brain tissue. (F) Represent different distribution *m/z* 734.5 PC 32:0 and *m/z* 826.5 PC36:1K.

[OA][CHCA] can also be used in negative mode to ionize the lipids. Figure 4.11 shows MALDI spectrum in negative mode for the detection of lipids on brain tissue. The highest peak is *m/z* 902 ST-OH 42:3.

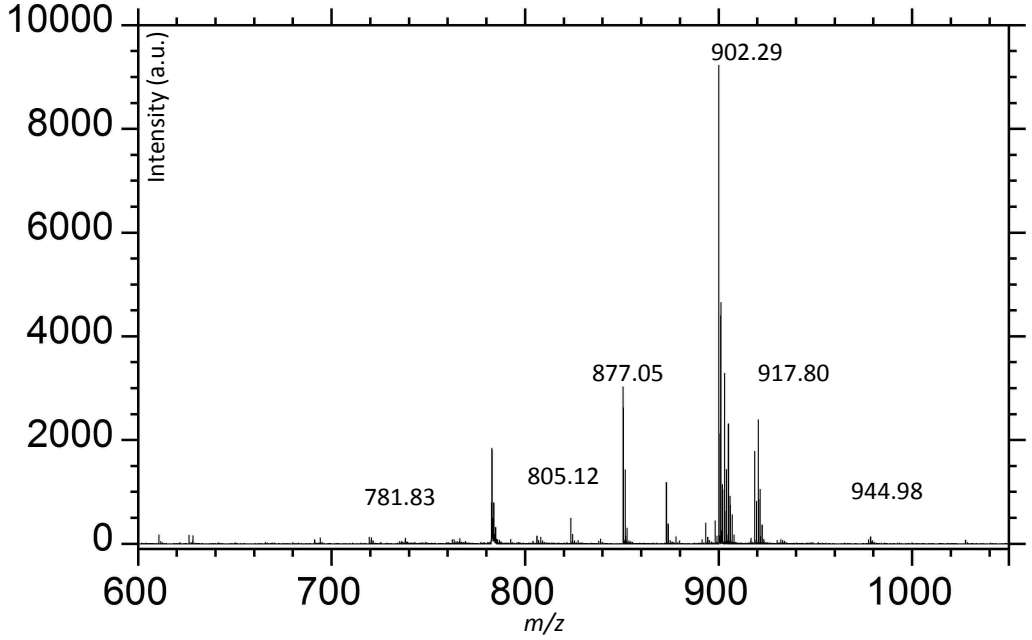

Figure 4.11. MALDI mass spectrum of rat brain tissue in negative ion reflectron mode with [OA][CHCA] matrix.

4.4 Conclusion

In this study, we synthesized a novel matrix for the detection of phospholipids in both negative and positive ion mode. [OA][CHCA] was characterized with ^{1}H NMR and ESI-MS. The matrix was tested using the peptides angiotensin II and GLU^{1} fibrinopeptide standards. The results reveal that [OA][CHCA] shows higher signal intensity and RSD as compared with DHB. [OA][CHCA] was successful at detecting hydrophobic proteins and was used for lipid imaging in rat brain tissue sections.

Furthermore, [OA][CHCA] detected phospholipids directly on tissues in both negative and positive ion modes and was comparable with DHB. [OA][CHCA] surpassed DHB in several experiments by providing more homogenous deposition on tissue compared with DHB. Finally, [OA][CHCA] showed higher signal intensity and better reproducibility than the commonly used DHB, and was shown to be stable under vacuum.

4.5 References

[1] M. Sud, E. Fahy, D. Cotter, A. Brown, E. A. Dennis, C. K. Glass, A. H. Merrill, Jr., R. C. Murphy, C. R. Raetz, D. W. Russell, S. Subramaniam. LMSD: Lipid \ maps structure database. *Nucl. Acids Res.* **2007**, *35*, D527.

[2] M. L. Cuzner, A. N. Davison, N. A. Gregson. chemical composition of vertebrate myelin and microsomes. *J. Neurochem.* **1965**, *12*, 469.

[3] E. J. Murphy, M. B. Schapiro, S. I. Rapoport, H. U. Shetty. Phospholipid composition and levels are altered in down syndrome brain. *Brain Res.* **2000**, *867*, 9.

[4] X. L. Han, D. M. Holtzman, D. W. McKeel, J. Kelley, J. C. Morris. Substantial sulfatide deficiency and ceramide elevation in very early Alzheimer's disease: Potential role in disease pathogenesis. *J. Neurochem.* **2002**, *82*, 809.

[5] N. Braidy, A. Poljak, C. Marjo, H. Rutlidge, A. Rich, T. Jayasena, N. C. Inestrosa, P. Sachdev. Metal and complementary molecular bioimaging in Alzheimer's disease. *Front. Aging Neurosci.* **2014**, *6*.

[6] P. Greenspan, E. P. Mayer, S. D. Fowler. A selective fluorescent stain for intracellular lipid droplets. *J. Cell Biol.* **1985**, *100*, 965.

[7] R. G. Buice, L. A. Cassis, R. A. Lodder. Near-IR and IR imaging in lipid metabolism and obesity. *Cell Mol. Biol*. **1998**, *44*, 53.

[8] D. Chapman. Infrared spectroscopy of lipids. *J. Am. Oil Chem.* **1965**, *42*, 353.

[9] C. D. Cerruti, F. Benabdellah, O. Laprevote, D. Touboul, A. Brunelle. MALDI imaging and structural analysis of rat brain lipid negative ions with 9-aminoacridine matrix. *Anal. Chem.* **2012**, *84*, 2164.

[10] C. Eriksson, N. Masaki, I. Yao, T. Hayasaka, M. Setou. MALDI imaging mass spectrometry-A mini review of methods and recent developments. *Mass Spectrom.* **2013**, *2*, S0022.

[11] J. L. Norris, R. M. Caprioli. Imaging mass spectrometry: A new tool for pathology in a molecular age. *Proteomics Clin. Appl.* **2013**, *7*, 733.

[12] A. S. Woods, S. N. Jackson. Brain tissue lipidomics: Direct probing using matrix-assisted laser desorption/ionization mass spectrometry. *AAPS J.* **2006**, *8*, E391.

[13] D. Touboul, A. Brunelle, O. Laprevote. Mass spectrometry imaging: Towards a lipid microscope? *Biochime.* **2011**, *93*, 113.

[14] S. N. Jackson, H. Y. J. Wang, A. S. Woods. Direct tissue analysis of phospholipids in rat brain using MALDI-TOFMS and MALDI-ion mobility-TOFMS. *J. Am. Soc. Mass Spectrom.* **2005**, *16*, 133.

[15] P. Greenspan, S. D. Fowler. Spectrofluorometric studies of the lipid probe, nile red. *J. Lipid Res.* **1985**, *26*, 781.

[16] S. Shimma, Y. Sugiura. Effective sample preparations in imaging mass spectrometry. *Mass Spectrom.* **2014**, *3*, S0029.

[17] H. Y. J. Wang, S. N. Jackson, J. McEuen, A. S. Woods. Localization and analyses of small drug molecules in rat brain tissue sections. *Anal. Chem.* **2005**, *77*, 6682.

[18] C. Schone, H. Hofler, A. Walch. MALDI imaging mass spectrometry in cancer research: Combining proteomic profiling and histological evaluation. *Clin. Biochem.* **2013**, *46*, 539.

[19] J. A. Hankin, S. E. Farias, R. Barkley, K. Heidenreich, L. C. Frey, K. Hamazaki, H. Y. Kim, R. C. Murphy. MALDI mass spectrometric imaging of lipids in rat brain injury models. *J. Am. Soc. Mass Spectrom.* **2011**, *22*, 1014.

[20] R. Lemaire, J. C. Tabet, P. Ducoroy, J. B. Hendra, M. Salzet, I. Fournier. Solid ionic matrixes for direct tissue analysis and MALDI imaging. *Anal. Chem.* **2006**, *78*, 809.

[21] E. Astigarraga, G. Barreda-Gomez, L. Lombardero, O. Fresnedo, F. Castano, M. T. Giralt, B. Ochoa, R. Rodriguez-Puertas, J. A. Fernandez. Profiling and imaging of lipids on brain and liver tissue by matrix-assisted laser desorption/ionization mass spectrometry using 2-mercaptobenzothiazole as a matrix. *Anal. Chem.* **2008**, *80*, 9105.

[22] C. D. Calvano, S. Carulli, F. Palmisano. Aniline/alpha-cyano-4-hydroxycinnamic acid is a highly versatile ionic liquid for matrix-assisted laser desorption/ionization mass spectrometry. *Rapid Commun. Mass Spectrom.* **2009**, *23*, 1659.

[23] G. Stubiger, O. Belgacem. Analysis of lipids using 2,4,6-trihydroxyacetophenone as a matrix for MALDI mass spectrometry. *Anal. Chem.* **2007**, *79*, 3206.

[24] S. N. Jackson, A. S. Woods. Direct profiling of tissue lipids by MALDI-TOFMS. *J. Chromatogr. B Analyt. Technol. Biomed. Life Scis.* **2009**, *877*, 2822.

[25] W. Bouschen, B. Spengler. Artifacts of MALDI sample preparation investigated by high-resolution scanning microprobe matrix-assisted laser desorption/ionization (SMALDI) imaging mass spectrometry. *Int. J. Mass Spectrom.* **2007**, *266*, 129.

[26] A. Fulop, M. B. Porada, C. Marsching, H. Blott, B. Meyer, S. Tambe, R. Sandhoff, H. D. Junker, C. Hopf. 4-Phenyl-alpha-cyanocinnamic acid amide: Screening for a negative ion matrix for MALDI-MS imaging of multiple lipid classes. *Anal. Chem.* **2013**, *85*, 9156.

[27] D. A. Stoyanovsky, L. J. Sparvero, A. A. Amoscato, R. R. He, S. Watkins, B. R. Pitt, H. Bayir, V. E. Kagan. Improved spatial resolution of matrix-assisted laser desorption/ionization imaging of lipids in the brain by alkylated derivatives of 2,5-dihydroxybenzoic acid. *Rapid Commun. Mass Spectrom.* **2014**, *28*, 403.

[28] N. X. Xu, Z. H. Huang, J. T. Watson, D. A. Gage. Mercaptobenzothiazoles: A new class of matrices for laser desorption ionization mass spectrometry. *J. Am. Soc. Mass Spectrom.* **1997**, *8*, 116.

[29] K. Teuber, J. Schiller, B. Fuchs, M. Karas, T. W. Jaskolla. Significant sensitivity improvements by matrix optimization: a MALDI-TOF mass spectrometric study of lipids from hen egg yolk. *Chem. Phys. Lipids.* **2010**, *163*, 552.

[30] S. R. Shanta, L. H. Zhou, Y. S. Park, Y. H. Kim, Y. Kim, K. P. Kim. Binary matrix for MALDI imaging mass spectrometry of phospholipids in both ion modes. *Anal. Chem.* **2011**, *83*, 1252.

[31] R. Estrada, M. C. Yappert. Alternative approaches for the detection of various phospholipid classes by matrix-assisted laser desorption/ionization time-of-flight mass spectrometry. *J. Mass Spectrom.* **2004**, *39*, 412.

[32] C. Meriaux, J. Franck, M. Wisztorski, M. Salzet, I. Fournier. Liquid ionic matrixes for MALDI mass spectrometry imaging of lipids. *J. Proteomics.* **2010**, *73*, 1204.

[33] I. M. Warner, B. El-Zahab, N. Siraj. Perspectives on moving ionic liquid chemistry into the solid phase. *Anal. Chem.* **2014**, *86*, 7184.

[34] D. W. Armstrong, L. K. Zhang, L. F. He, M. L. Gross. Ionic liquids as matrixes for matrix-assisted laser desorption/ionization mass spectrometry. *Anal. Chem.* **2001**, *73*, 3679.

[35] S. G. Park, K. K. Murray. Infrared laser ablation sample transfer for MALDI imaging. *Anal. Chem.* **2012**, *84*, 3240.

[36] T. Jaskolla, M. Karas, U. Roth, K. Steinert, C. Menzel, K. Reihs. Comparison between vacuum sublimed matrices and conventional dried droplet preparation in MALDI-TOF mass spectrometry. *J. Am. Soc. Mass Spectrom.* **2009**, *20*, 1104.

CHAPTER 5: CONCLUSIONAND FUTURE DIRECTIONS

5.1 Concluding Remarks

The studies reported herein describe novel ionic liquid-based matrix compounds using 1-aminopyrene (AP) and AP-derived ***g***roup of ***u***niform ***m***aterials ***b***ased on ***o***rganic ***s***alts (GUMBOS) for the analysis of peptides using MALDI MS. A number of solid phase salts, i.e. GUMBOS, were synthesized using AP as a cation and various anions to tune the hydrophobicity of the GUMBOS. The performance of these tunable GUMBOS as MALDI matrices for the analysis of hydrophobic and hydrophilic peptides was evaluated in terms of sensitivity and reproducibility in comparison to conventional matrix compounds. Detection of hydrophobic biomolecules remains an obstacle for analysis by MALDI. This stems from the fact that most matrices for MALDI are hydrophilic and therefore have low affinity for hydrophobic biomolecules. Herein, 1-aminopyrene (AP) and AP-based GUMBOS were investigated as MALDI matrices for hydrophobic peptides, and their performance was evaluated in terms of sensitivity and reproducibility. AP was selected for these studies because it exhibits strong absorption of appropriate laser radiation, as well as displaying hydrophobic characteristics and ability to protonate the analytes. In this study, we synthesized and tested a series of AP-based GUMBOS including [AP][chloride], [AP][ascorbate], and [AP][bis(trifluoromethane) sulfonamide] ([AP][NTf_2]). The relative hydrophobicity of these compounds and conventional MALDI matrices were estimated by measuring their 1-octanol/water partition coefficients ($K_{o/w}$), which indicated that these compounds could be made much more hydrophobic. The matrix compounds were then examined as MALDI matrices for analysis of hydrophobic (valinomycin and gramicidin) as well as hydrophilic (angiotensin II) peptides. For

hydrophobic peptides, these matrices provided enhanced sensitivity and better spot-to-spot reproducibility as compared to the conventionally used matrix compounds. It was observed that these GUMBOS compounds tend to form small crystals on the MALDI target. These new classes of materials are promising matrices for effective detection of various biomolecules. A mixture of hydrophobic (valinomycin) and hydrophilic (angiotension II) peptides was analyzed using AP and AP-based GUMBOS and compared with conventional matrix compounds for peptides. The selectivity between these matrices was dependent on the hydrophobicity of the matrices. Increasing the hydrophobicity of the matrix increases the affinity to hydrophobic peptides. We observed that CHCA, [AP][Asc], and [AP][Cl], showed good affinity for hydrophilic peptides. Interaction of analytes with MALDI matrices that are composed of AP and AP-based GUMBOS was investigated using a hydrophobic (gramicidin) and a hydrophilic peptide (angiotensin II). Fluorescence anisotropy and Scatchard analysis were used to study and understand the interaction between matrices and peptides. Our results show strong binding of AP, a hydrophobic matrix, with gramicidin, a hydrophobic peptide and weak binding with angiotensin II, a hydrophilic peptide. Conversely, it appears that the hydrophilic matrix [AP][ascorbate] ([AP][Asc]), binds strongly with angiotensin II and demonstrates weaker binding with gramicidin. Thus, by changing the hydrophobicity of matrices we can tune the binding affinity of peptides. The binding results correlated well with MALDI MS results and were found to complement each other. It is important to synthesize new matrix materials for the analysis hydrophobic peptides. Hydrophobic AP and AP-based GUMBOS demonstrated stronger interaction and higher detection with a hydrophobic peptide such a gramicidin, whereas hydrophilic AP-based matrices detected

the hydrophilic peptide, angiotensin II, with higher signal intensity. This study presents a unique approach towards predicting matrix-analyte interactions in MALDI by use of fluorescence spectroscopic measurements and related analysis techniques.

Herein we report the use of novel GUMBOS, oleylamine α-cyano-4-hydroxycinnamic acid [OA][CHCA], as a matrix for MALDI IMS detection of lipids in tissue using nebulizer spray to apply GUMBOS. Direct tissue analysis with a GUMBOS matrix was compared with that of 2,5-dihydroxybenzoic acid (DHB), a common matrix used to image lipids. The use of [OA][CHCA] yielded higher signal intensity and enhanced spectral quality, including resolution and noise. Formation of smaller crystals, improved homogeneity of the matrix with tissue, and better signal reproducibility was also found when our system was compared with the conventional matrix 2,5-dihydroxybenzoic acid (DHB). These enhancements were used to examine the distribution and localization of different classes of lipids in tissue.

5.2 Future Work

In ongoing work GUMBOS have been synthesized based on the conventional matrix for detecting hydrophobic and hydrophilic biomolecules directly on tissues such as the brain or kidney tissues of rats. Notably, GUMBOS matrices can be easily tuned, they give high homogeneity of crystals with analytes, and they have high sensitivity and selectivity. By adding various functional groups to the conventional matrix, the properties of the matrix can be changed in a way that will be helpful for detecting different peptides and proteins on tissues. They can be used as ions in the synthesis of GUMBOS matrices with varying hydrophobicity. Additionally, the use of binary matrices can be studied by mixing both hydrophobic and hydrophilic matrices in order to detect both hydrophobic

and hydrophilic peptides simultaneously with the same signal intensity. The ratio of hydrophobic and hydrophilic matrices can also be varied to optimize peptide detection. In addition, we can study the mass spectra of tissues after the digestion of tissue to help to understand what kind of peptides or proteins are present.

The mechanism of the interaction of matrices with analytes, in general, remains unclear. In order to develop better MALDI matrices, more investigation is needed to understand the mechanism after we fire the laser into target to form the plume. In this dissertation we studied the interaction between peptides and the matrix using fluorescence anisotropy and Scatchard analysis when the matrix and analyte are in a solvent. However, we have not yet studied interactions between the matrix and analyte when they are crystallized on the glass slide. We can use fluorescence anisotropy and Scatchard analysis to see the effect of changing the concentration of matrix while keeping the analyte concentration constant as they are mixed on the slide. In addition, the mixture of hydrophobic and hydrophilic analytes has not yet been studied in the laser plume. Also the interaction between matrices and analyte after solvent evaporation can be studied using confocal microscopy, fluorescence and X-ray.

Another direction we need to investigate is the use of GUMBOS in nanoparticle form (nanoGUMBOS) as matrices. Variations in the hydrophobicity will change the size of the nanoGUMBOS; therefore, investigation of the properties of the matrix and its binding with proteins or peptides in correlation to the change in size of the nanoGUMBOS is essential.

APPENDIX A SUPPORTING INFORMATION

Scatchard analysis was used to determine the type of binding and binding constants of hydrophobic and hydrophilic peptides with the MALDI matrices. The type of binding was determined based on the shape of the curve. For example, a linear correlation between v/ (v/cf) correlates to specific binding. In addition, the correlation between v/ (v/cf) was also used to calculate specific binding constants. The Scatchard plots corresponding to these studies are shown in figures A1-A8.

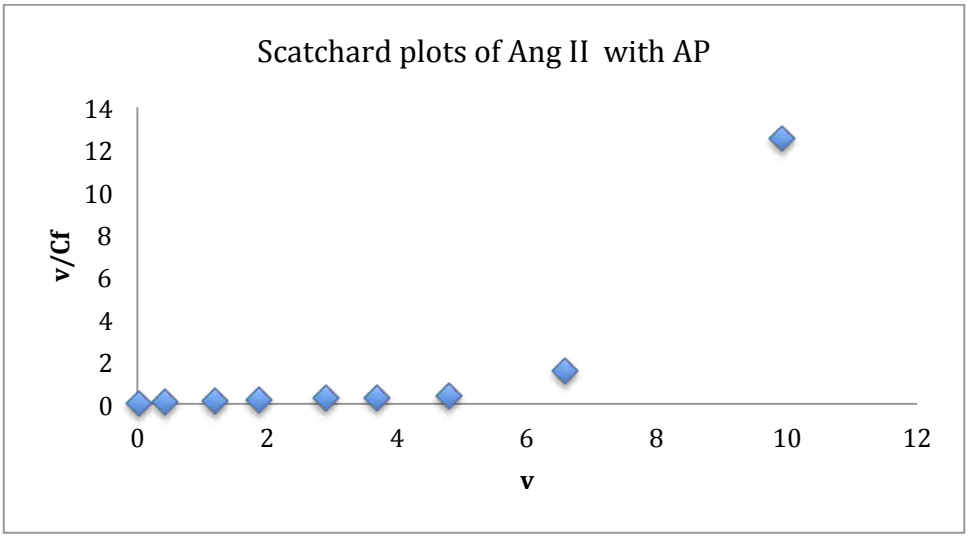

Figure A1: Scatchard plots of Ang II with AP

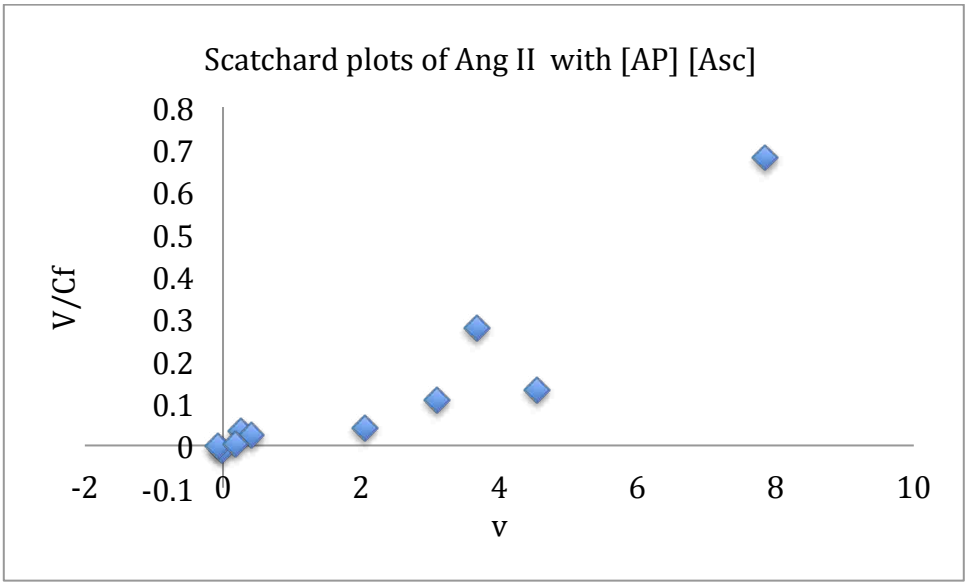

Figure A2: Scatchard plots of Ang II with [AP][Asc}

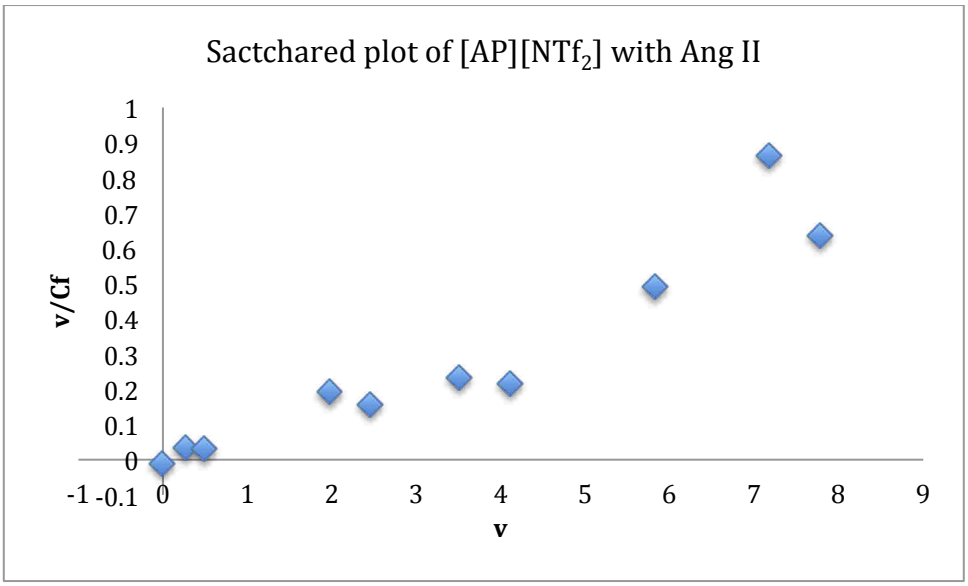

Figure A3: Scatchard plots of Ang II with [AP][NTf_2]

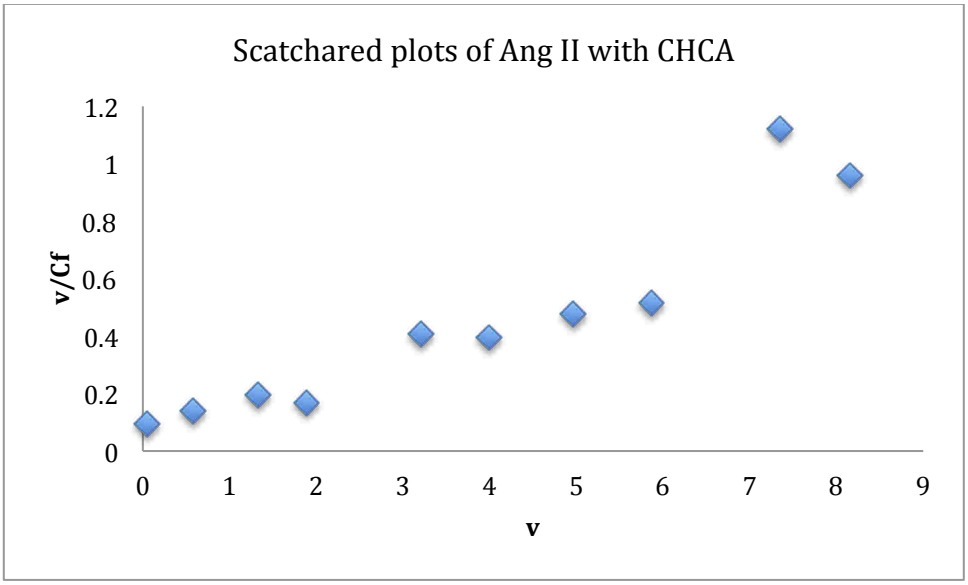

Figure A4: Scatchard plots of Ang II with CHCA

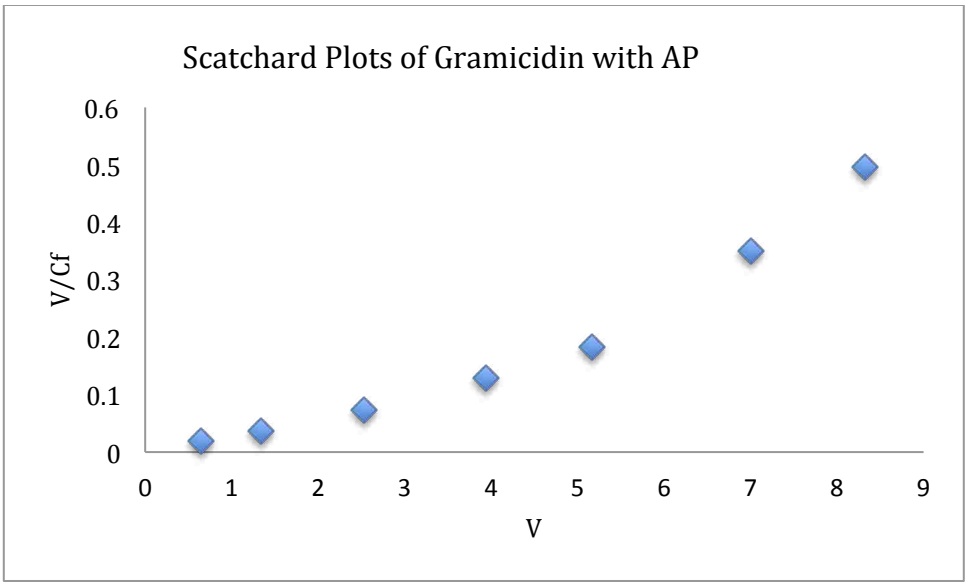

Figure A5: Scatchard plots of gramicidin with AP

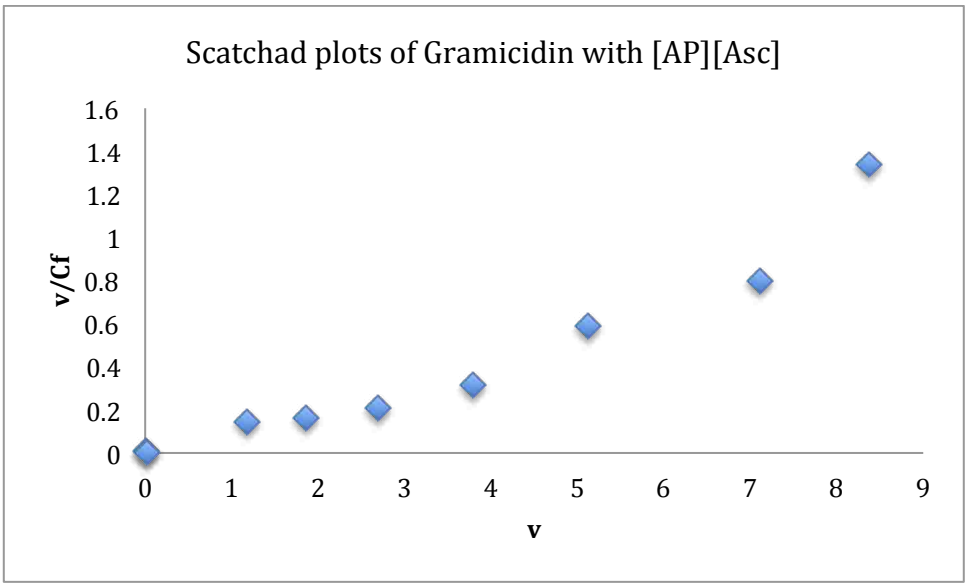

Figure A6: Scatchard plots of gramicidin with [AP][Asc]

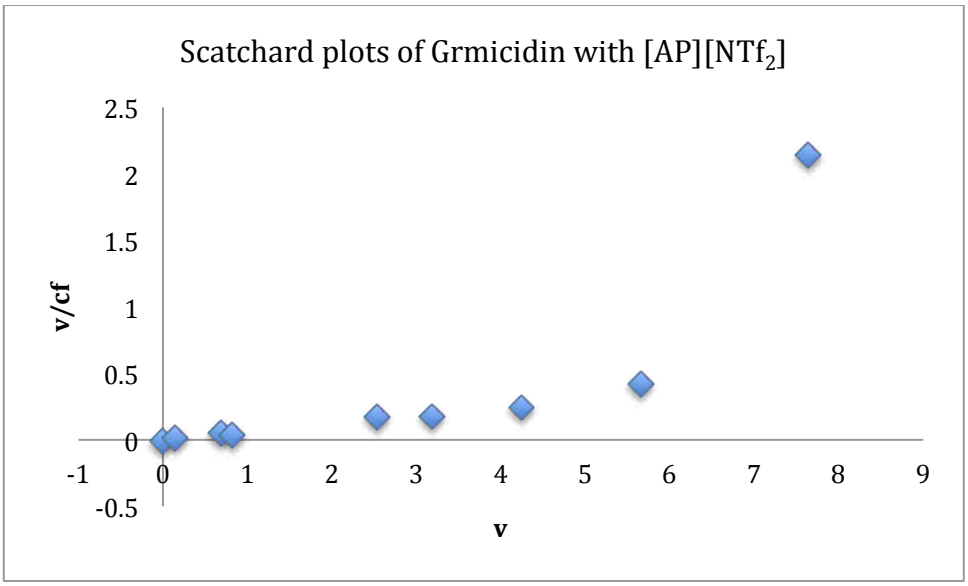

Figure A7: Scatchard plots of gramicidin with [AP][NTf_2]

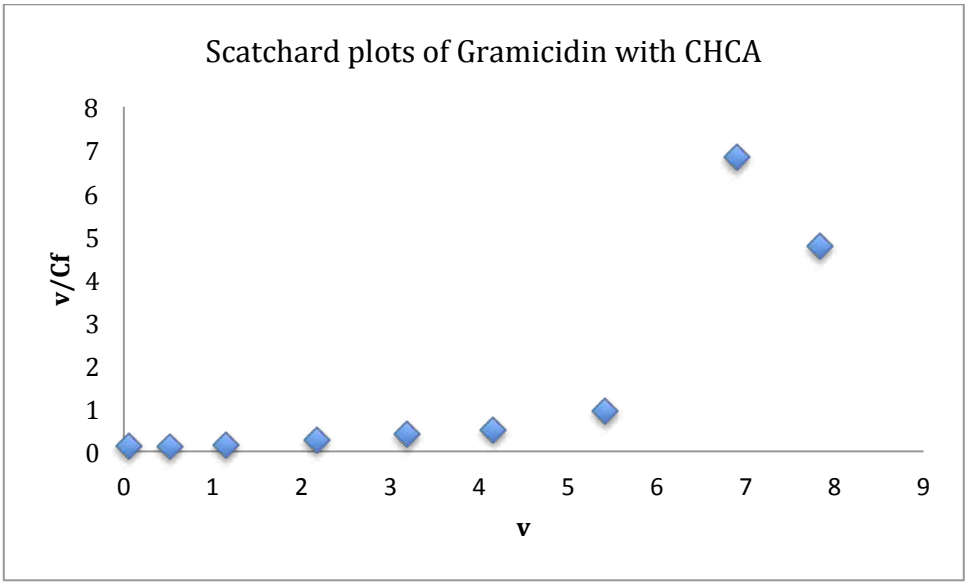

Figure A8: Scatchard plots of gramicidin with CHCA

Table A1: Average MALDI Signal intensity for [Glu^1]-fibrinopeptides B

Matrices	Average Intensity	SDV	RSD
2,5-DHB	2550	3739	147
[OA][CHCA]	8330	2357	28

The spectra for the [Glu1]-Fibrinopeptides B protein is shown using DHB and [OA] [CHCA] as the respective matrices for figures A9 and A10. From the spectra it was found that [OA] [CHCA] gave a smaller relative standard deviation and higher signal intensity as compared to DHB.

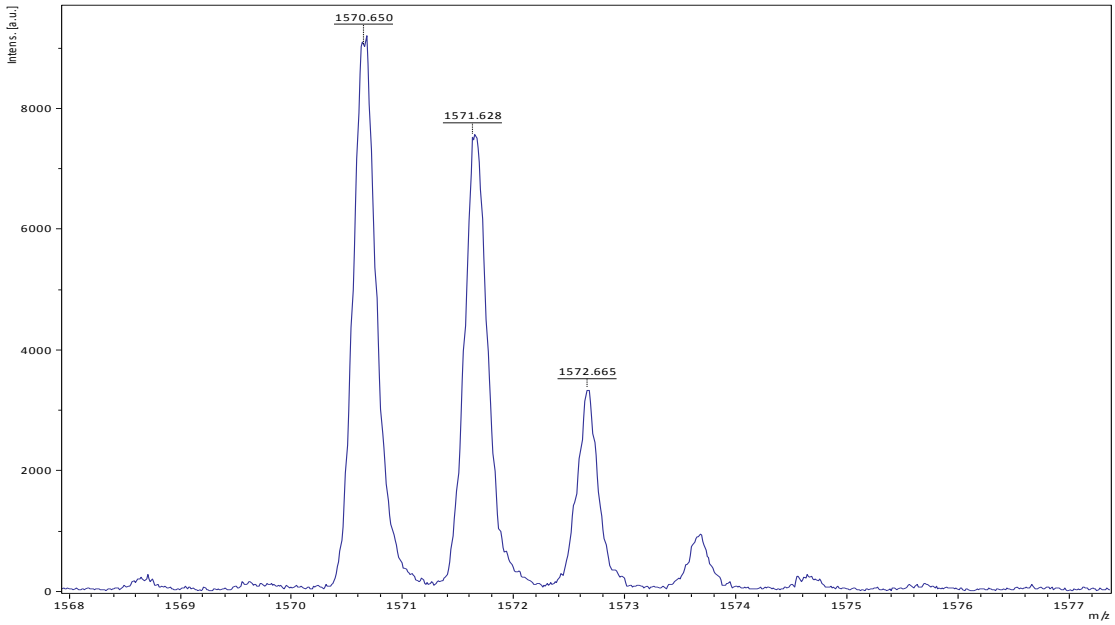

Figure A9: Positive ion mode MALDI MS spectrum of [Glu1]-Fibrinopeptides B using DHB

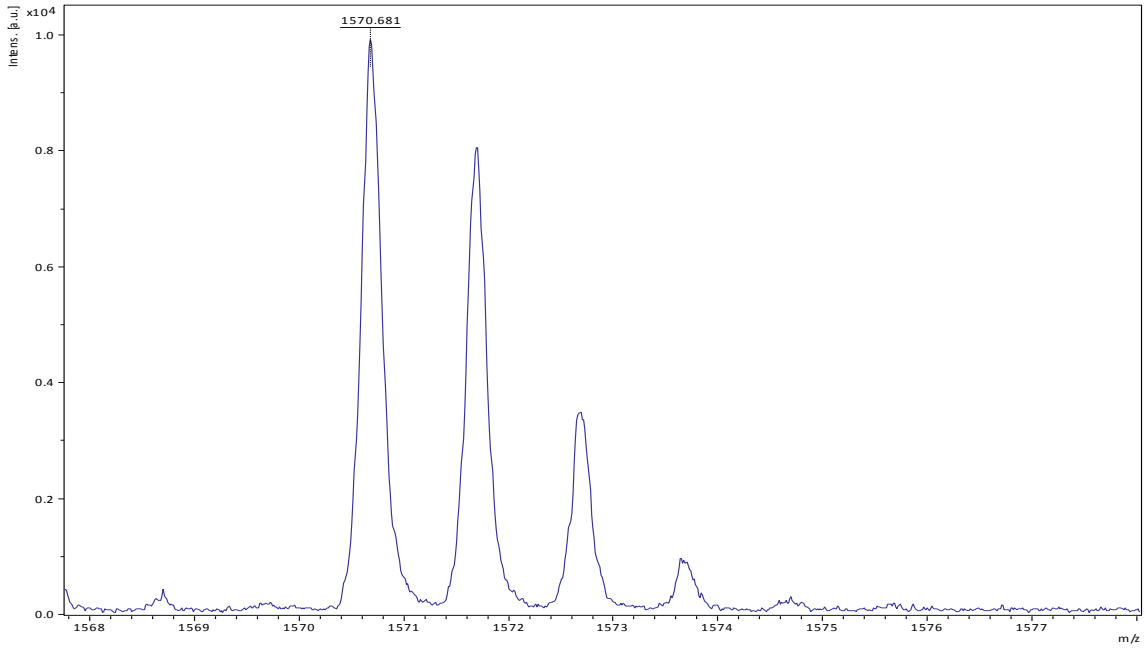

Figure A10: Positive ion mode MALDI MS spectrum of [Glu1]-Fibrinopeptides B using [OA] [CHCA]

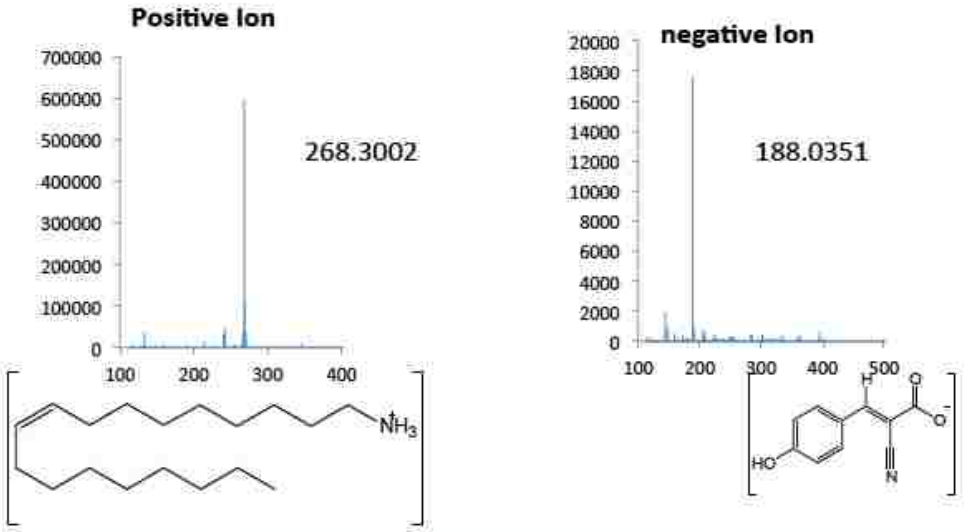

Compound	Molecular weight	ESI-Mass Spect Negative ion mode		ESI-Mass Spect Positive ion mode	
		Theoretical	Found	Theoretical	Found
[OA][CHCA]	456.335	188.0353	188.0351	268.30	268.3002

Figure A11. Positive and negative mode of ESI shows the formation of [OA] [CHCA]-based GUMBOS with a cation and anion.

APPENDIX B LETER OF PERMISSION

JOHN WILEY AND SONS LICENSE
TERMS AND CONDITIONS

Dec 04, 2014

This is a License Agreement between Hashim Al Ghafly ("You") and John Wiley and Sons ("John Wiley and Sons") provided by Copyright Clearance Center ("CCC"). The license consists of your order details, the terms and conditions provided by John Wiley and Sons, and the payment terms and conditions.

All payments must be made in full to CCC. For payment instructions, please see information listed at the bottom of this form.

License Number	3521930235114
License date	Dec 04, 2014
Licensed content publisher	John Wiley and Sons
Licensed content publication	Rapid Communications in Mass Spectrometry
Licensed content title	GUMBOS matrices of variable hydrophobicity for matrix-assisted laser desorption/ionization mass spectrometry
Licensed copyright line	Copyright © 2014 John Wiley & Sons, Ltd.
Licensed content author	Hashim Al Ghafly,Noureen Siraj,Susmita Das,Bishnu P. Regmi,Paul K. S. Magut,Waduge Indika S. Galpothdeniya,Kermit K. Murray,Isiah M. Warner
Licensed content date	Sep 19, 2014
Start page	2307
End page	2314
Type of use	Dissertation/Thesis
Requestor type	Author of this Wiley article
Format	Electronic
Portion	Full article
Will you be translating?	No
Title of your thesis / dissertation	GUMBOS as Matrix for Matrix-Assisted laser desorpation ionization times of fight mass spectrometry
Expected completion date	May 2015
Expected size (number of pages)	130
Total	0.00 USD

VITA

Hashim Al Ghafly earned his B.S. in Chemistry from King Saud University in Saudi Arabia. He later taught high school at Saihat High School in Saudi Arabia for ten years. Due to his enthusiasm and hard work as a teacher, he was awarded a scholarship to earn his Masters degree in the United States. By the end of spring 2009, he had earned his Masters in Mathematics from the University of Nebraska, Omaha. After obtaining his Masters degree with a high GPA, Hashim was awarded an extended scholarship to pursue his PhD in Chemistry at Louisiana State University. In 2010, he joined Dr. Isiah Warner's Research Group to become a part of the group's research progress and achievements. Hashim's research interest focuses on the Synthesis and studies of ***g***roup of ***u***niform ***m***aterials ***b***ased on ***o***rganic ***s***alts (GUMBOS) as matrix for Matrix-Assisted Laser Desorption/Ionization Mass Spectrometry. The aim of this study is to develop a method for improved detection of hydrophobic membrane peptides or proteins through their dissolution in novel GUMBOS, which will facilitate their uniform deposition on a MALDI target prior to their characterization by mass spectrometry. He is a member of the American Society for Mass Spectrometry (ASMS) and American Chemical Society (ACS). He is currently a candidate for the degree of Doctor of Philosophy in chemistry, which will be awarded at the may 2015 commencement.